EFFECTS OF ENERGY EXTRACTION ON SEDIMENT DYNAMICS IN INTERTIDAL ECOSYSTEMS OF THE MINAS BASIN

OEER Final Report
Jan 2010 – May 2012

Submitted by:

Dr. Danika van Proosdij (PI) and Casey O'Laughlin (MSc.)
Department of Geography, Saint Mary's University
923 Robie St. Halifax, NS, B3H 3C3
dvanproo@smu.ca
902 420-5738 (office) 902-496-8213 (Fax)

Collaborators:

Tim Milligan and Brent Law
Ocean Physics Section, Habitat Ecology Section, Bedford Institute of Oceanography

Ian Spooner
Department of Earth and Environmental Science, Acadia University
- Feb 18, 2013 -

SUMMARY

Sediments are the primary determinants of biological activities in the Upper Bay of Fundy, notably benthic habitat and ecosystem processes; being able to forecast their behaviour is a high priority as indicated in the SEA report (Whitford, 2008). These areas are of high importance for primary productivity and functioning of the estuarine ecosystem. However, our current understanding of sedimentary processes operating in the upper intertidal zone is extremely limited and significantly limits our ability to accurately model far field effects of energy extraction. We know that a decrease in velocity will affect the transport and deposition of sediments and alter their properties (e.g. grain size, cohesiveness, organic matter content) however the relative magnitude of these changes in upper intertidal zones such as tidal creeks and salt marshes is unknown. In addition, we do not know if these changes would fall within the bounds of natural variability or how processes would be either amplified or dampened under a changing climate.

The purpose of this research project was to assess how the dynamics of sedimentation change in response to changes in energy between neap and spring tidal cycles. The differences in tidal prism and energy between neap and spring tidal cycles were used as a proxy for energy extraction due to in-stream tidal power devices. The overall goal therefore was to gain a better understanding of the factors controlling sediment transport and deposition within intertidal ecosystem and how these processes may or may not change with changing tidal energy or amplitude.

The research was conducted over a 3 year period at two intertidal sites within the Cornwallis Estuary. Starrs Point and Kingsport were chosen specifically for contrasting levels of wave exposure which would likely result in differences in sediment transport processes and 'sensitivity' to changing tidal conditions. Similar types of instruments available at the Intertidal Coastal Sediment Transport (In_CoaST) Research Unit were used for all three experiments however were deployed in different configurations and at different sampling rates to focus on a range of research priorities. Instruments used included: one Nortek shallow water bottom mounted Acoustic Doppler Current Profiler, 3 Nortek Acoustic Doppler Velocimeters, 2 Optical Backscatter Sensors (OBS 3+ Campbell Scientific), surface mounted sediment traps, 1 Teledyne ISCO automated water sampler deployed on a tower and 1 RBR temperature, turbidity and salinity probe.

From August 2009 to September 2011, a total of 73 tides were sampled over a range of spring to neap tidal cycles. Complete data sets (all instruments and traps function with the exception of the ISCO sampler) were collected for 40 of these tides. A total of 624 sediment deposition and 431 suspended sediment samples were collected with almost a third of these being processed for disaggregated grain size (DIGS) analysis. In addition, data were

collected during a full range of natural variability in non-ice meteorological conditions. Data collected during these experiments represent the most comprehensive empirical data set ever collected within intertidal ecosystems in the Bay of Fundy.

Significant differences in sediment transport processes and controls on sediment deposition were found between the sheltered Starrs Point site (both within the creek and on the marsh surface) and the exposed Kingsport location.   The differences in sediment deposition may be linked to differences in both the availability of sediment and the opportunity for this sediment to be deposited. Overall current velocities were very low 5-10 cm·s^{-1} within the Starrs point tidal creek and less than 5 cm·s^{-1} within the vegetated canopy at both sites.   Measured shear stresses are insufficient to re-suspend sediment within the exception of the creek thalweg.   Water depth and tidal stage play an important role in controlling the hydrodynamics within these systems, particularly within the tidal creek system.   Tides which are restricted to the channel tend to be flood dominant while those that exceed the bankfull level are ebb dominant. Suspended sediment concentrations were highly variable ranging from < 50 mg·l^{-1} to 5,800 mg·l^{-1} particularly during flood and final ebb portions of the tide and during storms - mean during tides ~ 50-150 mg·l^{-1}. This suggests an ephemeral formation of a fluid mud layer which would dampen turbulence near the bed.   At Starrs Point, there was approximately seven times the mass of sediment deposited within the tidal creek when compared to the marsh surface.   In addition, approximately 1.5 times more sediment was deposited during overmarsh tides compared with channel restricted tides. The ADCP and OBS records indicate notable settling of sediment just after high tide which was not observed at the Kingsport site.   Significantly less sediment (approximately 10 times) was deposited within the exposed Kingsport site and the highest values were recorded, not surprisingly, during lower amplitude tides. The grain size spectra between tides were very similar, and the highly flocculated nature of the material leads to more rapid settling with higher suspended sediment concentrations and more resultant deposition with a greater volume of water (e.g. depth). While sediment availability is enhanced during heavy rainfall events it does not necessarily lead to higher deposition immediately after the storm.   Overall, these findings provide important baseline information regarding natural variability in biophysical processes and the ability of intertidal ecosystems to respond to changes in the environment (e.g. resilience) that can be applied to computer models currently being developed.

The amount of sediment deposited, particularly on the marsh surface, appears to be most sensitive to changes in water depth rather than changes in tidal energy. Therefore even a 5% reduction in tidal amplitude would reduce the number of over-marsh tides by a similar figure, and cause an increase in the occurrence of channel-restricted tides and result in significant changes in inundation time and flooding frequency on the marsh surface. The frequency of marshfull tides can potentially increase as well, in which case amplified

erosion of marsh edges may create an additional sediment source. Decreased inundation frequency of high marsh surfaces may impose a sediment deficit in marsh systems, as less material is distributed to the marsh surface from tidal creeks. High marsh areas will likely be the most significantly impacted with a loss of sediment input. This can show impacts in marsh sedimentation and resulting elevation, channel equilibrium, vegetation community structure, and ecological productivity.

Potential decreased ebb-flow magnitude is likely to be associated with decreased tidal amplitude, due to less water being put into storage on the marsh surface, as well as less frequent inundation events. Lower magnitude ebb flows may show less capacity for sedimentary work, reducing sediment mobility during ebb phases. The result may be creek infilling and a reduction in bank steepness, which would likely have continued impacts on creek hydrodynamics and sediment transport. A continuation and exacerbation of this cycle would constitute a non-linear response of fine-grained materials in tidal creeks, and would impact the movement of water in and out of the estuary through changes in deposition and erosion patterns and the resulting basin geometry. Either a circumstance of decreased sediment supply to the marsh surface, or an increase in in-channel sedimentation, will impact the form and function of salt marshes

While this research has led to an increased understanding of the factors controlling sediment transport and deposition, it has also raised our awareness of the spatial and temporal complexity of these processes. Future field data collection efforts should try to get a better picture of the significant fluctuations in suspended sediment concentrations in the exposed marsh and mudflat system, given the challenges during the Kingsport deployment. It is recommended that the research be expanded to include a greater range of seasonal conditions and simultaneous measurements at multiple locations. It will be critical that computer models be tested for a range of environmental conditions and at a sufficiently fine spatial scale to resolve differences in sediment transport processes between un-vegetated creek or mudflat surfaces and the marsh surface. In addition, given the sensitivity of intertidal sediment transport processes and deposition to water depth, it is recommended that a Basin wide GIS assessment be conducted to identify the areas that will be most sensitive (e.g. upper marsh) to changes in tidal amplitude.

Table of Contents

LIST of FIGURES

INTRODUCTION

Sediments are the primary determinants of biological activities in the Upper Bay of Fundy, notably benthic habitat and ecosystem processes; being able to forecast their behaviour is a high priority as indicated in the SEA report (Whitford, 2008). These areas are of high importance for primary productivity and functioning of the estuarine ecosystem. However, our current understanding of sedimentary processes operating in the upper intertidal zone is extremely limited and significantly limits our ability to accurately model far field effects of energy extraction. We know that a decrease in velocity will affect the transport and deposition of sediments and alter their properties (e.g. grain size, cohesiveness, organic matter content) however the relative magnitude of these changes in upper intertidal zones such as tidal creeks and salt marshes is unknown. In addition, we do not know if these changes would fall within the bounds of natural variability or how processes would be either amplified or dampened with climate change. These data will apply directly to on-going modeling initiatives at the Bedford Institute of Oceanography.

Scientific Objectives

The purpose of this research project was to assess how the dynamics of sedimentation change in response to changes in energy between neap and spring tidal cycles. The differences in tidal prism and energy between neap and spring tidal cycles were used as a proxy for energy extraction due to in-stream tidal power devices. Specific questions addressed included:

1. How do current velocities and suspended sediment concentrations vary within confined intertidal environments such as tidal creeks over a spring to neap tidal cycle?

2. Using floc limit, a measure of how flocculated a suspension is, are there differences in the mobility and distribution of sediments during the spring/neap cycle?

3. What is the natural range of variability in sedimentary processes within mudflat and salt marsh environments over the spring to neap tidal cycle?

4. What influence do wave activity or precipitation events have on these patterns?

5. How do sedimentary processes vary between different intertidal environments (e.g tidal flat, tidal creek and salt marsh) and how might these systems respond to changes in tidal energy?

Simple numerical models of energy extraction from various channel networks show a general decrease in kinetic power density of tidal flows with increasing dissipation by turbines (Polagye and Malte, 2010; Sun *et al.*, 2008; Bryden *et al.*, 2004). According to Karsten *et al.* (2008), proposed tidal power installations in the Minas Passage will result in an overall lowering of tidal amplitude in the Minas Basin; a 5% reduction in tidal amplitude has been associated with moderate levels (e.g. 2.5 gigawatts) of energy extraction from the Minas Passage. Environmental effects of tidal power development in the Bay of Fundy have been previously considered (e.g. Yeo and Risk, 1979; Gordon 1994), but the magnitude of potential change still remains to be fully understood (Polagye *et al.*, 2011) and may or may not occur within a range of natural variability. It is hypothesized that intertidal sedimentation rates in the Minas Basin will demonstrate a non-linear response to modification of the tidal energy regime, due to naturally high suspended sediment concentrations (Polagye *et al.*, 2011; Polagye and Malte, 2010; Whitford, 2008), and based on previous work assessing estuarine response to anthropogenic alterations of hydrodynamics (e.g. van Proosdij *et al.*, 2009; Amos and Mosher, 1985; Turk *et al.*, 1980). Furthermore, changes in flooding patterns and frequency associated with a decreased tidal range may exert a significant impact on the species composition of high marsh communities.

This report will provide an overview of the experimental results from 2009 to 2011 and focus primarily on a comparison between processes operating with a sheltered tidal creek/adjacent saltmarsh surface and the exposed mudflat-salt marsh system. Detailed results, analyses and discussions are provided in two academic theses (O'Laughlin, 2012 – MSc; Poirier, 2012 – BSc) and two refereed journal articles (O'Laughlin and van Proosdij, 2012; O'Laughlin et al., in submission).

STUDY AREA

Two study sites were chosen within the Cornwallis estuary that represented two different types of intertidal systems. The first, Starrs Point (2009 and 2011) was a sheltered terminal creek at Starrs Point marsh, near the upper limit of the Minas Basin, at the mouth of the Cornwallis River (Figure 2, Figure 2). The second was an exposed section of mudflat with adjacent low marsh habitat near Kingsport (Figure 2). A headwater location was selected at Starrs Point for investigation of subtle variations in tidal parameters that occur in a low-energy segment of the tidal environment, where high rates of sediment deposition were anticipated as channel banks receive sediment for eventual distribution over the marsh surface. Accessibility also played a considerable role in site selection. Mean grain size and the diameter of the 50th percentile (d_{50}) of deposited sediment samples collected from the tidal creek are 6.2 and 6.1 μm respectively, which falls within the very fine silt category according to the Udden-Wentworth scale. Salinity is relatively constant (~30

practical salinity units). The marsh surface is characterized by a mix of high marsh platforms (dominated by *Spartina patens*) and deeply incised creeks, with a dominance of *Spartina alterniflora* on the upper creek banks and in low marsh areas. Creek banks are gently sloping and partially vegetated (Figure 3). Tidal flows navigate more than one kilometer of main channel before reaching the study location. A deep, incised ditch (~1 meter width, > 1 meter depth) continues for several hundred meters beyond the creek head and through an area of densely-vegetated low marsh, parallel to an agricultural dike (Figure 3)(most recent construction in 1955). The ditch is a former burrow pit that has been incorporated into the drainage network, as is common on Fundy marshes (MacDonald *et al.*, 2010; Bowron *et al.*, 2011; van Proosdij *et al.,* 2010).
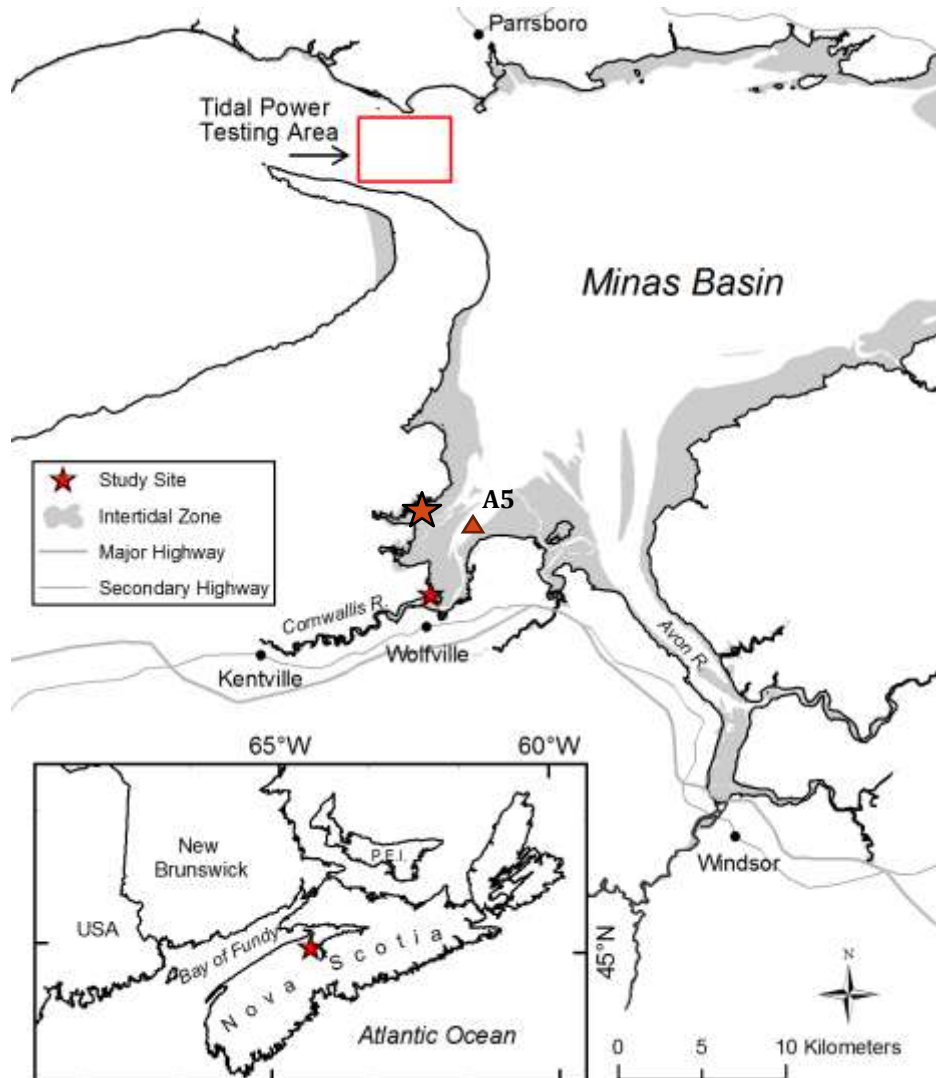
Figure 1: Experimental study sites relative to the tidal power test facility and intertidal zone. Approximate location of the A5 mooring station from DFO is also shown.
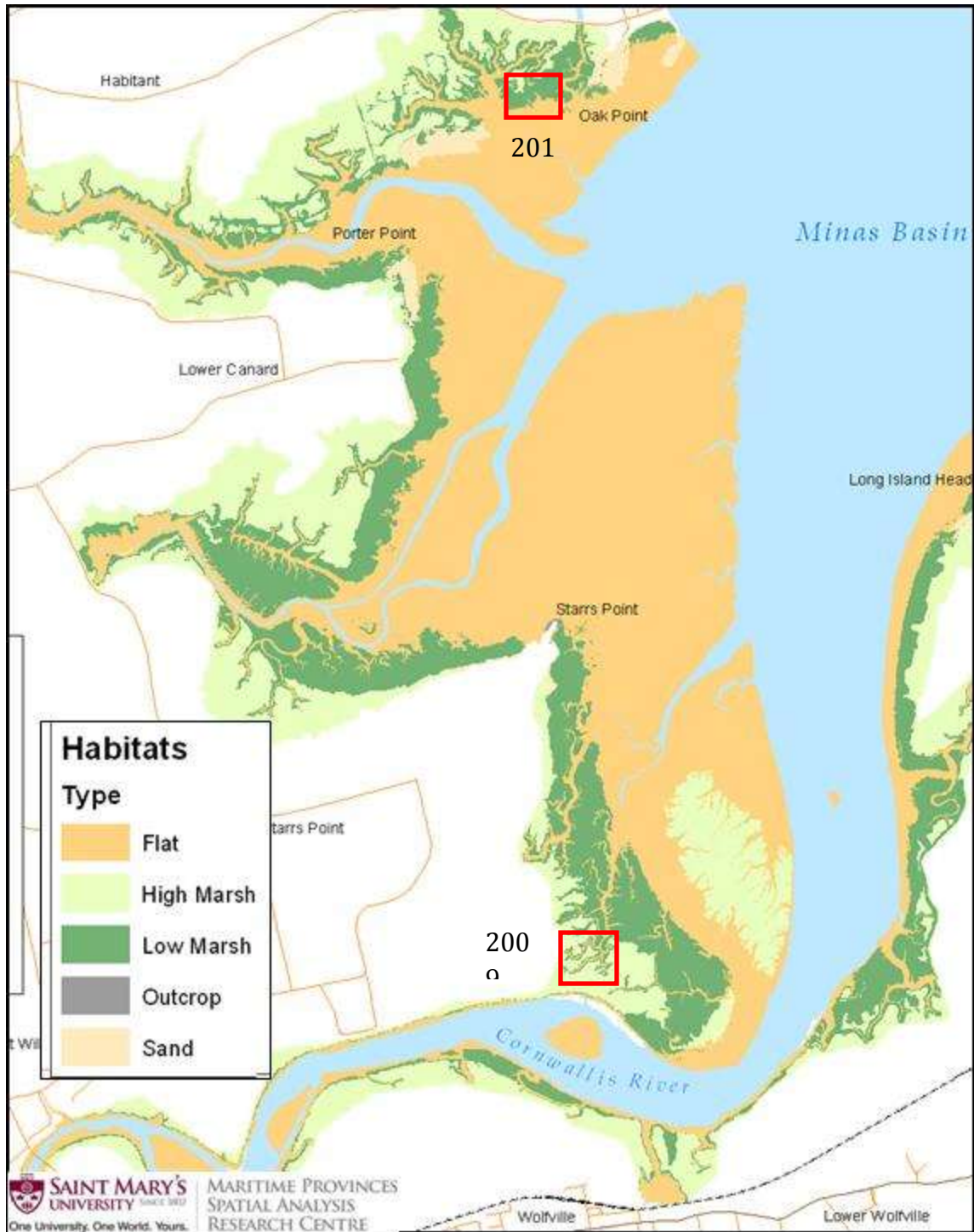
Figure 2: Location of study areas for 2009 and 2011 experiments (Starr's Point) and 2010 experiments near Kingsport in the Cornwallis Estuary.

The Kingsport site (2010) was located in an exposed section on the intertidal zone west of Oak Point (Figure 2). The sampling transect was located in a section low in the tidal frame, extending from the mudflat into the low marsh, dominated by *Spartina alterniflora.*

The mean grain size derived from surface scrape samples is 8.35 (± 2.58) µm, D_{50} of 9.52 µm. These sediments are therefore slightly coarser than at Starrs Point, falling into the fine silt category.

METHODS

Similar types of instruments available at the Intertidal Coastal Sediment Transport (In_CoaST) Research Unit were used for all three experiments however were deployed in different configurations and at different sampling rates to focus on a range of research priorities (Table 1).   Instruments used included: one Nortek shallow water bottom mounted Acoustic Doppler Current Profiler, 3 Nortek Acoustic Doppler Velocimeters, 2 Optical Backscatter Sensors (OBS 3+ Campbell Scientific), surface mounted sediment traps, 1 Teledyne ISCO automated water sampler deployed on a tower and 1 RBR temperature, turbidity and salinity probe.   Each OBS sensor was individually calibrated in the field (Puleo *et al.*, 2007; Hoitink and Hoekstra, 2005; Voulgaris and Meyers, 2004a) with suspended sediment from the co-located ISCO sampler.

Field Deployments
Starrs Point (sheltered tidal creek):

In 2009, sampling efforts were concentrated within the tidal creek itself to examine variability in hydrodynamic processes, sediment composition and deposition in the thalweg and non-vegetated bank.   The ADCP was deployed in the creek thalweg sampling at a continuous rate of 1 HZ with 2MHZ frequency with a bin size of 5 cm. A temperature and salinity probe was deployed at the mouth of the creek to monitor incoming tidal conditions. One ADV with co-located OBS was also deployed in the thalweg sampling at a rate of 16 Hz in 1 min bursts every 5 minutes at 10 cm above the bed (Figure 4). Another ADV/OBS pair was stationed midway up the creek bank and ran continuously at 4 Hz over the entire sampling period. Changes in surface elevation were measured at each site using a grid of stationary pins (50 pins at 20 cm spacing) and reflectorless total station (Figure 5). The total station was mounted on a post at a fix point and points were taken at the pin/mudflat interface and elevation determined via triangulation and 3D surfaces will be modeled in ArcGIS.   Unfortunately considerable amounts of floating vegetative debris became entangled around the pins as the season progressed making accurate measurement near impossible. In addition, it was also found that snails congregated in these areas as well, resulting in local disturbance of the sediment surface.

Samples of deposited sediment were collected with surface-mounted sediment traps and pre-weighed filter papers (Whatman 5, 90 mm paper filters), based on the design by van Proosdij *et al.* (2006a, 2006b) (Figure 5 inset). This trap design allows for re-suspension of

deposited materials within a tidal cycle and can be used to characterize net sediment deposition on non-vegetated creek banks and tidal flats. Four traps were deployed within an approximately 2 m² plot on the creek bank, with three filter papers in each trap, and were leveled using a spirit level.
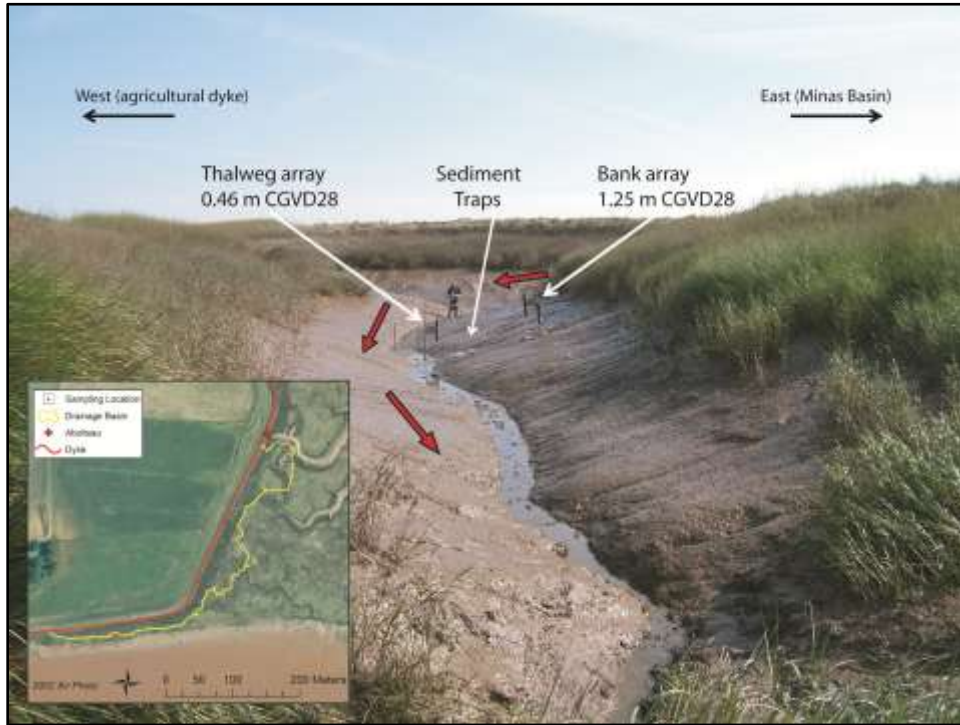
Figure 3:   2009 experimental set-up within end member tidal creek at Starrs Point.   Localized drainage basin indicated within the inset.
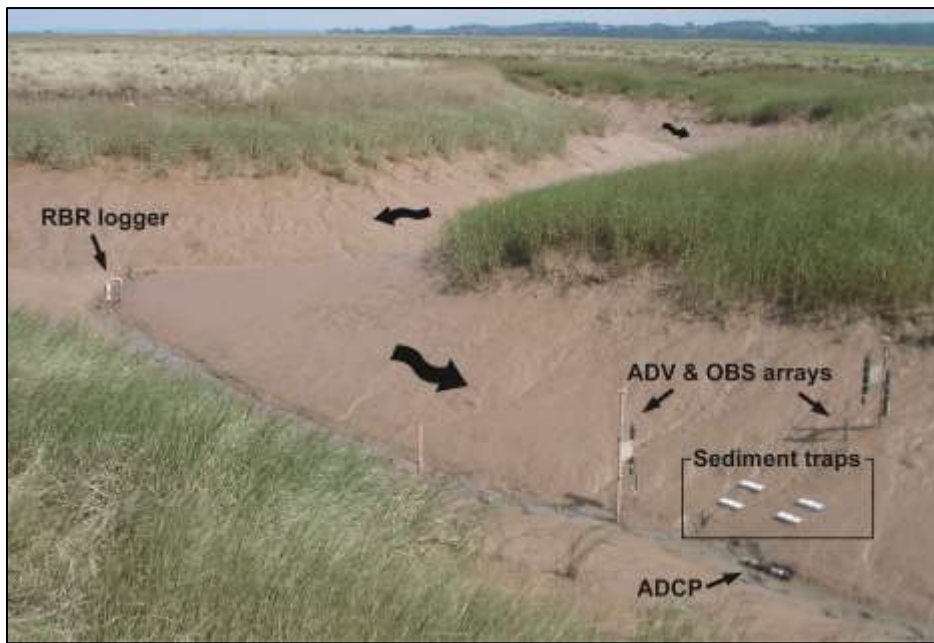
Figure 4: Closer view of the experimental set-up for the 2009 deployment at Starrs Point.

Figure 5: ISCO sampling platform on the high marsh surface adjacent to the tidal creek used in both 2009 and 2011 deployments. Structure was removed during the winter months. Surface mounted sediment traps used in 2009 depicted within the inset.

This study focused on in-creek deposited sediment to enable full characterization of tides that remain confined to channels and do not flood the marsh surface. Traps were not deployed in rainy weather. Deposited samples were air dried for 24-48 hours before weighing to determine the total amount of sediment deposited on each paper, on each trap, and at each trap location over the course of the study. The traps were not rinsed prior to analysis since minimal salt accumulated over individual tidal cycles. Salinity was measured with a RBR XR-420 logger positioned at the mouth of the study creek, and remained relatively constant over the experimental period. Statistical analyses on deposited sediment samples were completed using a nested ANOVA and standard two-sample t-tests (SYSTAT 13).

In 2011, building upon findings from the 2009 experiments, the experimental design was extended to include the vegetated low marsh on the bank of the tidal creek, marsh crest and extending into the high marsh platform (Figure 7). The position of the ADCP remained in relatively the same position as did the ISCO tower. The sampling bin volume was increased from 5 to 30 cm in order to try and get measurements over more of the water column. The sampling rate remained at 1 Hz. The traps were re-designed to include only one filter paper each and collect statistically independent samples.

Figure 6: Surface elevation pins within the Starrs point creek in late June, 2009.
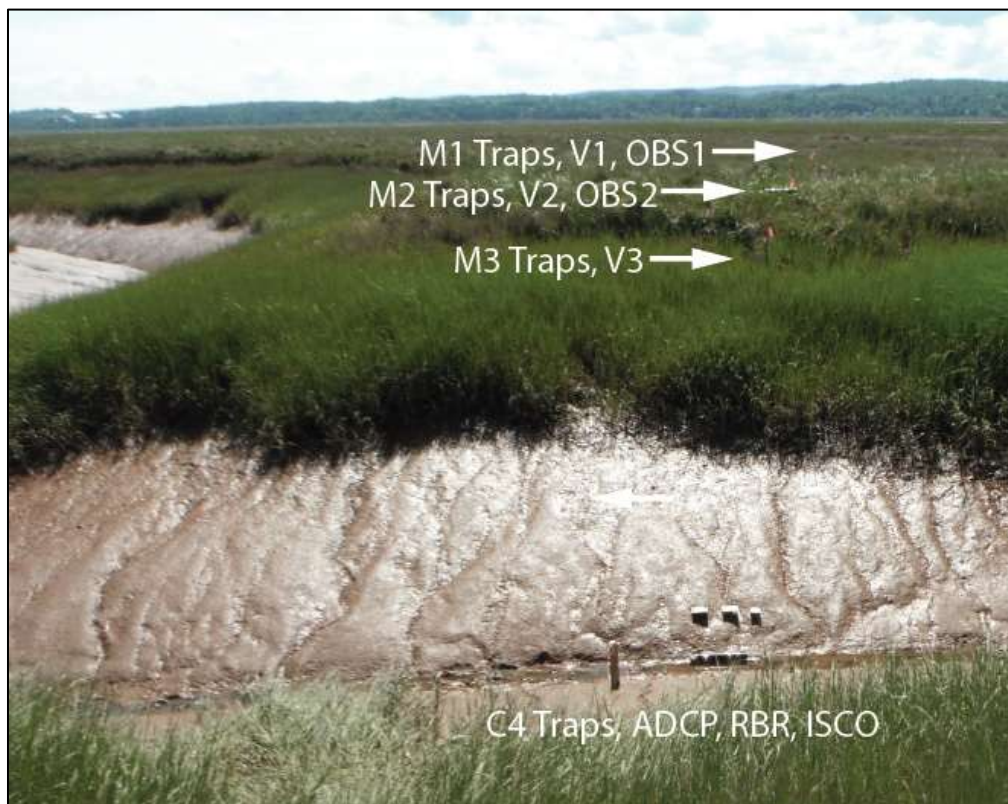
Figure 7: Experimental set-up for 2011 deployment including C4 station (creek), M3 (low marsh bank), M2 (transition zone cliff) and M3 (high marsh platform).

Figure 8: ADV and sediment covered traps at M1 on August 31st, 2011 (Photo by C. Skinner, 2011). Note deployment of the ADVs at M1 and M2 side lying in order to sample as close to the bed as possible.

Year	Instrument	Station	Bin size or sampling elevation	Sampling rate	Type
2009	ADCP	Creek thalweg	5 cm, high resolution	1Hz, 2 MHz freq	continuous
	ADV (2)	Thalweg & bank	10 cm above the bed	16Hz, 4 Hz	Thalweg 1 min burst every 5 min, bank continuous
	OBS	Thalweg & bank	10 cm above the bed		
	ISCO	thalweg	10 cm above the bed	200 ml	Every 30 minutes
	Traps (4 x 3 filters)	Along thalweg			
2010	ADCP	mudflat	5 cm, high resolution	1Hz, 2 MHz freq	continuous
	ADV (3)	Low marsh (V1-3)	10 cm above bed	16 hz	5 min burst every 10 min
	OBS	V1 & V3	10 cm above bed	16 hz	5 min burst every 10 min
	ISCO	V1	10 cm above bed	200 ml	Every 30 minutes
	Traps (12)	3 per site with 1 filter	2 cm above bed		
2011	ADCP	Creek thalweg	30 cm, standard mode	1 Hz	continuous
	ADV (3)	M1 (HM),M2 (edge), M3 (LM creek bank)	10 cm M3, 15 cm M1 & 2	16 hz	5 min burst every 10 min
	OBS	M1,M2			
	ISCO	thalweg	10 cm above bed	200 ml	Every 30 minutes
	Traps (12)	3 per site with 1 filter			

Table 1: Summary of sampling rates for all field experiments.

Kingsport (open exposed mudflat and low marsh system)

In 2010, a shallow water, upward looking Nortek Acoustic Doppler Current Profiler (ADCP) was deployed on the mudflat approximately 5 m away from the edge of the low marsh. Data were collected at a continuous rate of 1 HZ with 2MHZ frequency with a bin size of 5 cm. A temperature and salinity probe (RBR) was deployed in the immediate area to monitor incoming tidal conditions. Three ADVs were installed approximately 20 m apart perpendicular to the edge of marsh (Figure 9, Figure 10). All instruments were adjusted to sample at 10 cm above the bed at a rate of 16HZ in 5 minute bursts every 10 minutes. Station V1 was located approximately 2 m landward of a small low marsh cliff 30-50 cm in height and contained one ADV, one OBS and the inlet nozzle for the Teledyne ISCO water sampler (Figure 11, Figure 12). The ISCO water sampler was deployed off of a small tower at the top of the marsh cliff and powered by a solar panel (Figure 11). V2 only contained one ADV while station V3 at the edge of the marsh contained both an ADV and OBS. Sediment deposition was measured using three surface mounted sediment traps per station. Sediment collected on the filter papers were dried, weighed and one sample per station will be processed for grain size using a Multisizer 3 Coulter Counter. One rising stage bottle (Figure 12) per station was deployed starting on the second deployment sequence when it was found that the ISCO water sampler was not collecting samples consistently. The method however only measures suspended sediment concentration on the rising tide. A low boardwalk was installed with removable boards to minimize trampling and re-suspension in the vicinity of the instruments. Boards were removed after the traps and instruments were deployed so as to minimize flow interference.

A portable weather station (Campbell-Scientific) was installed on the adjacent dyke at Starrs Point marsh in all years to record hourly-averaged records of meteorological parameters, including wind speed and direction, rainfall, temperature and atmospheric pressure. Webtide' (Dupont *et al.*, 2005) was used to develop a one-year record (15-minute intervals) of predicted tide elevations at the study location.

Both sites in all years were impacted by biological processes associated with snail and crab populations that varied over the course of the summer (Figure 13), peaking in July/early August. Snails in particular seem to congregate along rills formed by freshwater seepage and late ebb drainage along the muddy tidal creek banks (Figure 14, Figure 15).
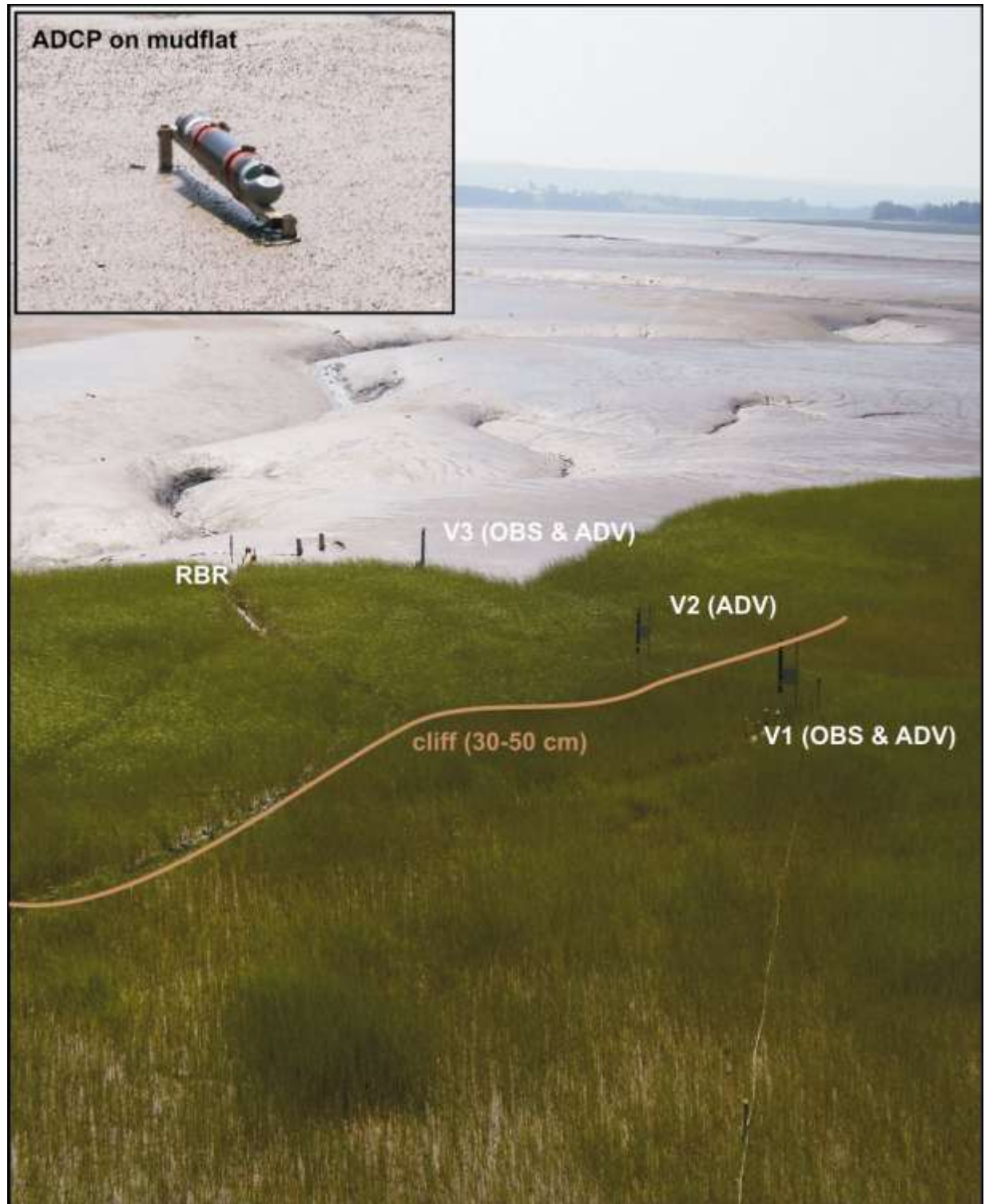
Figure 9: Position of ADCP, ADV, OBS and RBR along transect at Kingsport in 2010. Three sediment traps deployed at each station as well as one rising stage bottle sampler.

Figure 10: View of high marsh cliff and low marsh ramp looking west from the ISCO tower at Kingsport (June 2010)

Figure 11: Casey O'Laughlin (MSc candidate) and Will Flanagan securing the ISCO water sampler at Kingsport.
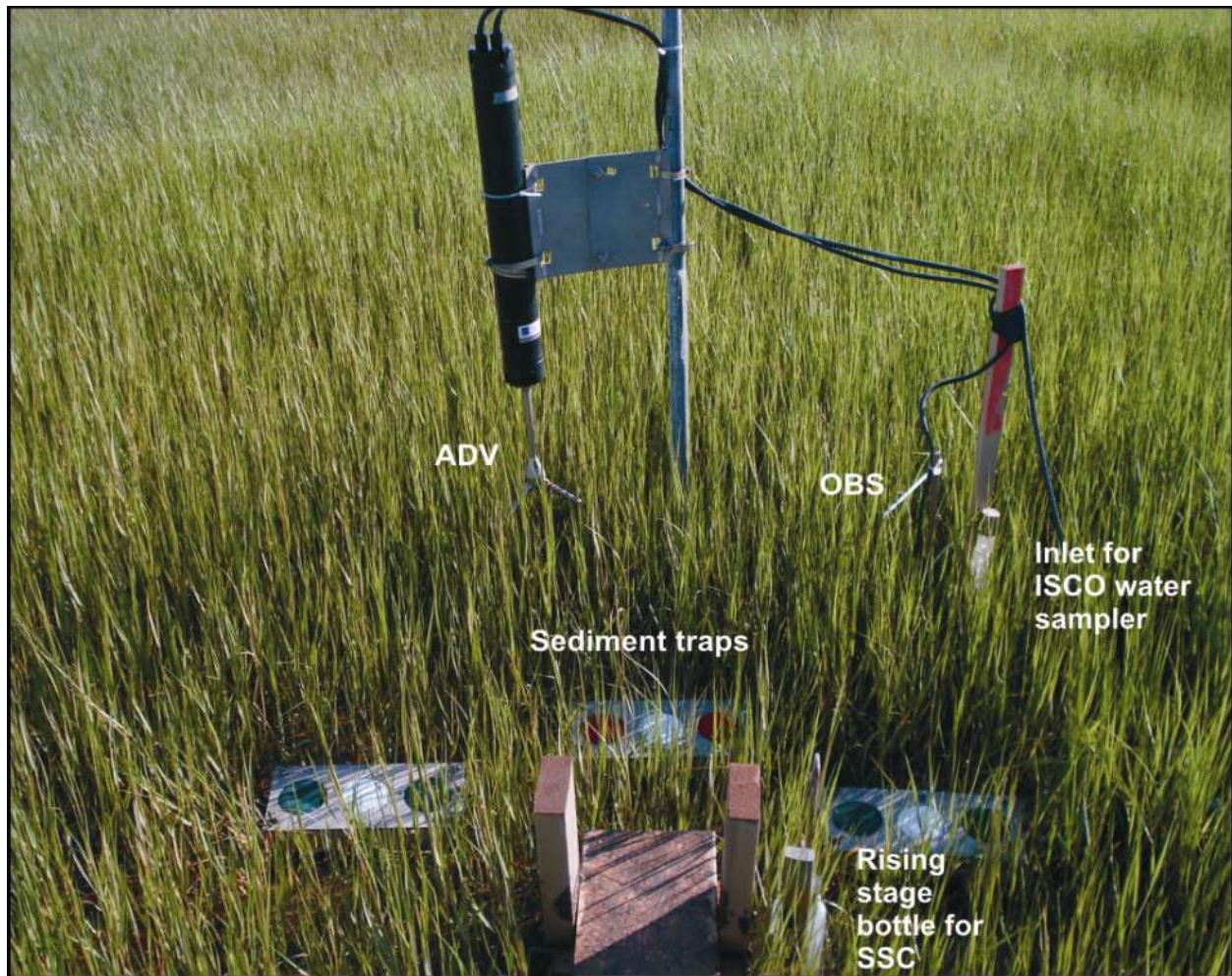
Figure 12: Experimental configuration at station V1 at the Kingsport salt marsh in 2010.

Figure 13: Rising stage bottle, ISCO nozzle and milling crabs and snails at Starrs Point (July 15, 2011)

Figure 14: Snail populations congregating along tidal creek rills at Starrs Point (July 15, 2011)

Figure 15: Snails and station V4 at Kingsport including position of ADCP, rising stage bottle, RBR, traps and removable boardwalk (July 2010).

Lab Analysis

Sediment scrape samples were collected after each tide in 2010 and 2011 and processed for organic matter, water content and grain size.

Sediment trap filters were weighed after air drying for 24-48 hours, to determine the total amount of sediment collected on each paper, on each trap, and at

Figure 16: Example of sediment trap filters from Starrs Point in 2009.

each trap location. Samples were not rinsed prior to weighing, since salinity measured at the mouth of the study creek (with a RBR XR-420 logger) remained relatively constant (~30), and the amount of salt accumulated over individual tidal cycles was presumably minimal relative to the amount of sediment. One filter from each trap was heated in a muffle furnace to determine organic content, while material from a second was used for grain size analyses. Statistical analysis of samples of deposited sediment was completed using nested ANOVA and standard two-sample t-tests (SYSTAT 13). Suspended sediment concentrations were determined from bottle samples and standard suction filtration methods.

In order to perform the disaggregated grain size analysis on both deposited and suspended samples, all organic material within the samples needed to be eliminated. Hydrogen peroxide solution at a concentration of 30% was used to dispose of the organic matter. A small amount was placed into 20 ml beakers and 2.5 ml of hydrogen peroxide solution was applied to them. The beakers were placed on hot plates, starting at a temperature of 60°C, and heating up to 100°C. If necessary, an additional 2.5 ml of hydrogen peroxide solution was added. After all of the liquid solution was evaporated, the remaining sediment was only inorganic content. During this process, the content of organic matter was quantified. The net weight of the sediment after being processed with hydrogen peroxide was subtracted from the initial net weight and the percentage of organic matter was therefore obtained.

Disaggregated inorganic grain size (DIGS) analysis was performed on samples of suspended and deposited sediment, using a Beckman-Coulter Multisizer III

electroresistance particle counter, following methods described by Milligan and Kranck (1991), Kranck et al. (1996a, 1996b), Curran et al. (2004), and Milligan and Law (2005). Small subsamples (0.1 - 0.5 g) for DIGS analysis were extracted from field samples of deposited sediment. Material was generally abundant on filters at the Starrs Point site, and subsamples were easily removed from filter papers after drying. Subsamples were treated with hydrogen peroxide (30%) to remove organic materials, added to ~10 ml of deionized, reverse osmosis water, and placed in a sonic bath for 10 minutes to disaggregate particles. For processing samples of suspended sediment, known volumes of sample laden-water were filtered onto Millipore 8.0 mm SCWP (cellulose acetate) pre-weighed filters using standard gravimetric methods. Millipore filters were selected based on previous studies that recommend these filters due to high retention of particles less than their nominal pore sizes (Sheldon, 1972; Sheldon and Sutcliffe, 1969). Filters were oxidized at <60° C in a low temperature oxygen/plasma asher, to prevent the fusing together of mineral grains while removing the filter. Once subsamples were isolated, they were diluted in a 1% NaCl solution and re-sonicated for 2 minutes using a sapphire-tipped ultrasonic probe, before processing with the Coulter Multisizer III. Both 30 and 200 μm aperture tubes were used in these analyses, the size distributions measured of which were merged to create continuous grain size spectra. In addition, grain size statistics were calculated on the merged grain spectra using GRADISTAT (Blott and Pye, 2001). Due to the more limited amount of sediment deposited on the filters at the Kingsport site, these filters were placed in beakers with SuperQ water and sonicated to remove the sediment particles. The sample was then processed in a similar manner to the suspended sediment samples.

Data Processing

Acoustic data recorded by the ADCP were filtered, viewed and interpreted using the standard settings in Storm (ver. 1.14, Nortek). Flow velocity and average signal strength were considered for each tidal cycle. ADCP data collected for this study were not calibrated for quantitative estimates of suspended sediment concentration however can be used as a measure of relative concentrations within a tide. Wave conditions during the sampling periods were investigated using raw pressure signals from the bank ADV, where consistently identified centimeter-scale ripples on the water surface reflect field observations. Mean current velocity and subsequent parameters derived from ADV records were estimated through time-averaging over 5-minute measurement bursts. Instantaneous horizontal flow components (x, y) were rotated into down-stream (u) and cross-stream (v) velocities following methods outlined by Roy *et al.* (1996) and Lane *et al.* (1998), and velocity was calculated as $\sqrt{u^2 + v^2}$. Instantaneous turbulent components (u_t, v_t, w_t) were derived using the relationship $u = U + u_t$, and turbulence intensities (i_u, i_v, i_w) were calculated as the root mean square of turbulent components. Turbulent kinetic energy (TKE) was calculated using:

$$TKE = \frac{1}{2}\, \rho\, (u_t{}^2 + v_t{}^2 + w_t{}^2)$$

Equation (1)

where ρ is water density at 20°C (ρ = 1025 kg·m^{-3}) (Neumier and Amos, 2006; Voulgaris and Meyers, 2004). Mean kinetic energy ($\overline{KE}$) in the tidal creek was estimated with:

$$\overline{KE} = a\,(\tfrac{1}{2}\, \rho\, u^2),$$

Equation (2)

where a is channel cross-sectional area and u is upstream current velocity (Karsten *et al.*, 2008). Friction velocity (u_*) was computed using the Reynolds stress method (Soulsby, 1983; Kim and Friedrichs, 2000):

$$u_* = (-\overline{u_t\, w_t})^{1/2},$$

Equation (3)

where u_t and w_t are instantaneous components of down-stream and vertical velocity, respectively. Friction velocity can then be applied to calculate bed shear stress (τ_0) (N·m^{-2}):

$$\tau_0 = \rho\, u_*{}^2$$

Equation (4)

where z is the measurement elevation above the sea bed, and h is the total local water depth in the channel (Kim and Friedrichs, 2000; Biron *et al.*, 2004; Voulgaris and Meyers, 2004).

DIGS distributions were parameterized using a non-linear, least-squares fit 'inverse floc model', through a semi-automated MATLAB routine developed by Curran et al., (2004) and based on work by Kranck and Milligan (1991) and Kranck et al. (1996a, 1996b). Deposited sediment DIGS distributions are expressed as the log of equivalent weight percent versus log of particle diameters, normalized over the size range (Kranck et al., 1996a, 1996b; Milligan and Kranck 1991). Suspended samples are expressed using log of concentration in parts per million (PPM) (Law et al., 2008). DIGS distributions of deposited sediment samples were then parameterized using a non-linear, least-squares fit model, based on work by Kranck *et al.* (1996a, 1996b) and Kranck and Milligan (1991).

Figure 17: Idealized DIGS distribution (solid line) showing concentration versus diameter on log-log axes. The floc-settled (dotted line) and single-grain (dashed line) components are determined by the inverse floc model. Graphical locations of model parameters of model parameters (d$_f$, d̂, m) are shown. Modified from deGelleke (2011).
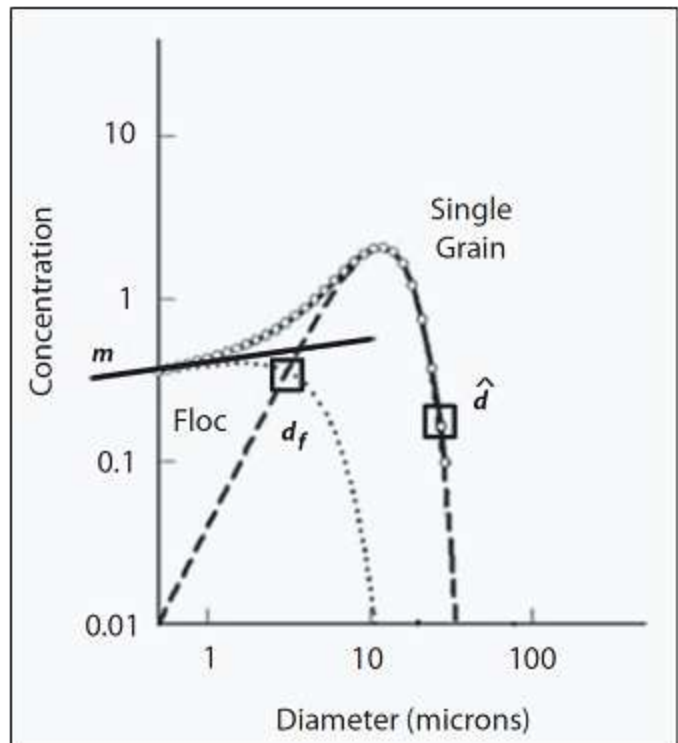
Figure 17 illustrates the components of the Inverse Floc model. The source slope *m* represents the property of the source material; the roll off diameter *dhat* reflects the largest grain size in suspension; the floc limit *df* represents the particle diameter whose flux to the bed as single grains and as flocs is equal; finally, the floc fraction *Kf* represents the mass fraction of floc-deposited mud to the bed. The model assumes a single source of material and no re-suspension (Curran et al., 2004).

RESULTS and DISCUSSION

The purpose of this research was to examine the variables affecting sediment transport and deposition over a range of tidal and meteorological conditions and how these processes differ between sheltered and exposed intertidal environments. From August 2009 to September 2011, a total of 73 tides were sampled over a range of spring to neap tidal cycles (Appendix A). Complete data sets (all instruments and traps function with the exception of the ISCO sampler) were collected for 40 of these tides. The most common reason for incomplete data sets was rain which prevented trap deployment or contaminated the filters. Others included programming errors, dangerous field conditions (e.g. hurricane) or instrument malfunction. Fortunately hydrodynamic measurements are available for 67 of the tides and will provide a solid contribution to hydrodynamic model validation. A total of 624 sediment deposition and 431 suspended sediment samples were collected with almost a third of these being processed for grain size (Table 2). In addition, data were collected during a full range of natural variability in non-ice meteorological conditions. Data collected during these experiments represent the most comprehensive empirical data set ever collected within intertidal ecosystems in the Bay of Fundy.

Type of Data	2009	2010	2011
Date range	Aug 5 – Sept 26	June 25 – Sept 11	Jun 1 – Sept 2
Ecosystem	Creek thalweg & un-vegetated bank	Mudflat – low marsh	Creek, vegetated bank & high marsh
Depth range @ ADCP	2.8 – 5.2 m	3.5 – 6.5 m	3.5 – 5.6 m
# tides (# successful*)	18 (16)	36 (17)	19 (7)
# tides with ADCP	16	34	17
# tides with ADV & OBS	16	36	19 bank, 14 marsh
Total # traps x # tides	180	360	84
ISCO samples (# x tides)	118	128	185
Primary student thesis	Casey O'Laughlin (MSc Applied Science)		Emma Poirier (Honours Environnemental Sci.)
Notable storms	Hurricane Bill (Cat 1)	Hurricane Earl (Cat 1)	none

Table 2: Summary of data collected during experiments during the summer months from 2009 to 2011.

This section of the report will first present and discuss hydrodynamic and sedimentary processes associated with the sheltered salt marsh and tidal creek environment at Starrs Point followed by a comparison with Kingsport.   It will conclude with an examination of the implications of these findings for our understanding of the potential far-field environmental effects of potential tidal power development.

Hydrodynamics and Sediment Transport

Hydrodynamics and sediment transport processes are significantly influenced by tidal stage in relation to surrounding intertidal topography. This is particularly evident within the sheltered salt marsh tidal creek system at Starrs Point.   The drainage basin of the studied creek has a total volume of approximately 9,800 m³ and a submerged area over 13,800 m² at the mean bankfull level (4.5 m). Channel morphology can be quantified by the tidal asymmetry factor (γ), which considers changes in surface area as a function of water level to determine if a given channel has stronger flood or ebb currents, given by:

$$\gamma = \delta \, \frac{\Delta h}{\bar{h}} - \frac{\Delta b}{\bar{b}}$$

<div align="right">Equation (1)</div>

where $\bar{h}$ and $\bar{b}$ represent average channel depth and embayment width, and Δh and Δb describe the amplitude of depth and width variation over a tidal cycle. Flood or ebb dominance is demonstrated when $\gamma \geq$ or ≤ 0, respectively (Friedrichs and Perry, 2001; Blanton *et al.*, 2002). Equation (1) describes the study creek as flood dominant, which is typical for macrotidal channels with relatively high equilibrium marsh (Friedrichs and Perry, 2001). However, tides that exceeded the bankfull level showed notable ebb-dominance during initial ebb phases and as water depth in the creek fell below bankfull. A broad range of maximum tidal amplitudes (2.7 to 5.7 m) were considered for this study. Tides were categorized by water depth, into two groups: over-marsh tides (amplitude > 4.5 m & tidal prism > 9800 m³) and channel-restricted tides (amplitude < 4.5 meters & tidal prism < 9800 m³) (Figure 18). This division was based primarily on the visual appearance of these data when plotted as stage curves (Figure 19) (Allen, 2000). Over-marsh tides are therefore defined as those which fully inundate the high marsh surface, while channel-restricted tides do not surpass the general bankfull level and remain confined to the creek network.
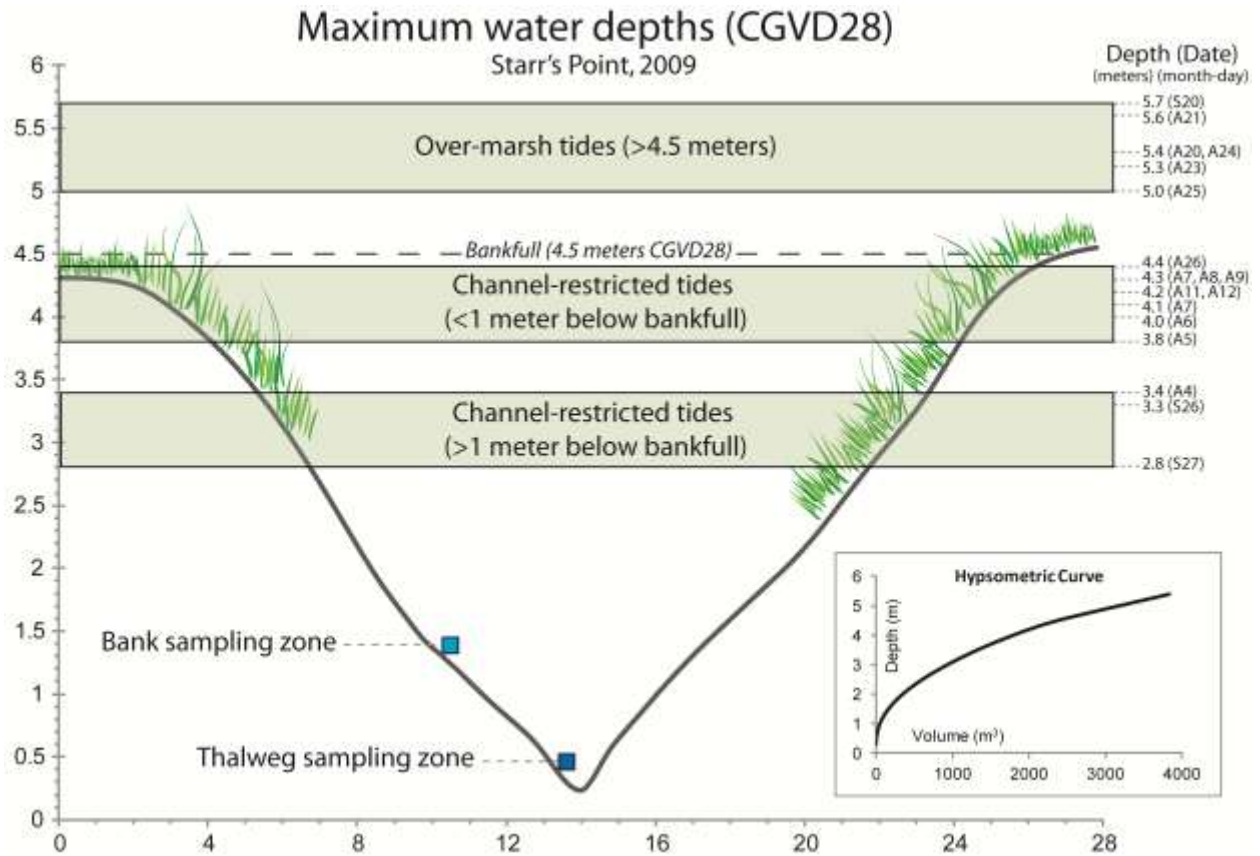
Figure 18: Tides were separated into two dominant groups: over-marsh and channel-restricted. Channel- restricted tides may be further separated into zones relative to bankfull. Y axis represents elevation relative to CGVD28 vertical datum.
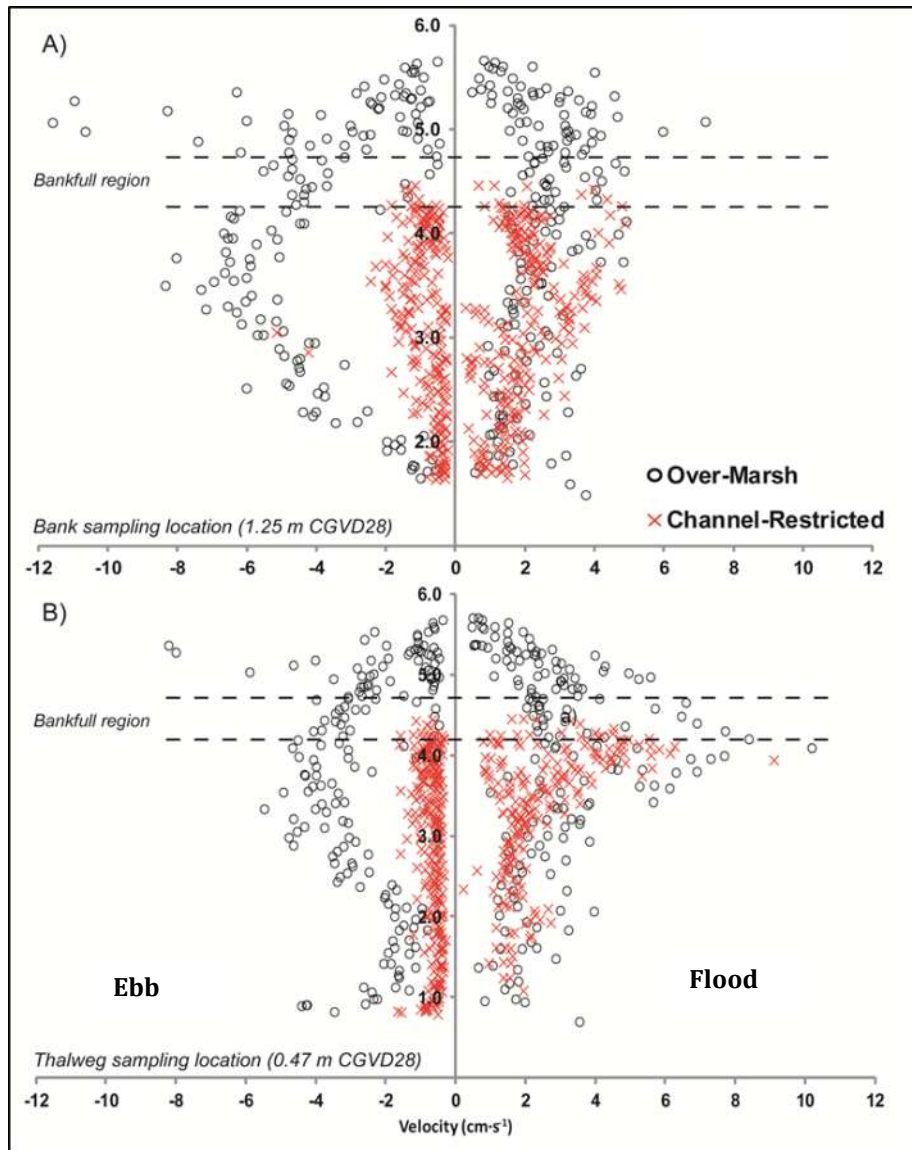
Figure 19: Stage-velocity curves for ADVs located in the thalweg and creek bank in 2009.

Stage-velocity plots indicate that surpassing the creek bankfull level at Starrs Point is a primary control on flow velocity and turbulence, especially during ebb phases. A series of morphological stages control flow as tidal water enters the creek. The tidal bore at this location is slight, and initial flood velocities are low ($0.5 - 3$ cm·s^{-1}). Tidal flow moves into the creek gradually and is detained at the creek head, while filling continues until water depth reaches ~2.0 meters above datum. Above this elevation, tidal flow is allowed access to the incised ditch which extends into the high marsh beyond the creek head, and a slight increase in flow velocity (up to 5 cm·s^{-1}) was found to occur at this stage. Above the bankfull level, over-marsh flows develop marked increases in velocity ($5 - 12$ cm·s^{-1}) (Figure 19).

Wave development during the sampling period was minor, where storm and non-storm conditions failed to produce waves greater than a few centimeters in height. Minor increases in flow velocity are seen during final ebb stages, associated with gravity-driven drainage of the marsh surface (Figure 20).

Figure 20: Upstream end of tidal creek at Starrs Point in 2011. Note presence of small waterfall at head of creek.
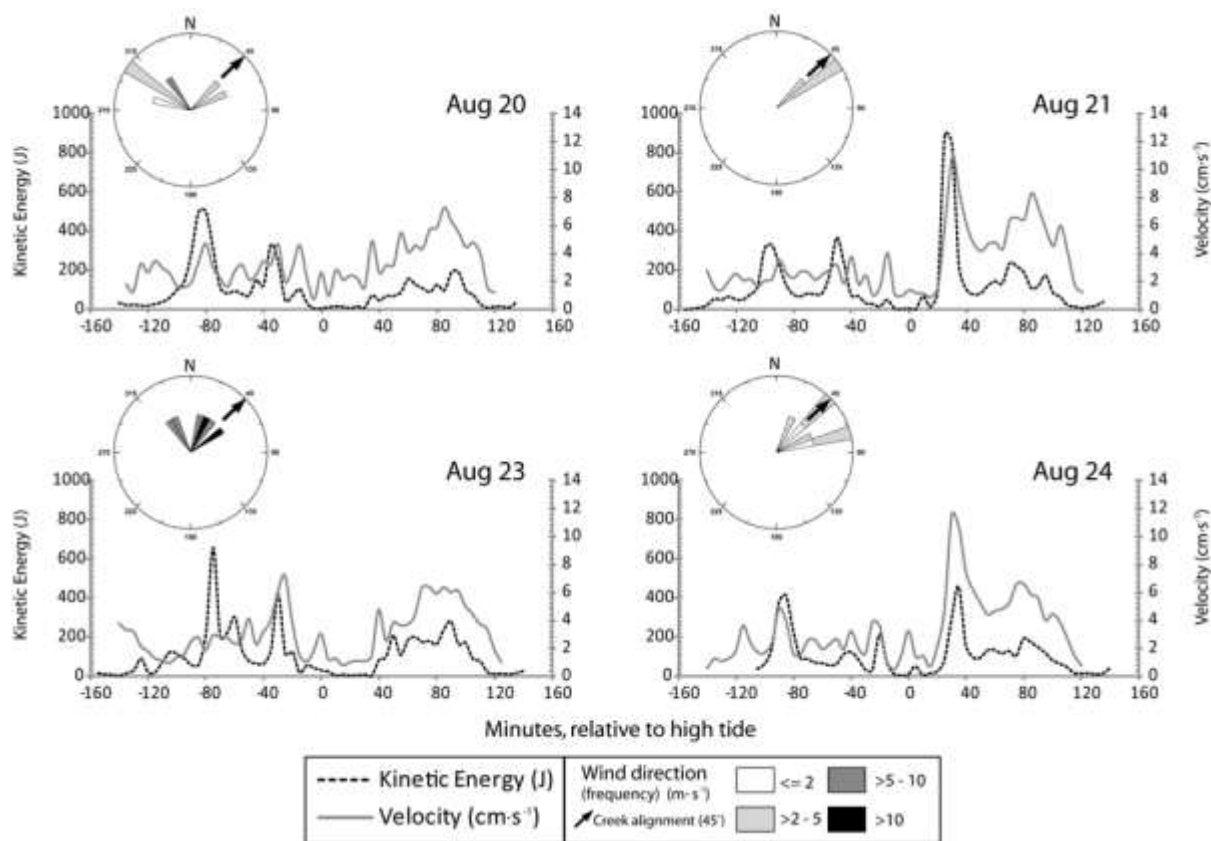
Figure 21: Variation in resolved velocity and kinetic energy during overmarsh tides at Starrs Point in 2009. Hurricane Bill passed through on Aug 23.

Velocity measurements demonstrate that over-marsh tides (> 4.5 m CGVD28) typically generate higher current velocities and greater estimates of TKE. The highest mean flow velocities (10 - 12 cm·s^{-1}) occurred during the early ebb stages of two over-marsh tides, while the marsh surface was well submerged (Figure 19). These enhanced flows may be linked to wind alignment with the channel at high tide (Figure 21). Other tides of comparable depth showed notably lower flow velocity during this stage. Interestingly, the increased wind speed associated with the passage of Hurricane Bill on August 23, 2009 did not produce higher velocities within the channel, likely due to the fact that these winds blew across (perpendicular to) the channel (Figure 21).

Peak flood tide velocity (9 – 10 cm·s^{-1}) on over-marsh tides occurred between 3.5 and 4.1 meters, just below the bankfull level, while the channel was full and at its widest and before flow spread over the marsh surface. Flow velocity decreased markedly above the bankfull level, and slack tide velocities (2 – 5 cm·s^{-1}) persist until early ebb stages. Velocity typically increased as water depth fell below bankfull and flow became channelized, and reached typical peak ebb flows of 5 – 8 cm·s^{-1}. The remainder of over-marsh tidal cycles was

consistently characterized by velocity decreasing to low values (0.5 – 1.5 cm·s^{-1}) and late ebb drainage, which was regularly measured at the thalweg position (Figure 19).
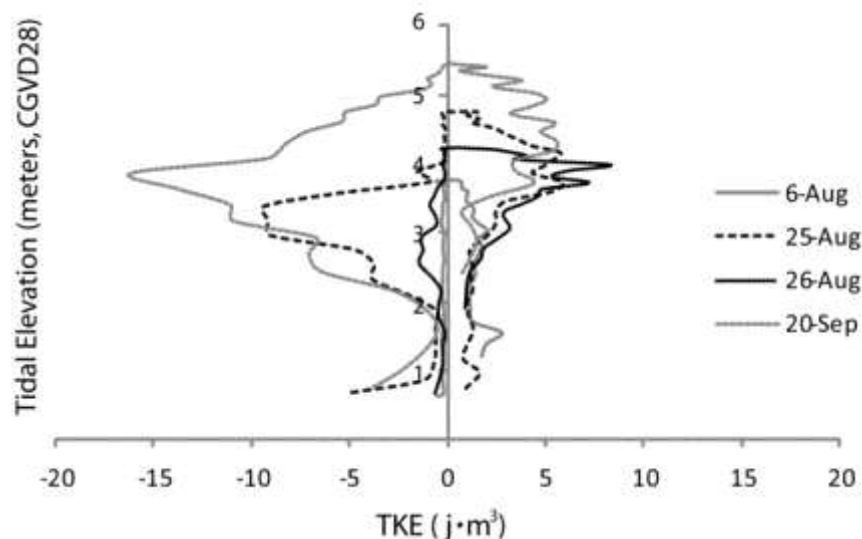
Figure 22: Turbulent kinetic energy stage curve for representative tides at

Channel-restricted tides displayed a strong tendency towards flood dominant velocity at both measurement locations. Velocity consistently increased with depth during flood stages, typically reaching peak velocities of 5 – 7 cm·s^{-1} just prior to high tide (Figure 19). The highest velocity associated with channel-restricted tides (9.1 cm·s^{-1}) occurred at the thalweg position on August 26, associated with a peak water depth in the tidal creek of ~4.4 meters, which is near the bankfull level. Ebb stages of channel-restricted tides consistently generated the lowest velocities (0.1 - 2 cm·s^{-1}) measured at this site, which remained nearly constant except for gravity-driven acceleration during final ebb. These slowly flowing ebb stages showed very low values (< 1) of velocity (cm·s^{-1}), TKE (J·m^{-3}), and KE (J), compared with the preceding flood stages.

As with velocity, higher estimates of TKE are associated with greater tidal prism, resulting in generally ebb-dominant TKE during over-marsh tides. Increase in TKE around the bankfull level with rising flood tide is consistently observed, although peak values of TKE (up to 1.5 j·m^{-3}) occurred during ebb stages of over-marsh tides, as flow is re-channelized and the marsh surface is emptied (Figure 22). Thalweg values of TKE are near-zero (0.01 – 0.1 j·m^{-3}) for the majority of ebb-stage flow during channel-restricted tides, compared with slightly greater flood values (0.1 – 0.8 j·m^{-3}). Kinetic energy (KE) in the tidal creek was slightly higher during flood stages of over-marsh tides, compared with similar stages of channel-restricted tides. Over-marsh ebb stages showed KE up to a magnitude greater than that noted during channel-restricted ebbs (Figure 22). Peak values of KE (90 – 118 J) are associated with tides that peaked near the bankfull level (e.g. Aug 25 & 26); maximum values occurred prior to high tide in these cases, and was seen to reduce dramatically with the onset of ebb tide. Early ebb phases of some over-marsh tides (e.g. Aug 21 & 24) showed

high KE with water depth above bankfull (4.8 – 5.1 m). Estimates of bed shear stress (τ_0) were higher for over-marsh tides (up to 0.4 N·m^{-2}), and achieved maximum with water depth near the bankfull level before and after slack tide, and during ebb drainage below bankfull. Channel-restricted tides show low bed shear stresses (< 0.08 N·m^{-2}) for the duration of all tidal stages, although a marginal flood dominance can be identified.

Resolved velocities and TKE values measured at the marsh plots in 2011 were significantly different between plots but not between tides. As expected, velocities were lower in the vegetated canopy (max 3-5 cm·s^{-1}) when compared to the tidal creek at both thalweg and bank locations (max 8-10 cm·s^{-1}). The marsh platform is generally covered with water up to a depth of approximately 1.5 m, this compares to 5.5 m in the creek. Velocity and TKE are clearly ebb dominant at all marsh stations, most noticeably at M1 furthest on the marsh platform. This agrees with other studies on marsh hydrodynamics (e.g. French and Stoddard, 1992; Friedrichs and Perry, 2001). In general, the highest velocities were recorded on the highest tides with the exception of station M3 on the vegetated creek bank (Figure 23). At that station, the highest velocities were recorded for tides near bankfull level.

The exposed Kingsport site share similarities in hydrodynamic processes with the sheltered Starrs Point system yet also differences. In order to try and isolate the effects of local topography (e.g. presence of marsh cliff, sloping marsh platform Figure 24), tides were examined which displayed conditions as close to 'calm' as possible (Figure 25). It was thought that the larger marsh cliff (2.1 m in height, approximately 5.8 m CGVD28) to the east (Figure 10) would act as a topographic threshold. In general, velocities at all three marsh stations were less than 3 cm·s^{-2} with the exception of June 28th (5.8 m CGVD28) that recorded flood tide velocities up to 8 cm·s^{-1} at the uppermost station V1 (Figure 24) and to a lesser extent (max 6 cm·s^{-2}) at V2 and V3 (Figure 24, Figure 25). Although it is one of the lowest tides, comparable tides of June 29 and June 28 do not exhibit the same patterns (Figure 25). The lowest velocities were experienced during the central portion of the tide which is not surprising given the low relative position within the water column. There is no clear effect of the larger marsh cliff.
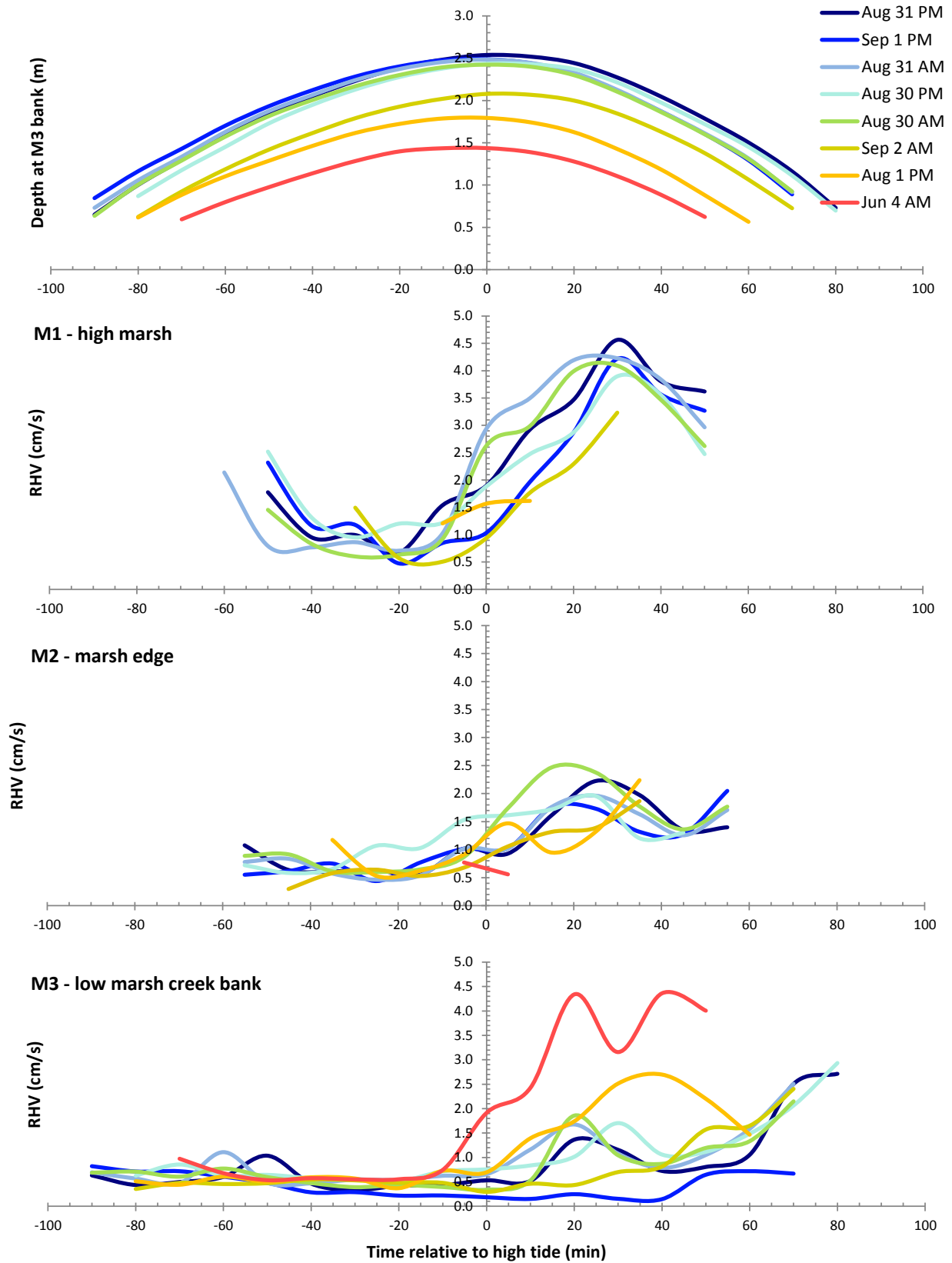
Figure 23: Water depth at M3 and resolved horizontal velocities at M1, M2 and M3 at Starrs Point in 2011.
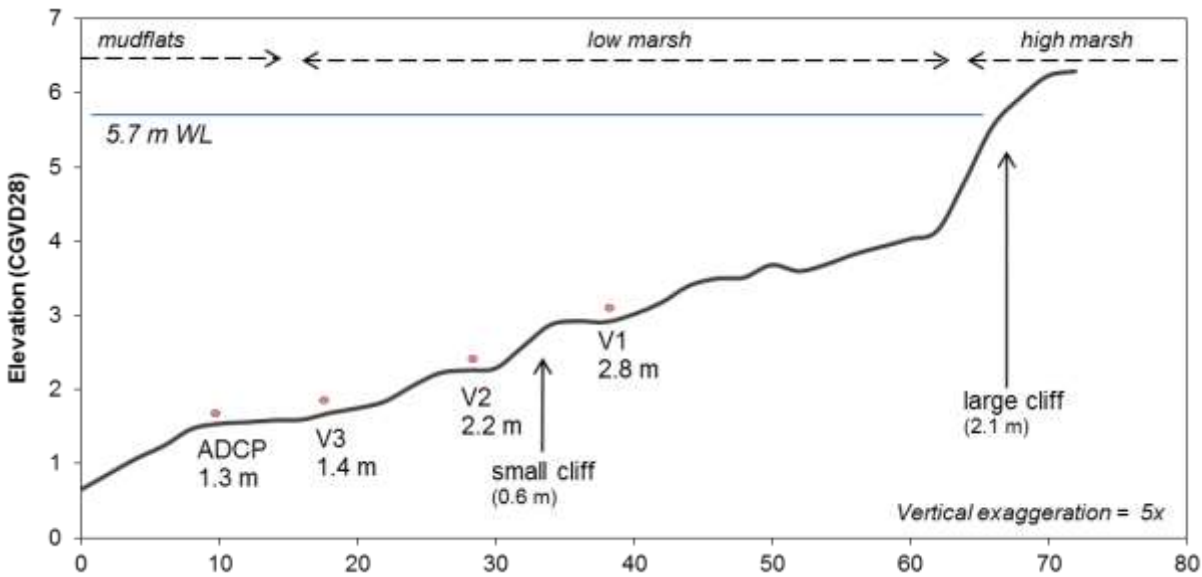
Figure 24: Cross sectional profile of Kingsport experimental transect in 2010.

In order to examine the potential influence of wind and waves on current velocity, tides were isolated that had a minimum hourly average wind speed of 4 m·s^{-1} (Table 4). It should be noted that the meteorological station was located on the dyke at Starrs Point and therefore may not entirely represent the absolute wind speed at Kingsport. The highest wind speeds were recorded during Hurricane Earl and this resulted in the highest velocities recorded (6-8 cm·s^{-1}) at stations V1 and V3 throughout the tide (Figure 26). No data are available for V2 due to instrument malfunction. The only other tide that demonstrated a similar pattern was on August 5th with a relatively low wind speed of 3.1 m·s^{-1} and one of the lowest tidal heights of the season (Table 4). The resolved velocity was maintained at around 4 cm·s^{-1} at V1 (Figure 26). Interestingly the evening tide on Sept 4 did not show corresponding increased flow velocities which are likely associated with a shift in wind direction from 101.9^0 (onshore) relative to North to 271.5^0 N (offshore). The remainder of the tides generally stayed below 2 cm·s^{-1} for the majority of the tide with the exception of the first and last 30-40 minutes of the tide where velocities increase to up to 4-5 cm·s^{-1} in water depths less than 2 m (Figure 26).
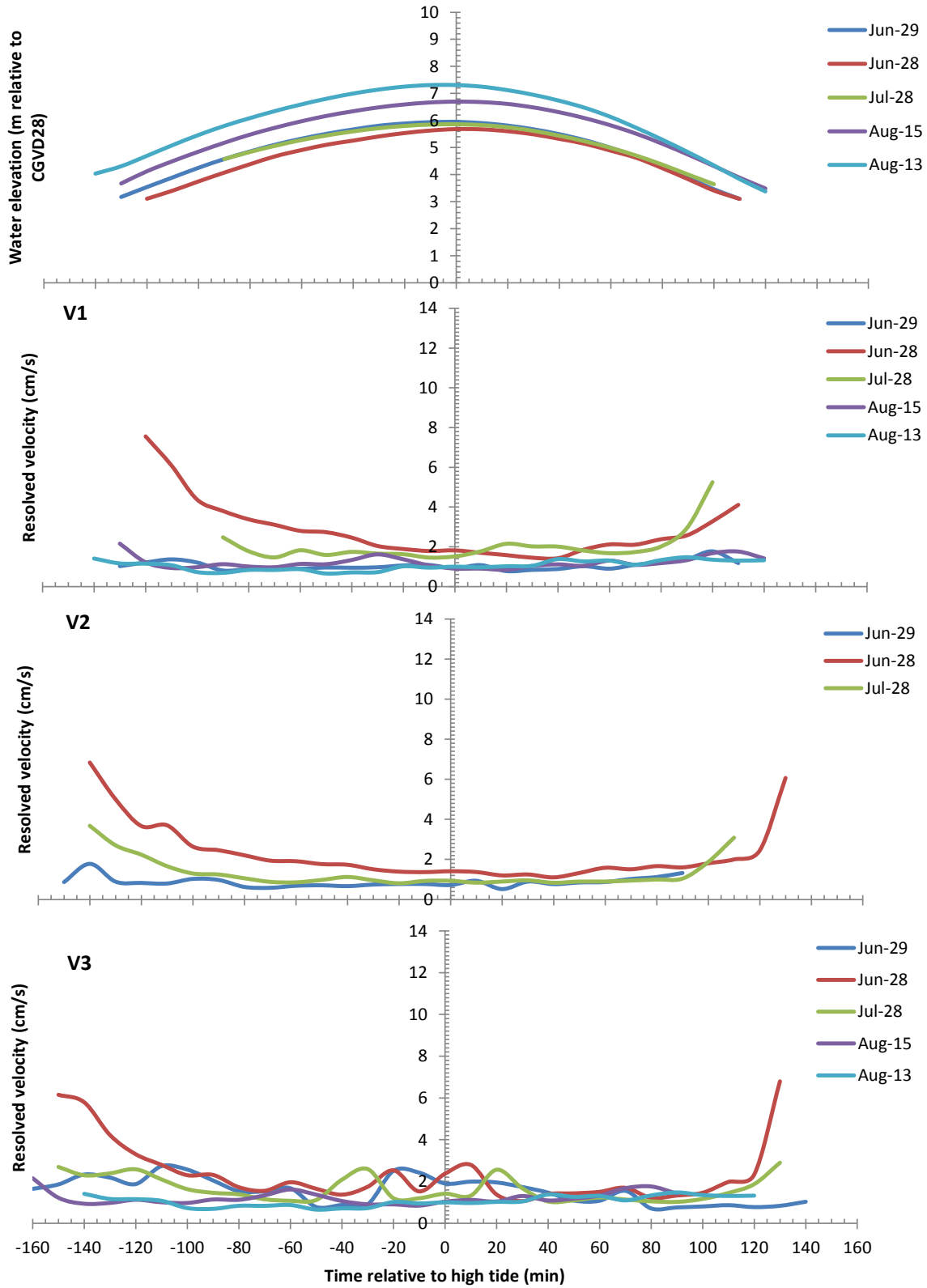
Figure 25: Water depth relative to datum and resolved velocity at marsh stations at Kingsport during 'calm' or low wave (less than 1 m/s wind speed) conditions in 2010.
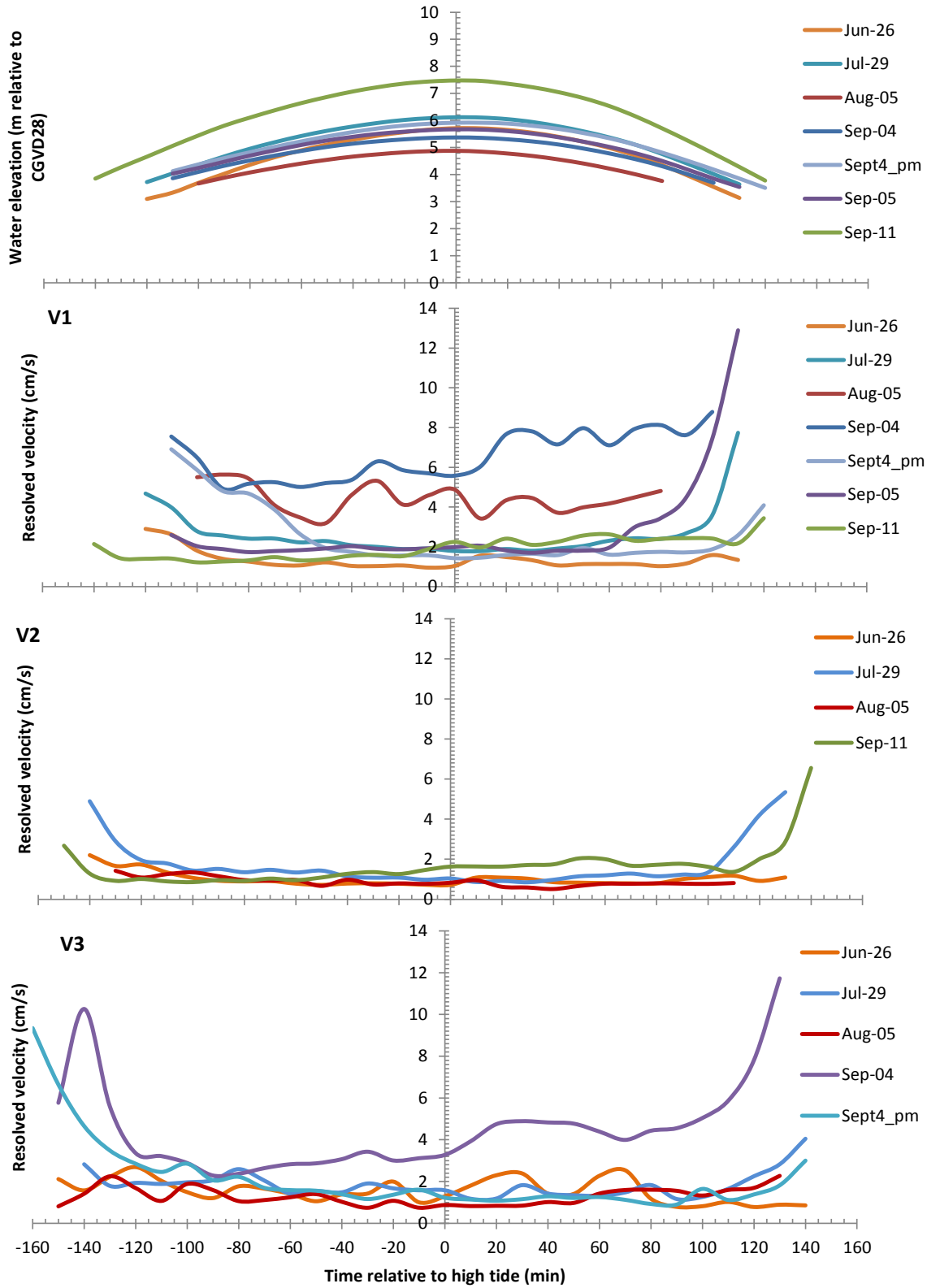
Figure 26: Tidal elevation and resolved velocity for marsh stations when wind speeds are generally greater than 4.0 m/s on June 25am (4.6 m/s), June 26 (4.6 m/s), July 29 (4.4 m/s), Aug 5 (3.1 m/s), Sept 4 am (Hurricane Earl 7.1 m/s), Sept 4 pm (6.8 m/s), Sept 5 (5.5 m/s) and Sept 11 (5.4 m/s) 2010.

Suspended Sediment Concentration

The variability in suspended sediment concentration was examined using the OBS records, ISCO water samples and the rising stage bottles where available. Major differences were observed between the sheltered Starrs Point site and Kingsport.

At Starrs Point in 2009, over-marsh tides generally showed higher suspended sediment concentration (SSC) compared with channel-restricted tides (Figure 27), most notably during early- to mid-ebb stages. Overall, a broad range of concentrations were reported by OBS sensors (1 - 1000 mg·l^{-1}) in the tidal creek under non-storm conditions. Maximum initial suspended concentrations (2000 - 3000 mg·l^{-1}) were measured ahead of Hurricane Bill (Aug 23rd, 2009), in response to periods of rain that occurred prior to the rising tide, increasing the potential for mobilization of exposed sediments on mudflats and creek banks. Regardless of varying maximum water depth, suspended concentration during flood phases of both channel-restricted and over-marsh tides is similar, showing a gradual reduction from moderate initial values (100 – 300 mg·l^{-1}) to a stabilized low concentration (~50 mg·l^{-1}). Stable concentrations around this level were noted at both thalweg and bank sampling locations, and persisted through high water and ebb stages on channel-restricted tides. Final ebbs of all tides were characterized by increasing concentration (up to 700 mg·l^{-1}); in many cases this is when peak per-tide concentrations occurred, associated with increased flow velocity via gravity-driven drainage. In addition, ebb phases of over-marsh tides brought about episodic, rapid increases to high concentration (600 – 1000 mg·l^{-1}) at only the thalweg location. Such increases occurred much earlier than increases associated with final ebb stages, and are linked to brief periods of flow acceleration with depth near the bankfull level. These rapid increases in concentration were not measured by the bank array. Periodic increases in bed shear stress appear to also lead to increased concentrations of suspended sediment (Figure 28) on the ebb tide. The maximum suspended sediment concentration measured during the study period occurred in close proximity to the passing of Hurricane Bill on August 23, 2009: at the thalweg, initial SSC was ~3500 mg·l^{-1}, and reached 2000 mg·l^{-1} during late ebb stages. Along with these high flood and ebb values, the stabilized, high water concentration (~100 mg·l^{-1}) was twice that of tides with similar depth and under non-storm conditions (~50 mg·l^{-1}). Moderate storm conditions were measured at the study site associated with Bill, including an average wind speed of 15 m·s^{-1}, and 40 millimeters of rain over a 5 hour period, ending just before high tide.

Suspended sediment concentrations measured at Starrs Point in 2011 are comparable to those recorded in 2009. Station M1 on the high marsh platform exhibited the greatest TKE value (0.45 J·m^{-3}) on the falling ebb tide (Figure 31). Corresponding suspended

sediment concentrations averaged around 100 mg·l^{-1} with increases up to approximately 450 mg·l^{-1} on the ebb tide on Sept 1 (Figure 31).
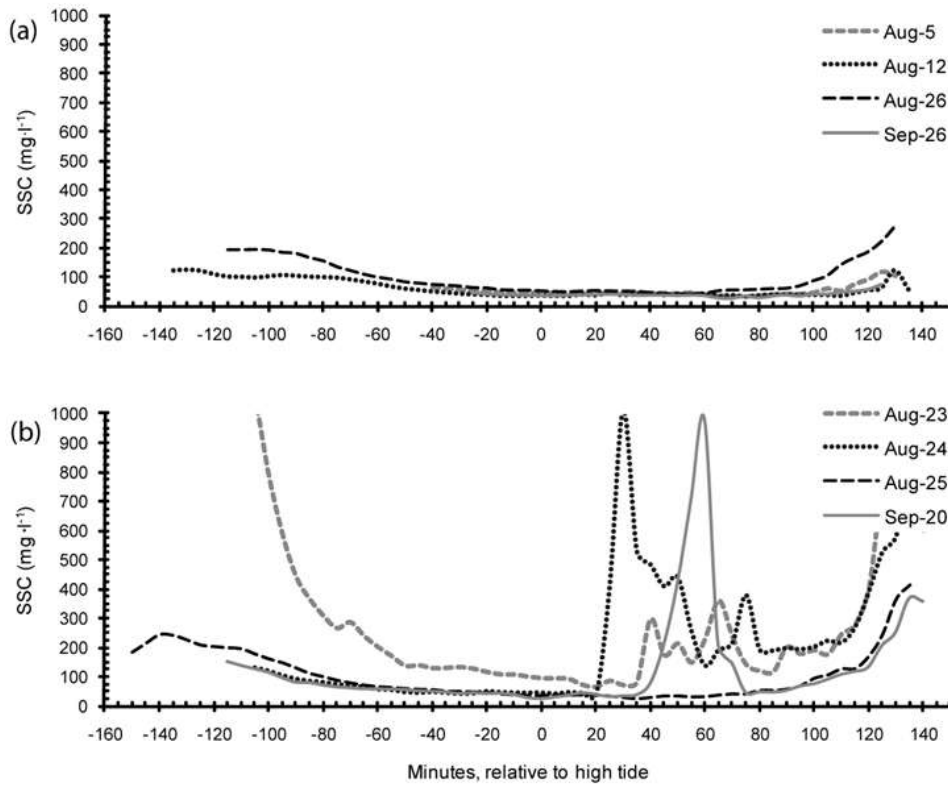
Figure 27: Time-series of suspended sediment concentration measured at the thalweg location, for (a) a series of channel-restricted tides and (b) a series of over-marsh tides. Impacts on the August 23 flood tide are credited to the passage of Hurricane Bill.
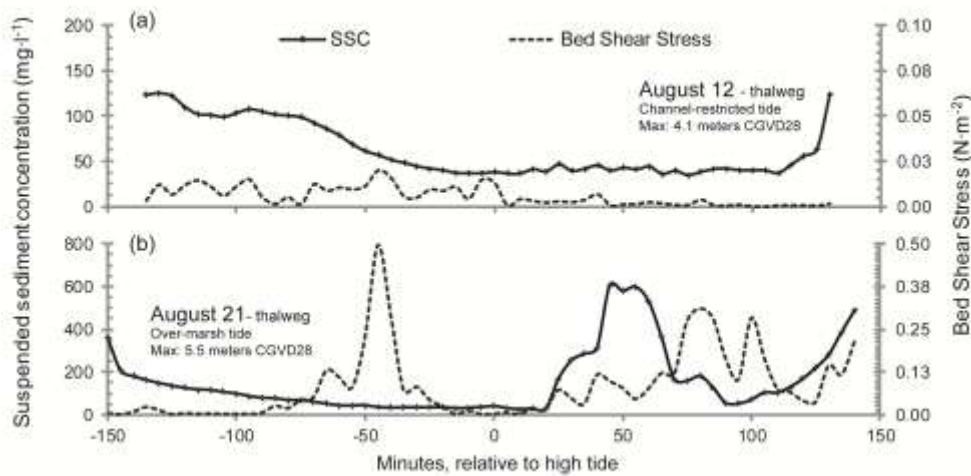
Figure 28: Influence of bed shear stress on suspended sediment concentration at Starrs Point on Aug 12 and Aug 21, 2009.
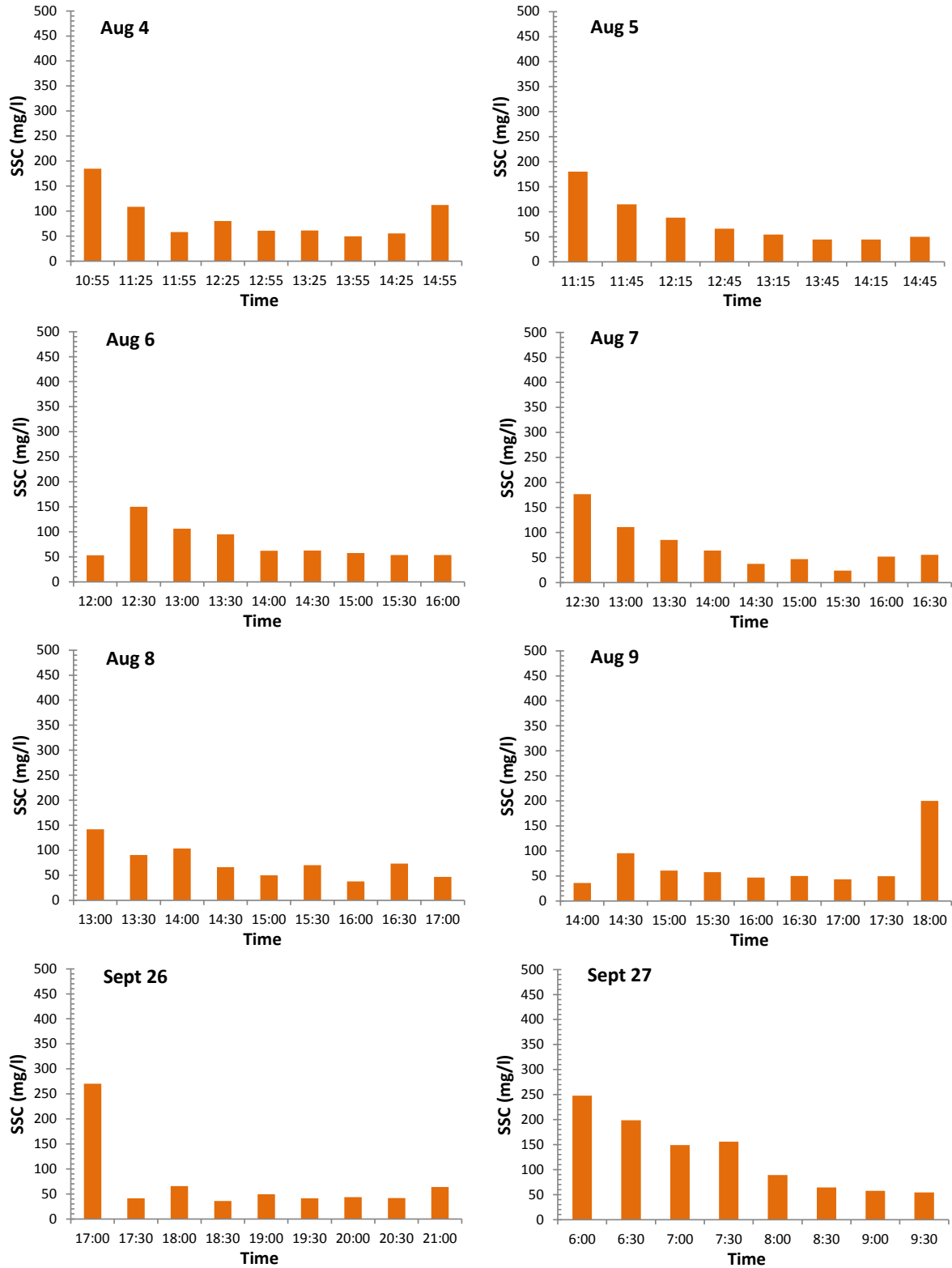
Figure 29: ISCO bottle samples collected during channel restricted tides within the tidal creek at Starrs Point in 2009.
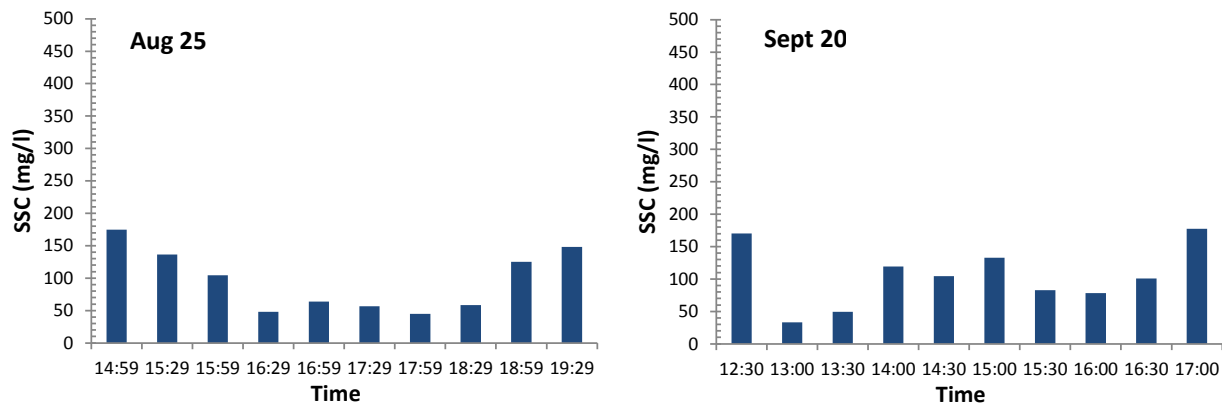
Figure 30: ISCO bottle samples collected during overmarsh tides in 2009. Samples for Aug 12, 20, 21 were lost.

This peak is preceded by a spike in TKE. However this relationship is not observed for any other tide. The TKE values at M2 on the marsh platform edge are lower than at M1, averaging 0.25 $J \cdot m^{-3}$ (Figure 31). Suspended sediment concentrations fluctuate around 250 $mg \cdot l^{-1}$ throughout the tide with highest values on the flood tide (Figure 31). Although there was no notable storm during the experimental period in 2011, smaller meteorological events may have exerted some influence on the amount of sediment in suspension. Increased wind activity and rain at the very end of August may have contributed to higher amounts of sediment in suspension.

The ISCO bottle samples at all four stations in 2011 supports patterns recorded using the OBS. The highest concentrations are recorded on the incoming tidal bore with the highest value (3, 867 $mg \cdot l^{-1}$) on August 1. The morning tides of Aug 30 and 31 recorded initial concentrations of 1,718 and 776 $mg \cdot l^{-1}$ respectively (Figure 32). Concentrations during all other tides did not exceed 400 $mg \cdot l^{-1}$. In most cases, concentrations decreased to around 100 $mg \cdot l^{-1}$ 60 minutes before and after high tide (Figure 32) and then increased during the ebb drainage. The only exceptions were on Aug 30 (pm) where a clear decreasing trend was recorded throughout the tide from around 450 to 75 $mg \cdot l^{-1}$ and on Sept. 2 (Figure 32).

Significant variations in suspended sediment concentration measured by the OBS were observed at Kingsport in 2010. Unfortunately, the wide range from 5 $mg \cdot l^{-1}$ to greater than 5,000 $mg \cdot l^{-1}$ often resulted in oversaturation of the instrument since the OBS used were not autoranging. While there appears to be data that make sense (Figure 35, Figure 36) when individual bursts are decomposed, we do not feel that the data as a whole are reliable enough for detailed analysis. In addition, there may have also been biofouling by vegetative debris or snails during the course of the experiment.
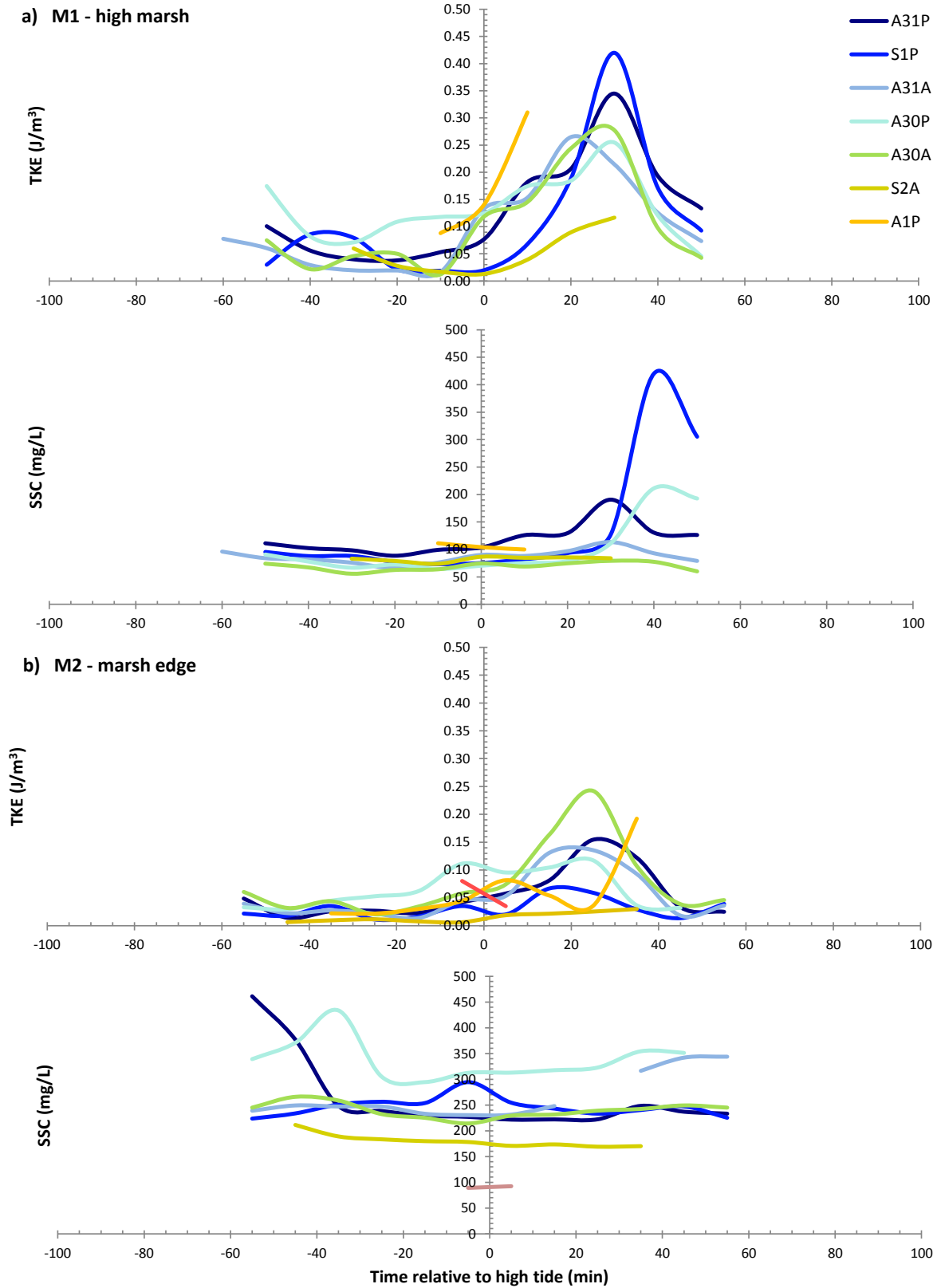
Figure 31: Relationship between turbulent kinetic energy (TKE) and suspended sediment concentration (SSC) measured by the OBS at station a) M1 and b) M2 at Starrs Point in 2011.
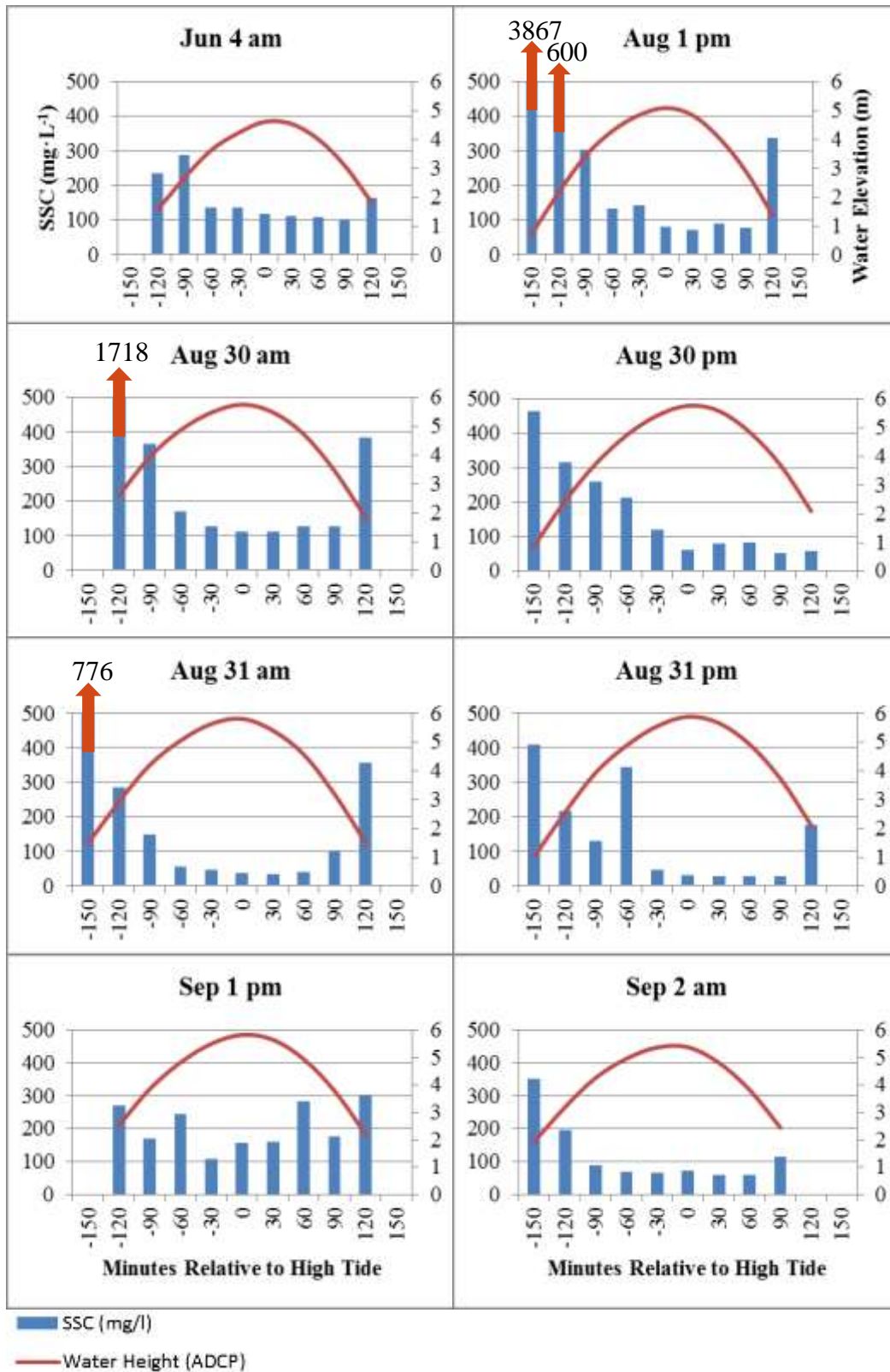
Figure 32: Variation in suspended sediment concentration measured from ISCO bottle samples in the creek at Starrs Point in 2011. Water depth measured by the ADCP.
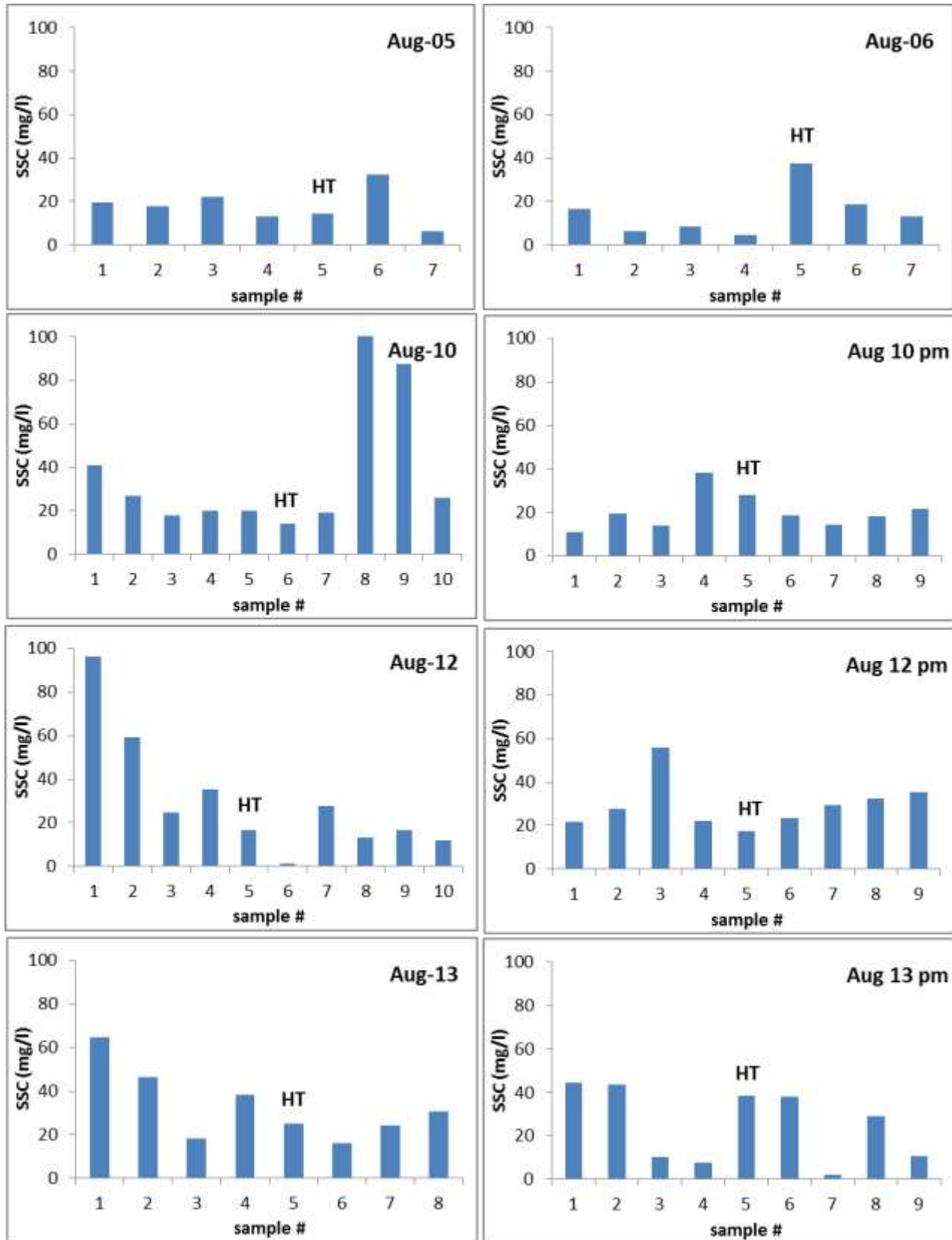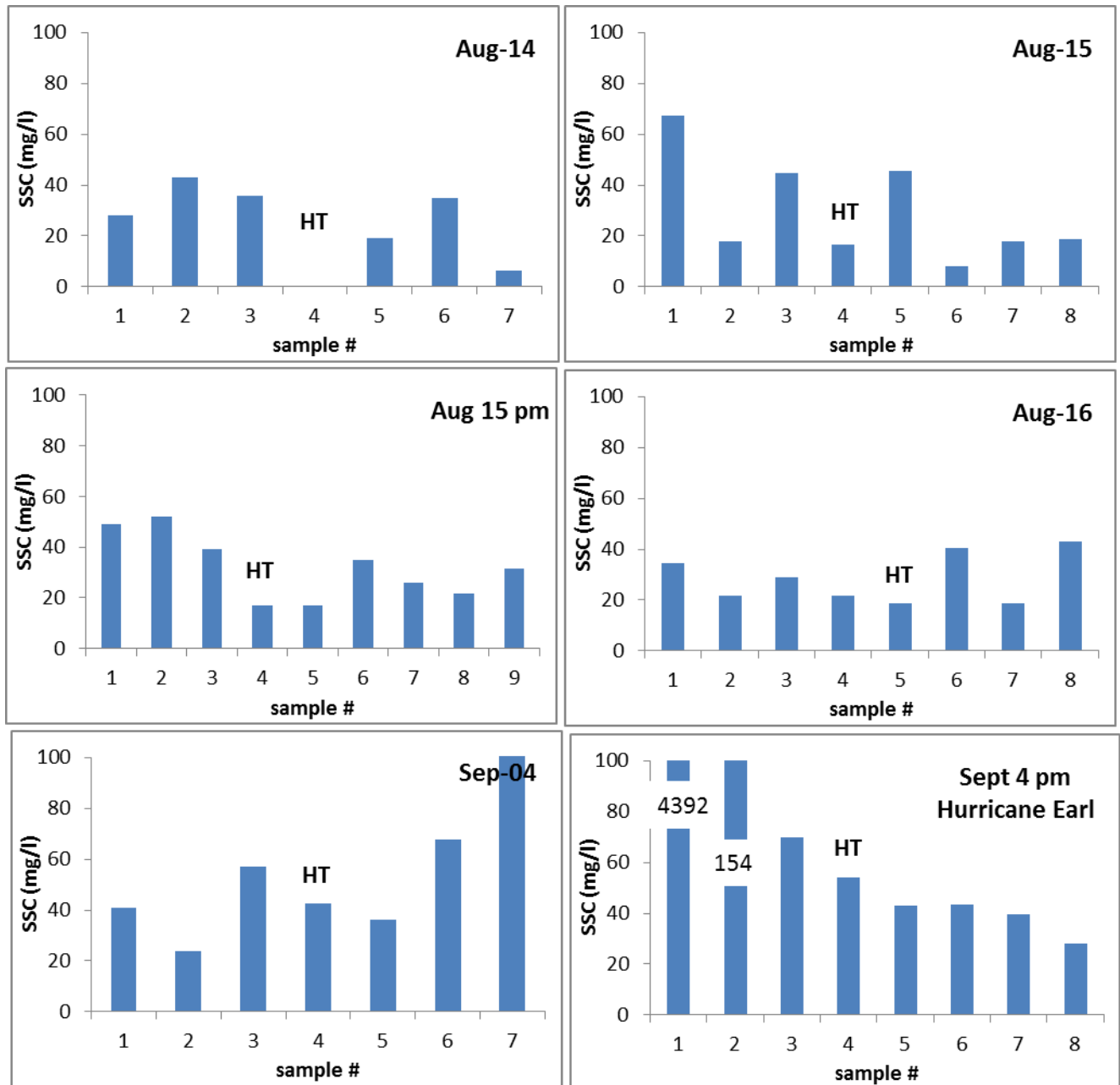
Figure 33: ISCO suspended sediment concentration at 30 minute intervals throughout the tide at Kingsport in 2010. Note difference in y axis scale from Starrs Point.

Despite significant challenges (e.g. tipping due to waves, too great a head elevation, etc..) with the ISCO automated water sampler during the Kingsport 2010 season, the samples collected do support the observation of significantly higher suspended sediment values at Starrs Point than at Kingsport during the initial flood and final ebb portions of the tide (Figure 32, Figure 33). Values during the tide however are similar, remaining less than 100 mg·l^{-1}. The highest value (4392 mg·l^{-1}) was recorded during the initial flood tide on

Sept 4th during Hurricane Earl (Figure 33).   It should be noted that the nozzle intake was located on the marsh surface at V1 during the whole Kingsport deployment.
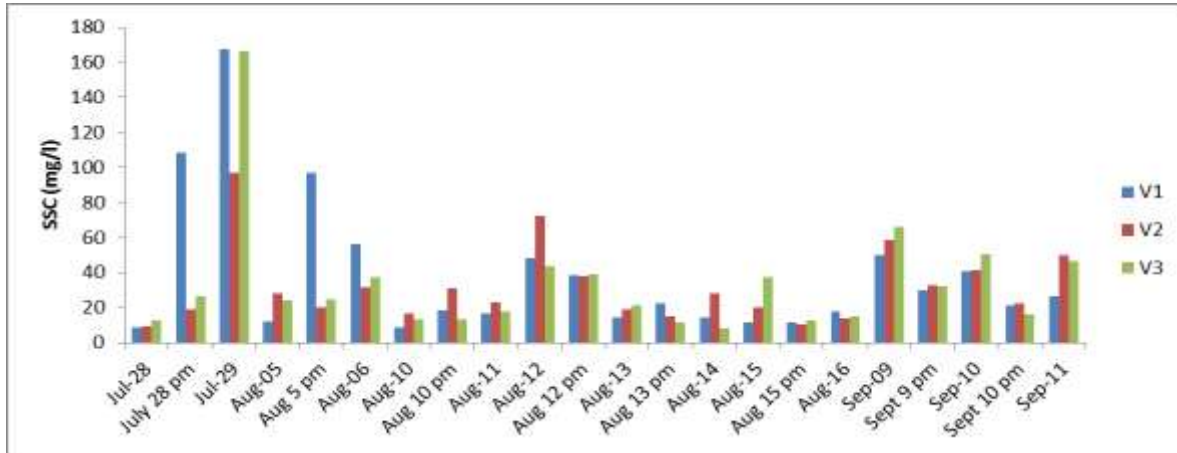
Figure 34: Suspended sediment concentration on flood tide at 15 cm above the bed measured by the rising stage bottle at Kingsport in 2010.   Station V1 is furthest from the mudflat and V3 is at the boundary between marsh and mudflat.
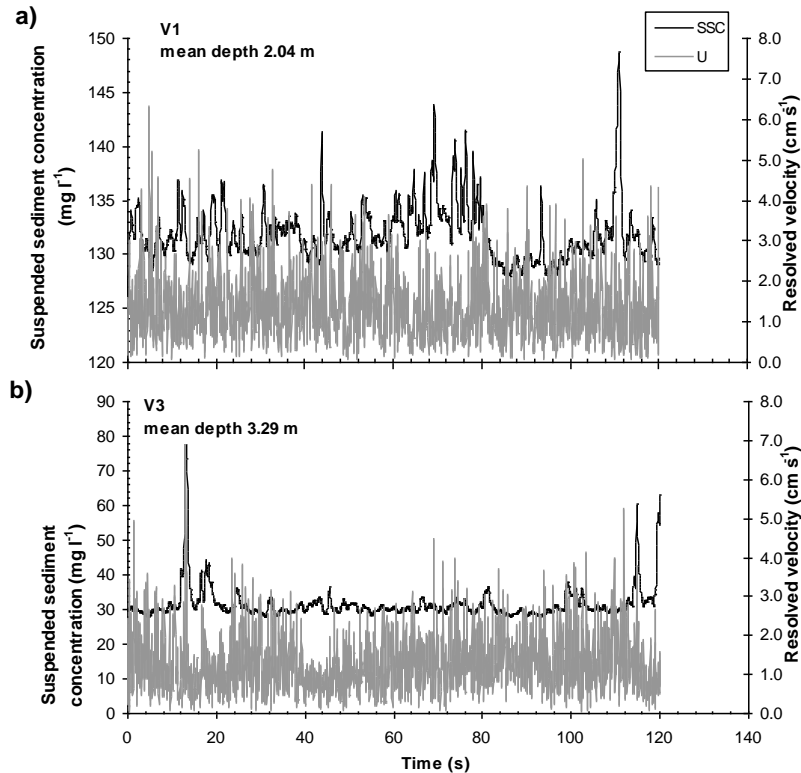
Figure 35: Example of suspended sediment concentration and resolved velocity recorded at a) V1 (top of cliff) and b) V3 (edge of marsh). Data were collected in the morning on August 10, 2010 during calm conditions and a 14.4 m tidal range on the rising tide (-100 minutes before high tide). Maximum water depth at the ADCP was 6.08 m. Note different scales for suspended sediment concentration between locations.

Rising stage bottles were added to each Kingsport station in late July after it was discovered that the OBS record was suspect. Interestingly, the July deployments saw the greatest incoming suspended sediment concentration overall (~160 mg·l^{-1}) (Figure 34). The high values are most noticeable during relatively higher wind conditions (Table 4), particularly at station V1. This station is adjacent to a small marsh cliff that was actively eroding when waves were lapping at it. Visual plumes of sediment were observed throughout the deployment. As the summer progressed, a more consistent pattern of higher concentrations being recorded at mudflat/marsh interface and decreasing further into the marsh surface emerged (Figure 34). This may potentially be attributed to increases in vegetation height.

Fluctuations in acoustic backscatter intensity (e.g. amplitude or signal strength) have been applied to investigate patterns of variability in suspended sediment dynamics, including measurement of size and settling velocities of suspended particles in both laboratory and field settings (e.g. Voulgaris and Meyers, 2004; Hill *et al.*, 2012; Thorne and Hanes, 2002; Fugate and Friedrichs, 2002). While it has been demonstrated that acoustic backscatter can be converted to quantitative estimates of SSC, Hoitink and Hoekstra (2005) describe complications related to unknown influences of flocculation, as well as anomalous scatterers in the water column (e.g. phytoplankton). Kim and Voulgaris (2003) found calibration of such datasets to be most accurate for fine sands, while silt and finer materials generated bias in acoustic measurements. High suspended sediment concentrations were also found to cause measurement inaccuracies due to significant signal attenuation in the water column (Thorne et al., 1993). In consequence, ADCP amplitude data discussed in this study are not quantified, but have been investigated as a relative indicator of SSC, in effort to link dynamics with sediment deposition on the scale of individual tidal cycles (e.g. Hill et al 2012).

The amplitude of the return signal measured by the ADCP shows variability in response to changing amounts of suspended material present in the water column, and is reported by the instrument as a signal strength (represented by 'counts'). As mentioned, amplitude data discussed here remains un-calibrated, and has been applied as an un-quantified, relative indicator of changing suspended sediment concentration. Examples of amplitude plots typical of over-marsh and channel-restricted tides are shown in Figure 37. Plots show that a gradual clearance, or reduction in suspended matter evidenced by decreasing signal strength at a given depth, is identifiable over the course of all tidal cycles measured. Channel-restricted tides in particular show a continuous and steady decrease in suspended content during the entire tidal cycle. This pattern persists until mid-ebb, when signal strength increases in response to the export of material that either remained in suspension for the duration of tidal cycles, or was re-mobilized by increased ebb flows (Figure 37). It is also notable that clearance of the water column (at ~1.5 - 2.0 meters above the bed)

routinely initiates within 10 minutes of high water (Figure 38). Clearance rates describing decreasing signal strength at 170 cm above the bed during the 30-minute period following high tide varied by up to one magnitude (0.02 - 0.2 counts/minute), and achieved maximum in response to channel-restricted tidal cycles. However, rates of change at 50 cm above the bed were higher during most over-marsh tidal cycles (~0.1 counts/minute) compared with that of channel-restricted cycles (~0.03 counts per minute) (Figure 38). This suggests that during the 30-minute period following high tide on channel-restricted tidal cycles, clearance of the mid to upper water column (e.g. 170 cm above the bed) is ongoing, but settling is not initiated nearer the bed (e.g. 50 cm above the bed).
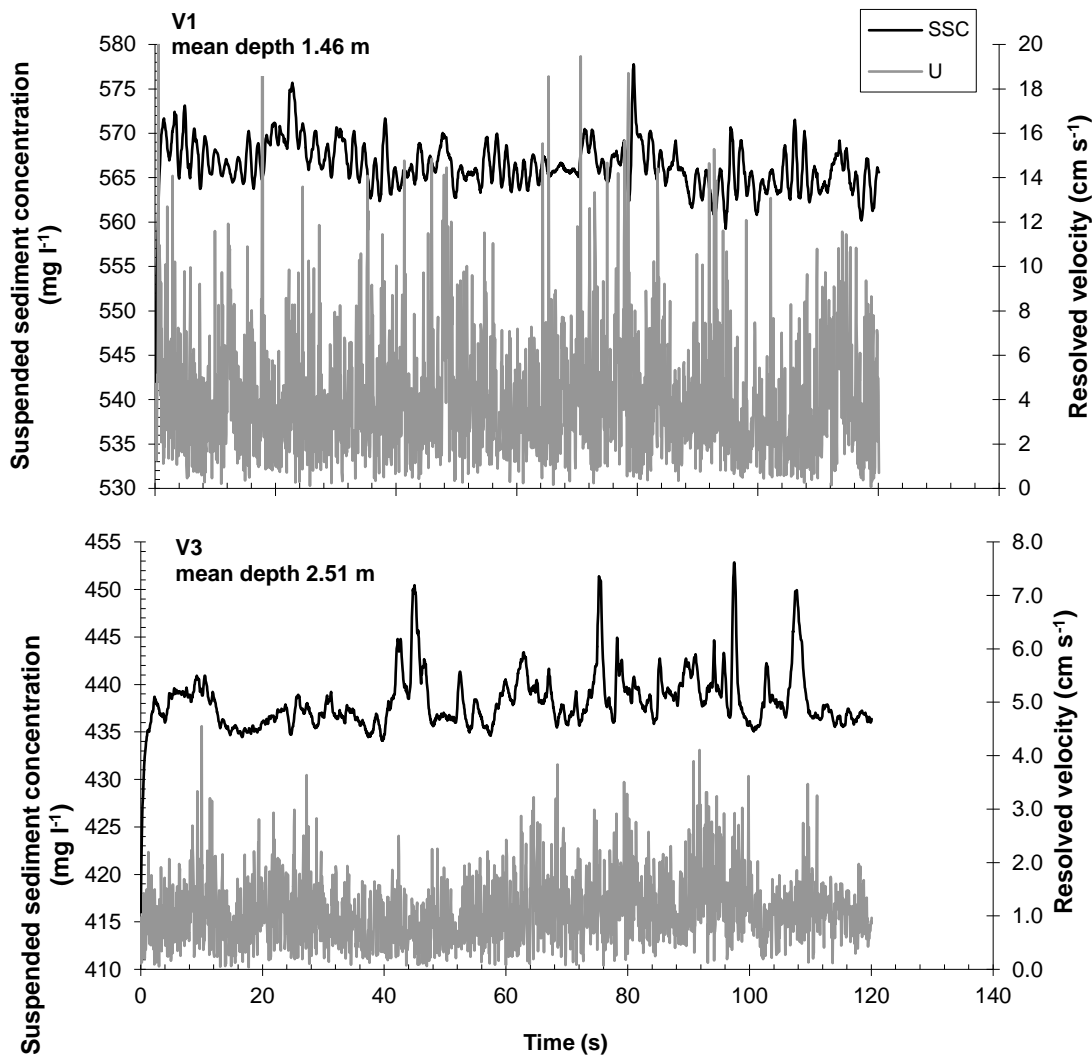
Figure 36: Example of suspended sediment concentration and resolved velocity burst recorded at a) V1 (top of cliff) and b) V3 (edge of marsh). Data were collected on August 5, 2010 with mean hourly wind speeds of 3.1m/s and a 11.8 m tidal range transitional tide , 40 minutes after high tide.

Conversely, over-marsh tides show higher rates of clearance near the bed compared with channel-restricted tides, characterizing variability that is likely related to an increased inundation period associated with over-marsh tidal cycles. This channel clearance was also observed in the ADCP records within the tidal creek in 2011 even at the larger bin resolution (Figure 39). All of acoustic profiles also illustrate re-suspension of sediments during the incoming tidal bore and final ebb drainage.

Examination of the ADCP records at Kingsport does not illustrate any apparent clearing of sediment from the water column. It does how show evidence of wave action, sediment re-suspension and higher velocities after high tide (Figure 41 to Figure 44). This is not evident for the relatively low tide on Aug 5, 2010 (Figure 40). The relatively weak Hurricane Earl passed through the Kingsport area in the morning of Sept 4, creating significant variability in resolved velocity and strong re-suspension at the ADCP (Figure 45). It is unclear however if this signals local re-suspension or increased material suspended in the water column brought in by the tide.
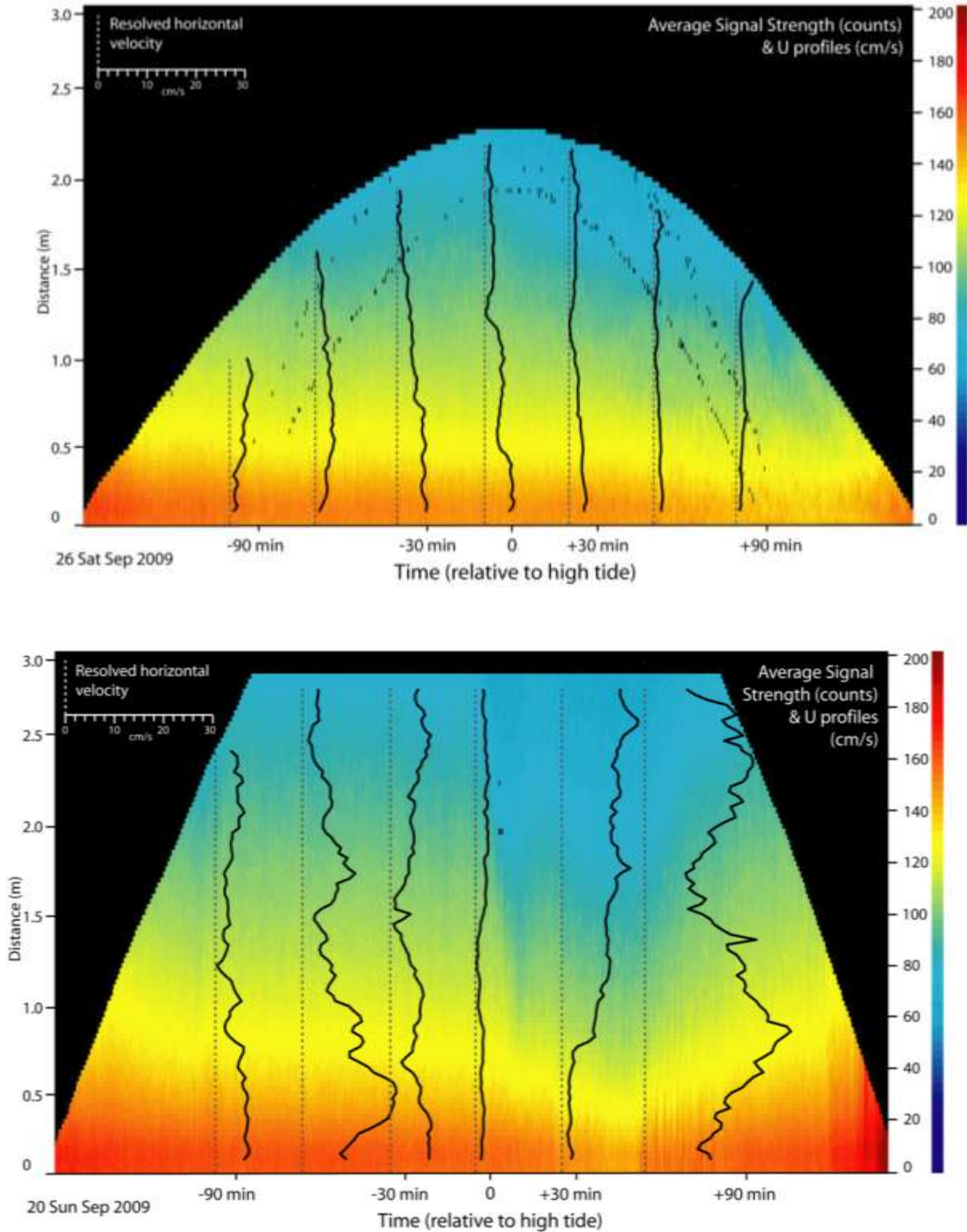
Figure 37: Relative variation in average ADVP signal strength as a proxy for suspended sediment concentration (red = highest concentrations) for a neap tide on Sept 26, 2009 and spring tide on Sept 20, 2009. Velocity profiles are illustrated by the black lines.
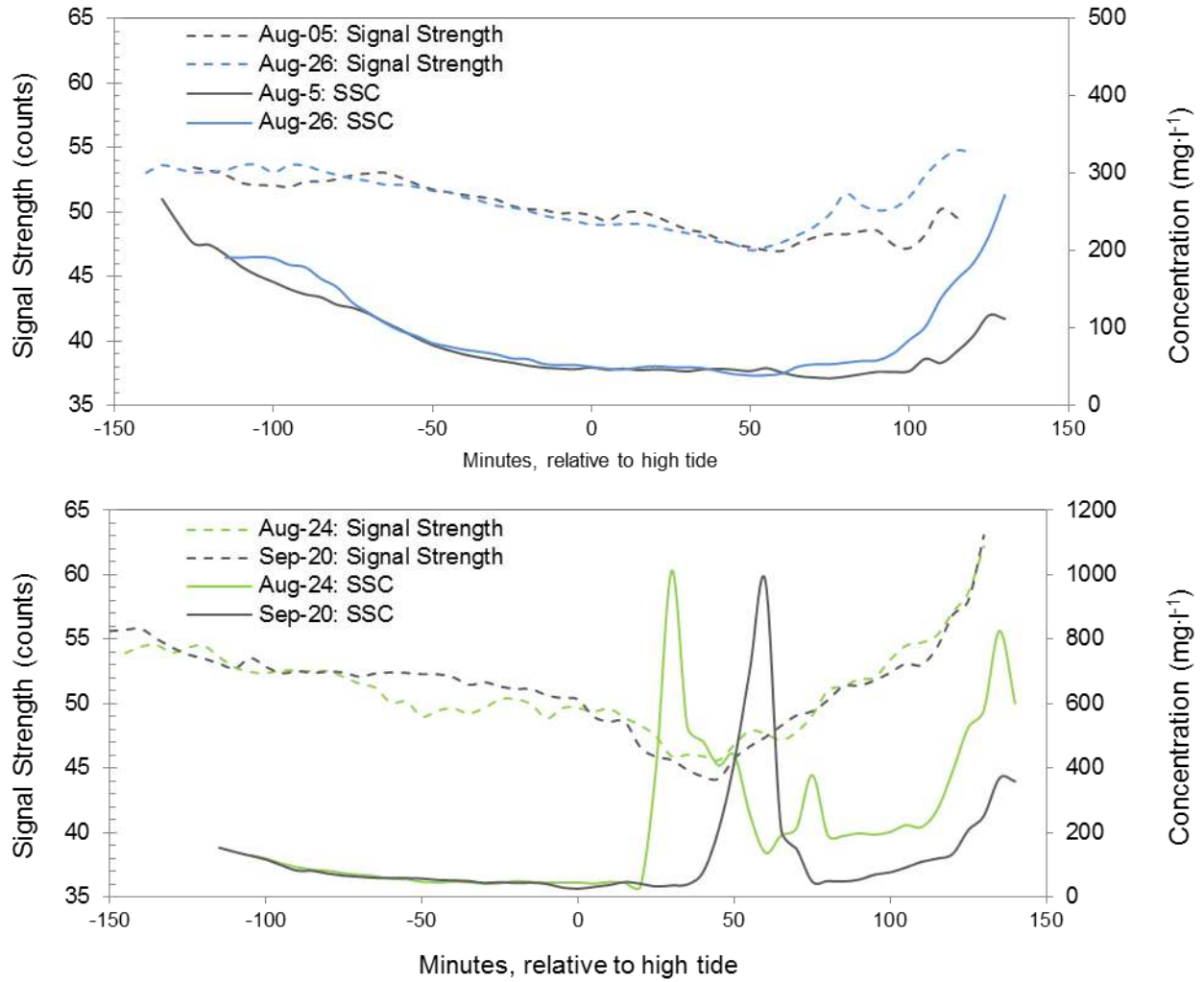
Figure 38: Time series, relative to high tide, of OBS-derived suspended sediment concentration (SSC) (solid lines) and the amplitude of the ADCP return signal (dashed lines) for two tidal cycles. The upper panel shows a channel restricted tide (Aug 6th) while the lower panel shows an over-marsh tide (Sept 20th). Note the variation in y-axis values.
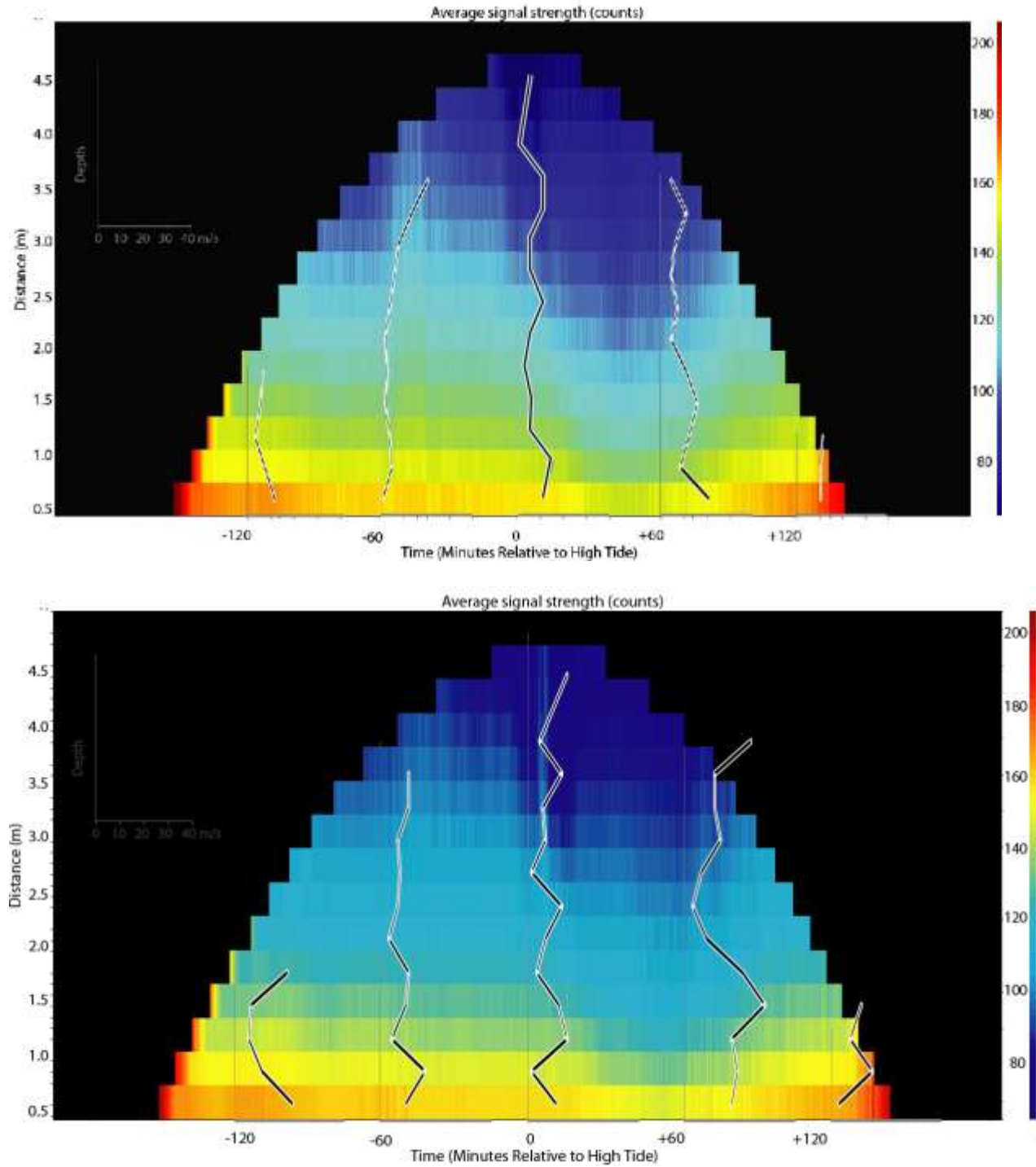
Figure 39: Examples of ADCP backscatter plots for overmarsh tides at Starrs Point on Aug 30 and Sept 2, 2011. Note evidence of potential clearing of suspended sediment approximately 30 minutes after high tide.
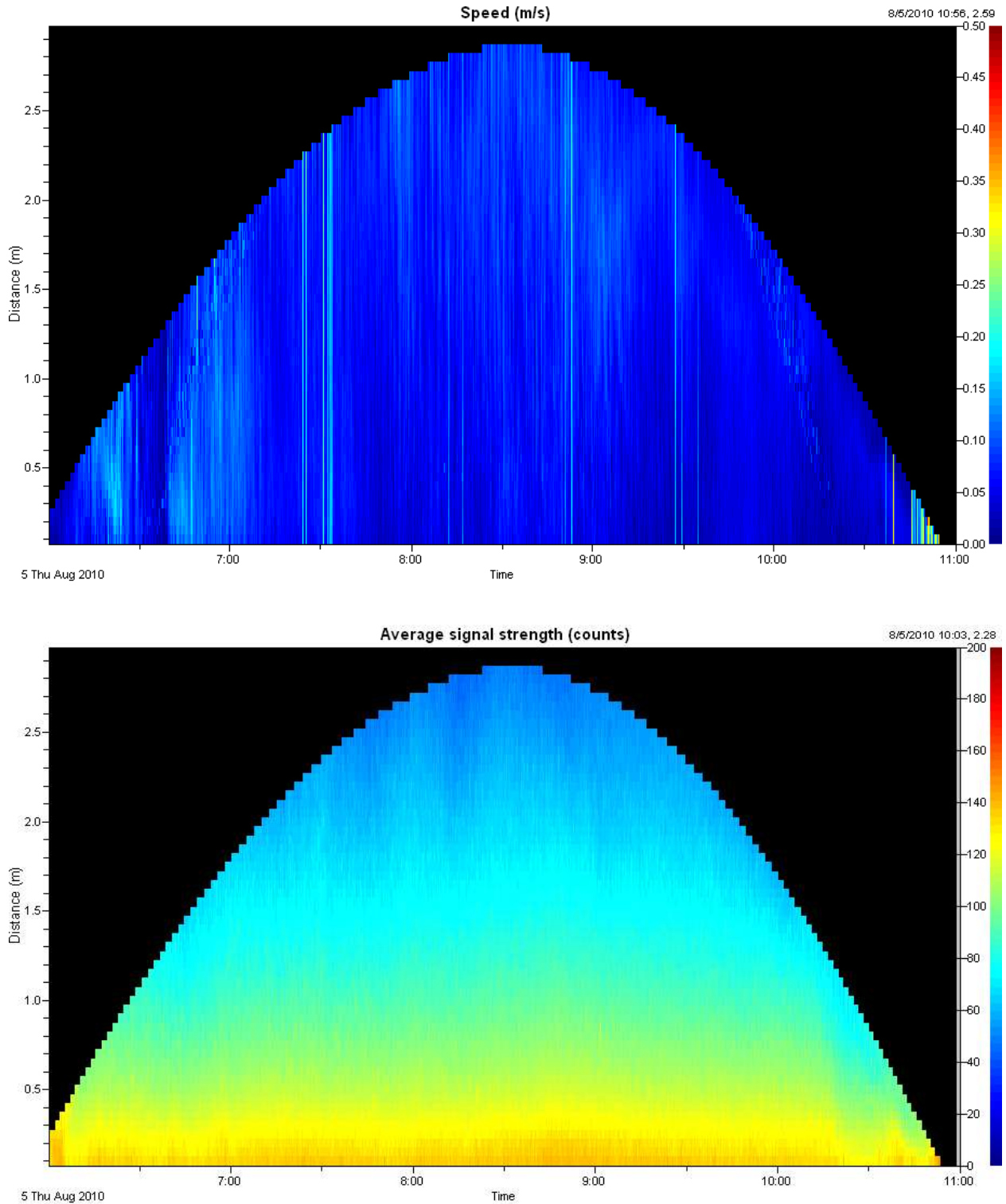
Figure 40:   ADCP resolved velocity and amplitude plots on Aug 5, 2010 at Kingsport mudflat.   Tidal height 5.4 m CGVD28, 24.1 mm rain, wind speed 3.1 m/s.
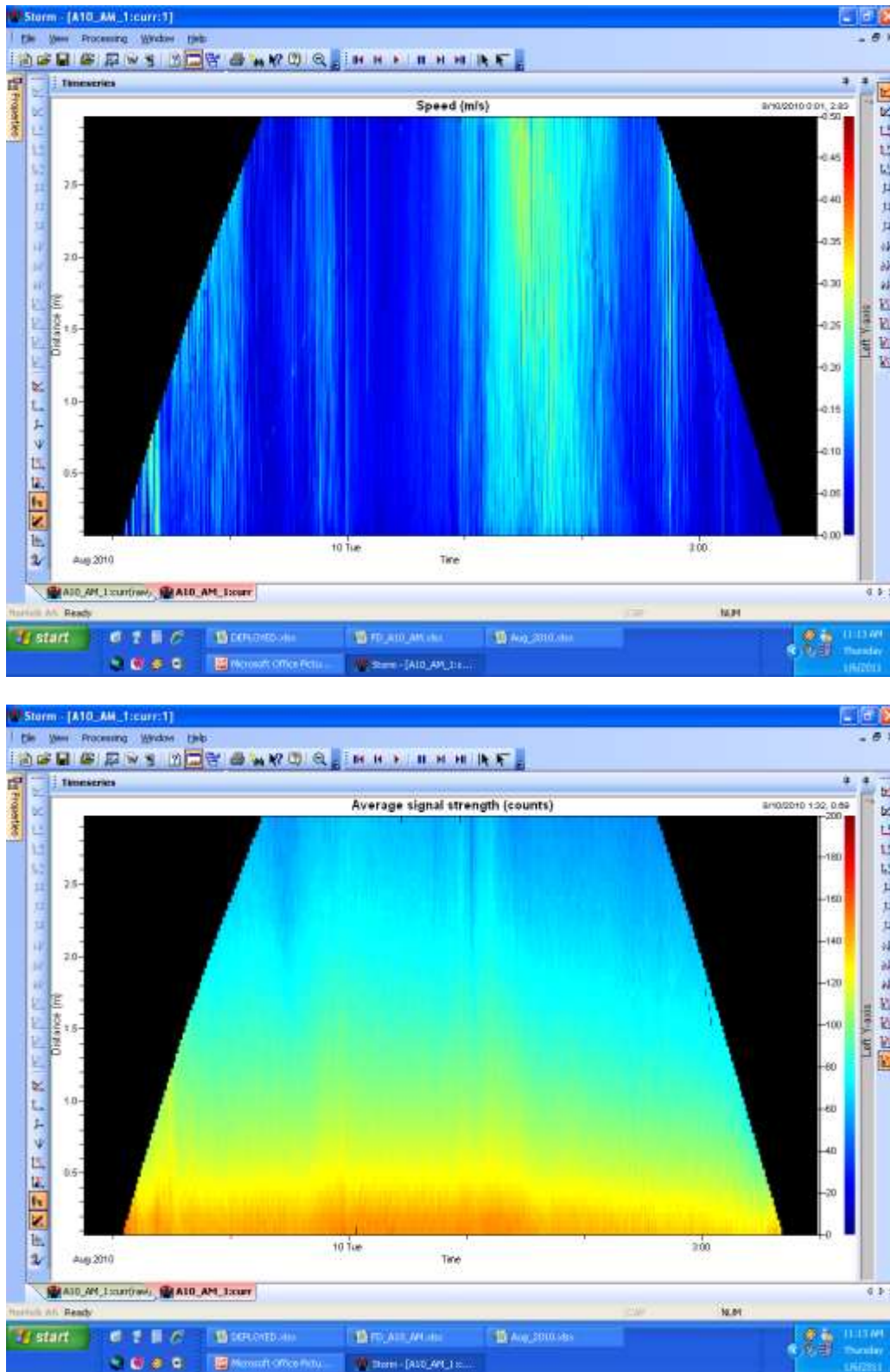
Figure 41 : Screen shot from Nortek STORM software for ADCP resolved velocity and backscatter on Aug 10, 2010. Tidal height 6.08 m CGVD28, spring cycle, rain 0.1 mm, 1.8 m/s wind speed.
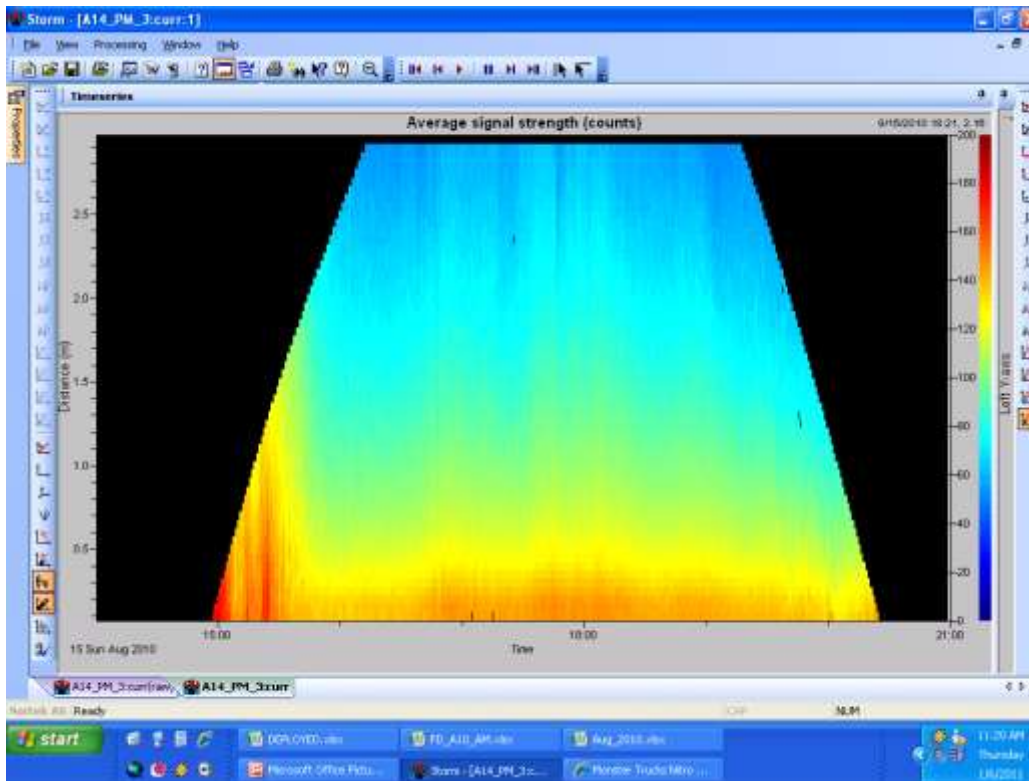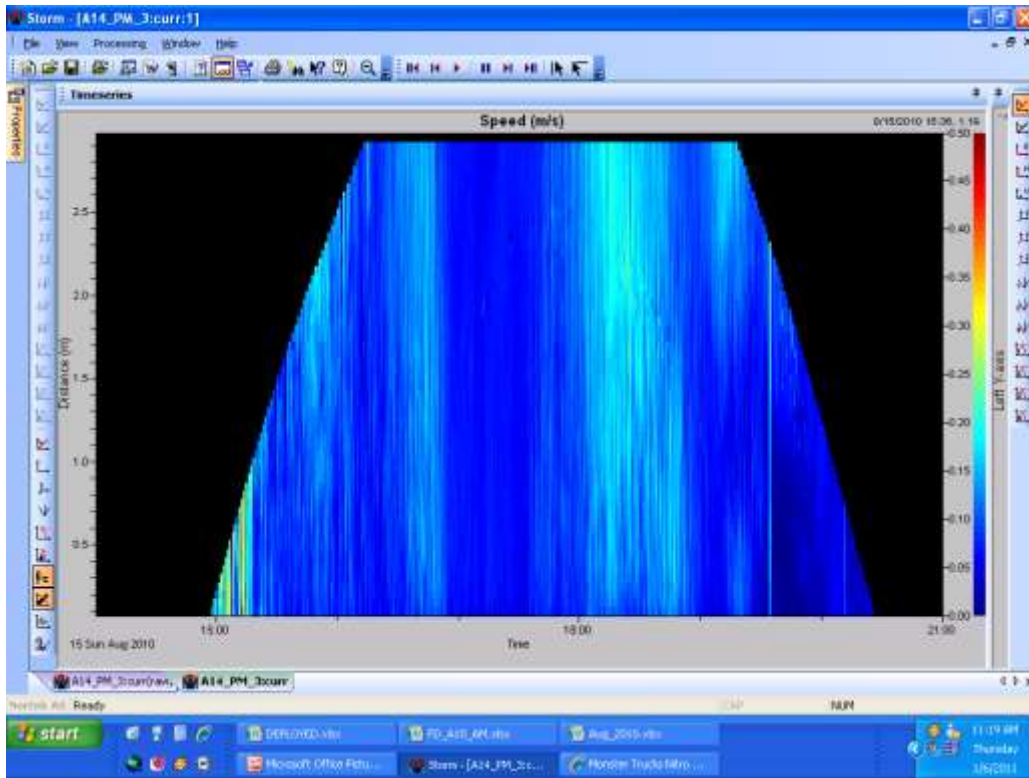
Figure 42: Screen shot from Nortek STORM software for ADCP velocity and backscatter on Aug 15, 2010 at Kingsport. High neap tide 6.67 m CGVD28, no precipitation, wind 1.1 m/s.
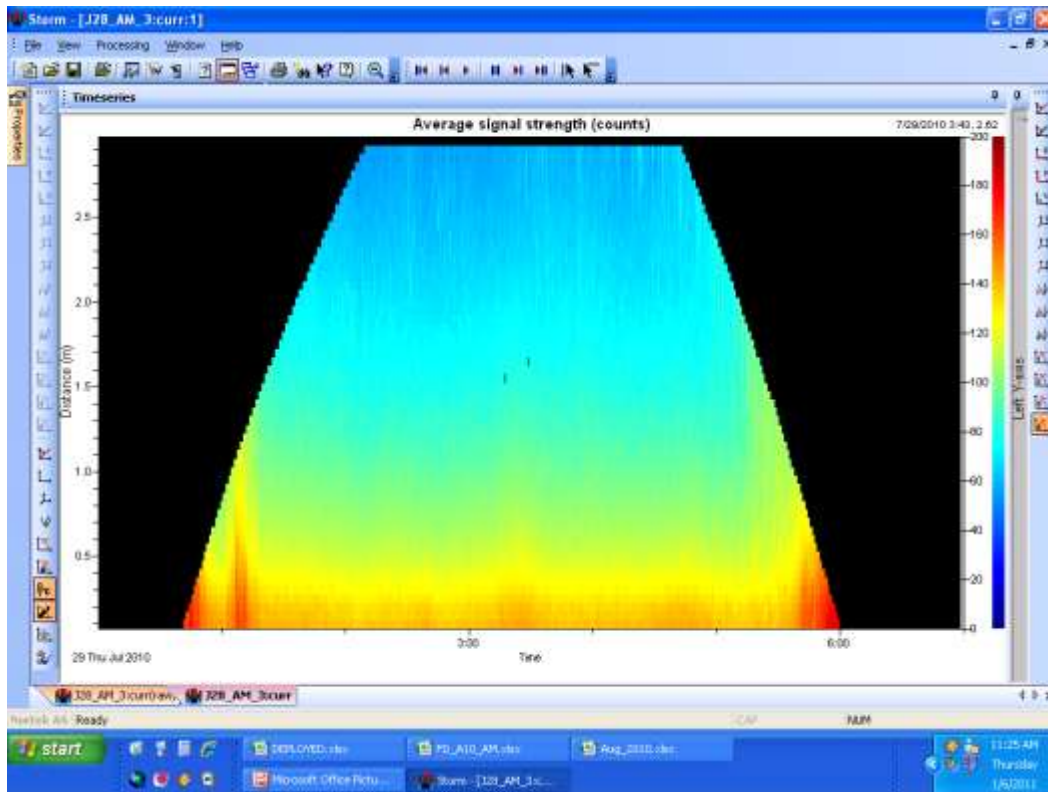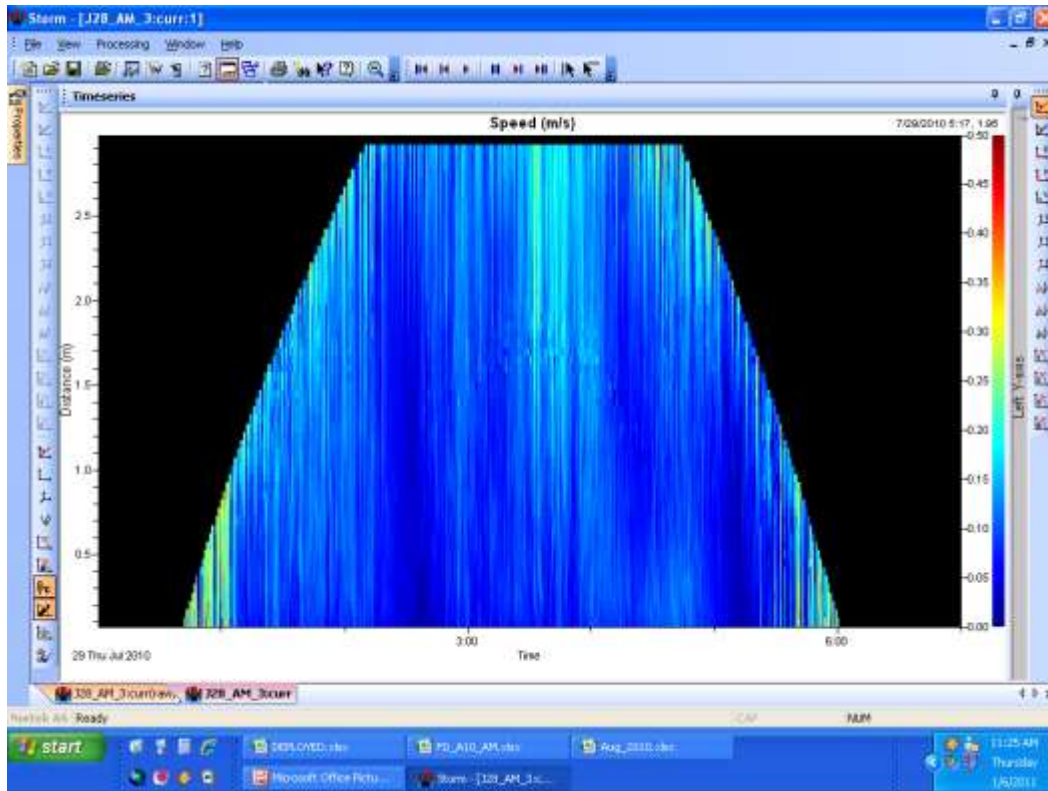
Figure 43: Screen shot of ADCP velocity and signal strength plots for July 29, 2010. High tide 6.06 m CGVD28, 3.5 mm precipitation and 4.4 m/s wind speed.
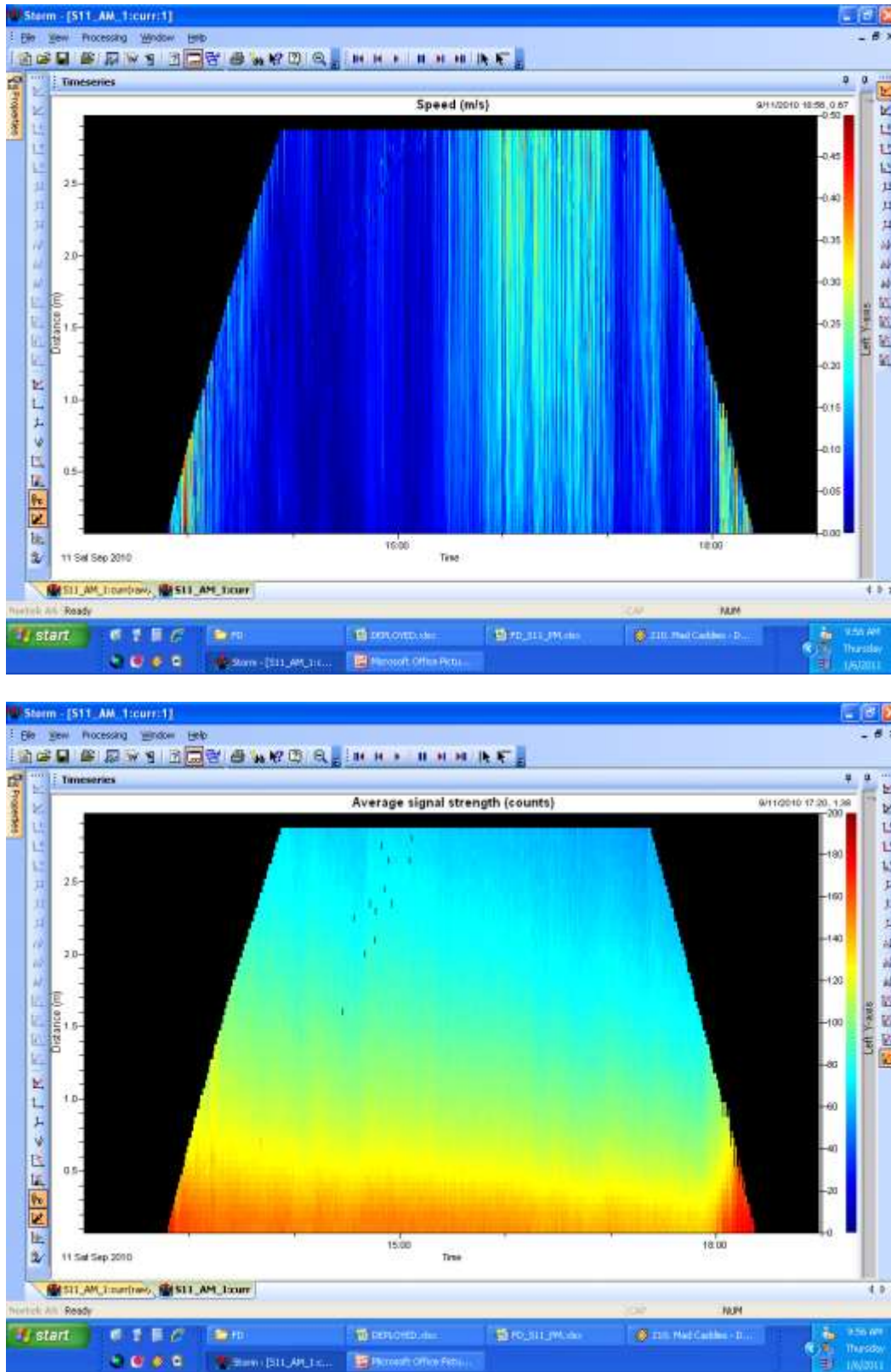
Figure 44: Screen shot of ADCP velocity and signal strength plots from Nortek STORM software on Sept 11, 2010. High tide 7.49 m, 0.1 mm precipitation and 5.4 m/s wind speed.
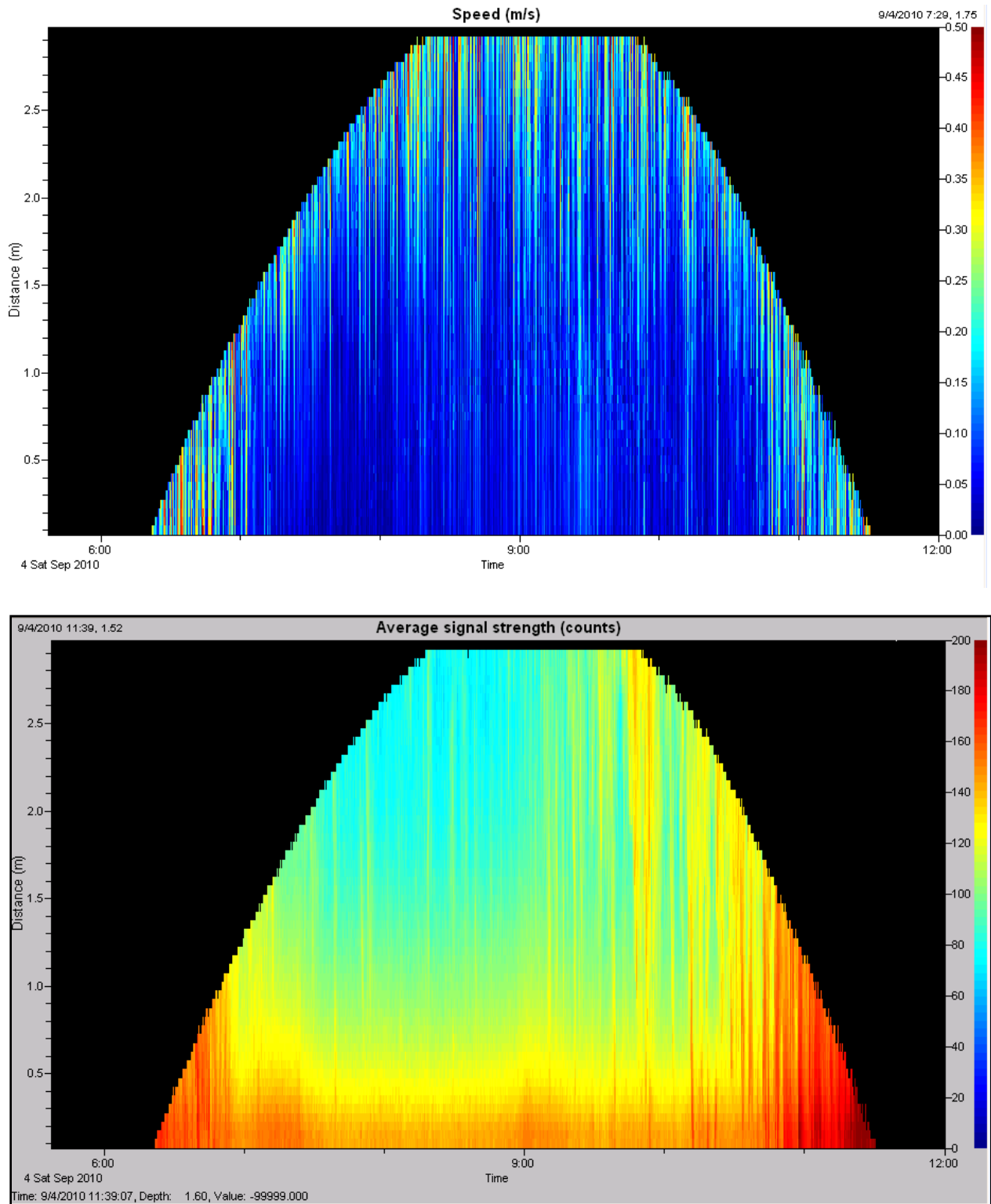
Figure 45: ADCP Storm plot for resolved velocity and signal strength (proxy for suspended sediment concentration) just before Hurricane Earl moved up the Bay on Sept. 4, 2010.

Sediment Deposition and Sediment Characteristics

There is a marked difference in sediment deposition between sites and between the tidal creek and vegetated marsh surface.   The sheltered Starrs Point site consistently recorded higher amounts of sediment deposition at all stations than at the more exposed stations at Kingsport (Table 3, Figure 46, Figure 47, Figure 51).   This is particularly evident within the creek itself which recorded almost seven times more deposition ($\sim 250\text{-}500$ g·m^{-2}) than the adjacent marsh surface ($\sim 15\text{-}125$ g·m^{-2}) (Figure 46). All stations are significantly different from each other ($p<0.001$ repeated measured ANOVA).   Interestingly, variable amounts of sediment were deposited at the creek station for similar tidal heights (Figure 46).The range of sediment deposition on the marsh surface both at Starrs Point and Kingsport fall within the range of data recorded at other sites within the Upper Bay (e.g. van Proosdij et al., 2006a; Silver, 2009; Davidson-Arnott et al., 2002).
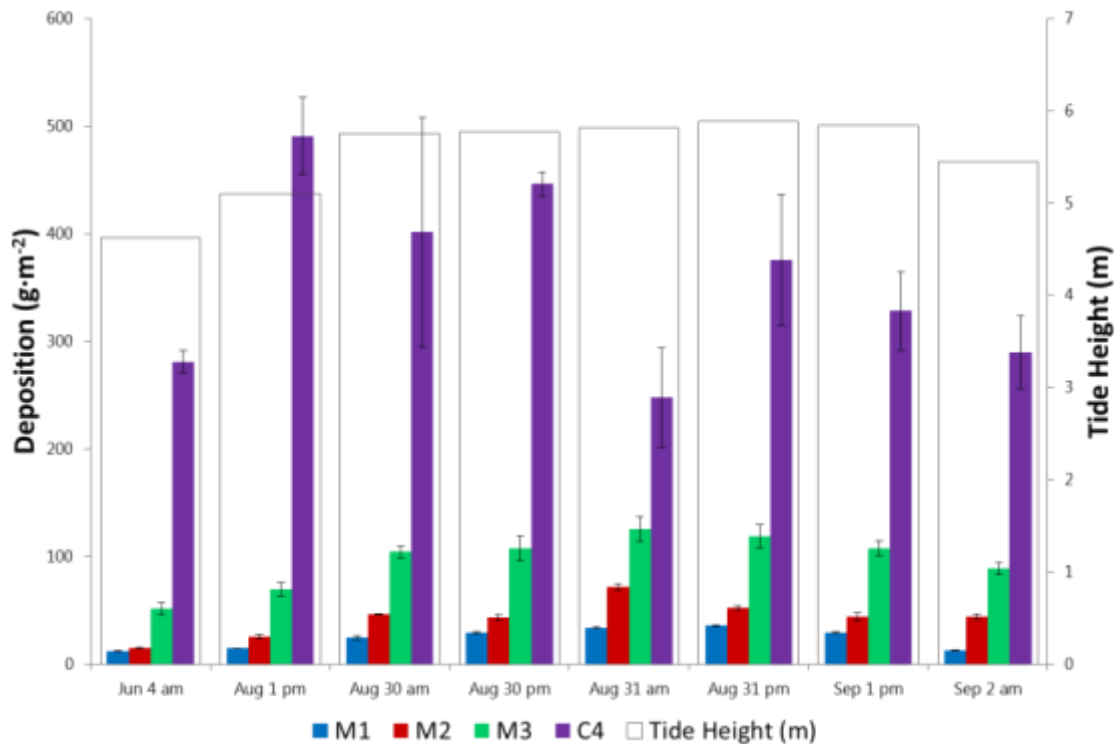
Figure 46:   Comparison of sediment deposition between creek and marsh sites at Starrs Point in 2011. Note similarity in tide height (m CGVD28).

The amount of sediment deposited on the marsh surface is a function of the availability and opportunity for suspended material to be deposited.   The availability and opportunity for sediment to be deposited is influenced by factors both intrinsic (within e.g. vegetation, biota, elevation within the tidal frame, topography) and extrinsic (external – e.g. tidal range, suspended sediment concentration, grain size, storms, tidal currents) to the marsh system (van Proosdij et al., 2006).
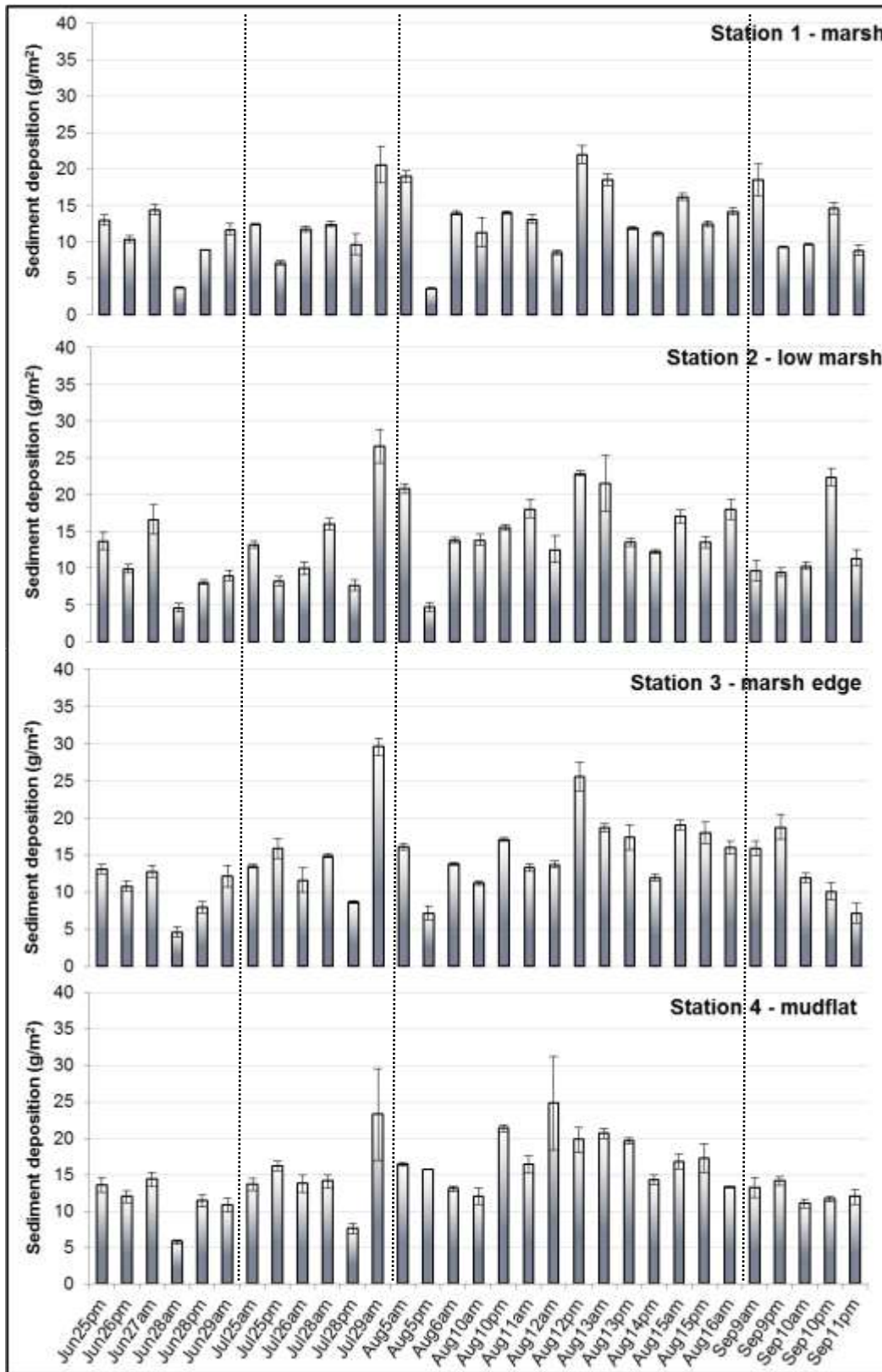
Figure 47: Variation in sediment deposition at Kingsport stations in 2010.

Availability of Sediment

The availability of sediment to be deposited is tied directly to the amount of suspended sediment within the water column. Suspended sediment concentrations are controlled primarily by meteorological and hydrodynamic conditions immediately pre and during the tidal cycle and will vary throughout the tidal cycle (Parry 2001; Reed et al. 1985; van Proosdij 2001; Wang et al. 1993). There is typically a pattern of higher concentration during the flood tide and recurrently another peak during the ebb tide (Christiansen et al. 2000; Dyer et al. 2000; Parry 2001; van Proosdij 2001). This was observed for the majority of tides at both Starrs Point and Kingsport.
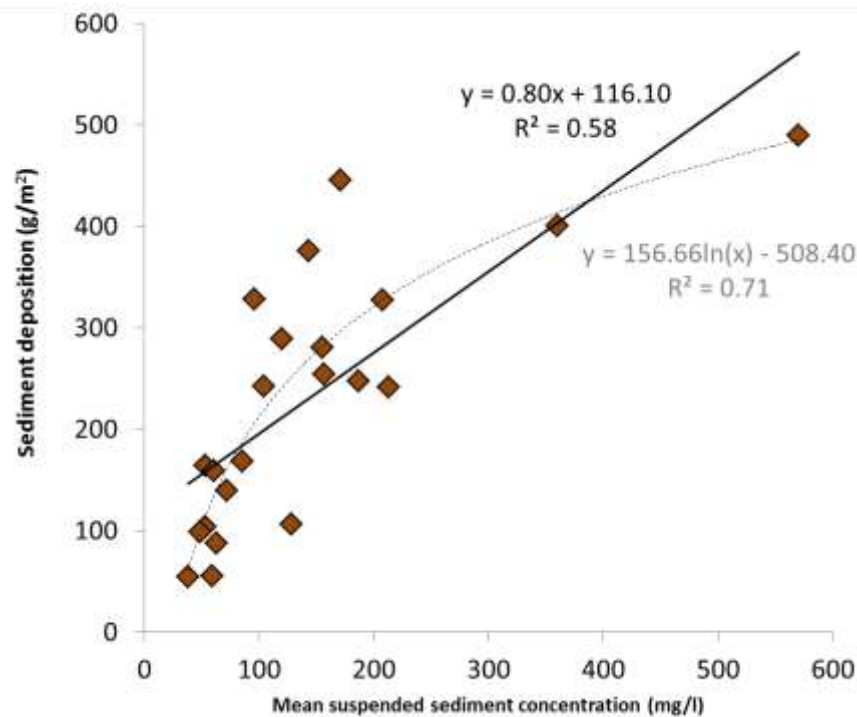
Figure 48: Relationship between mean suspended sediment concentration and sediment deposited within the creek at Starrs Point. Data from 2009 and 2011 were merged for the analysis.

There is a moderately strong positive correlation between mean suspended sediment concentration and sediment deposition within the tidal creek at Starrs Point for pooled data from 2009 and 2011 (Figure 48). Only the M2 station, immediately on the marsh platform, exhibited a strong correlation between suspended sediment and deposition (Figure 49). This relationship is consistent with findings of French et al. (2000) who found higher suspended sediment concentration closer to the marsh edge and decreasing concentrations as the water travelled through the marsh. This relationship was not observed at the exposed Kingsport site (Table 4, Figure 50).
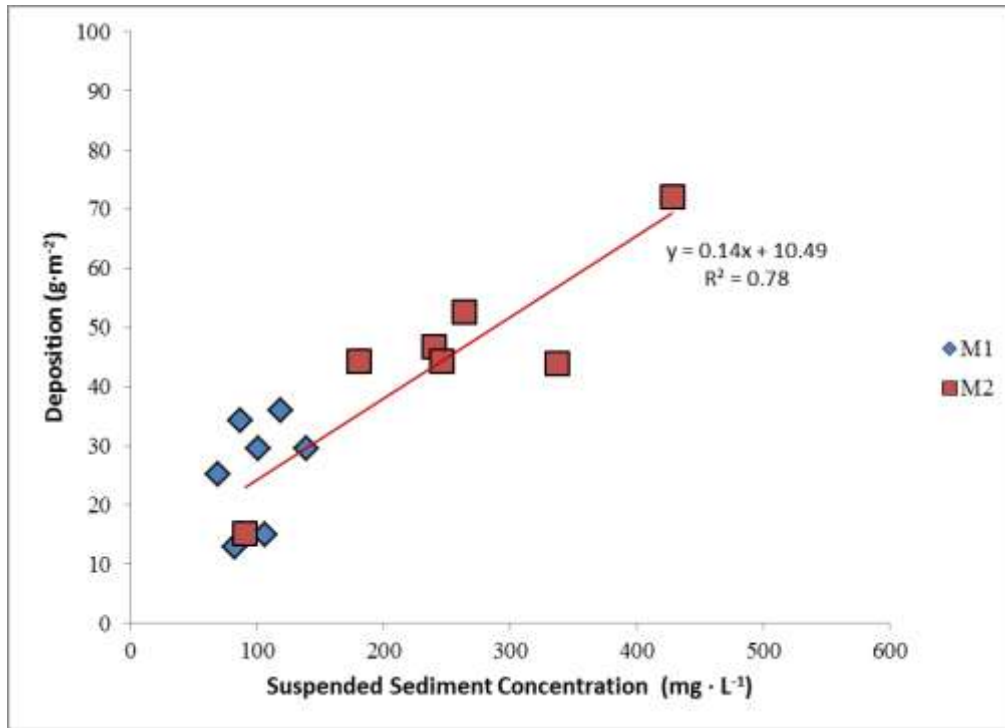
Figure 49: Relationship between suspended sediment concentration and deposition on the marsh surface at Starrs Point in 2011. M1 station located on the high marsh, M2 on the marsh platform at the creek edge.
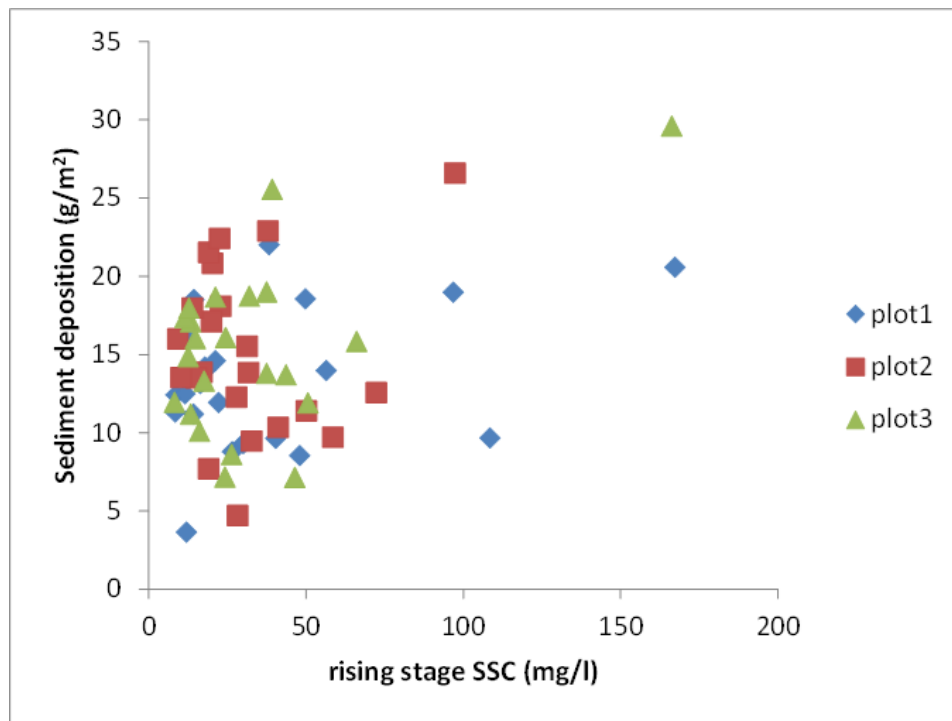
Figure 50: Relationship between suspended sediment concentration measured in the rising stage bottles at Kingport in 2010 and mean sediment deposition. Plot 1 is located furthest onto the marsh surface.

Site & Year	Date	Tide elevation (m CGVD28)	Sediment Deposition (g•m^{-2})	Organic matter content (%)	Floc fraction f	Mean grain size (μm)	Floc limit Df (μm)
Starrs Point 2009	Aug 4	3.40	186.38	7.88	0.69	6.32	11.67
	Aug 5	3.60	164.12	7.34	0.73	6.53	15.00
	Aug 6	3.75	140.08	8.16	0.70	6.53	15.25
	Aug 7	3.91	159.26	7.62	0.81	7.77	21.00
	Aug 8	4.03	103.79	7.92	0.85	6.10	21.00
	Aug 9	4.04	98.65	9.09	0.82	5.39	18.75
	Aug 12	4.16	87.93	8.44	0.87	5.91	23.00
	Aug 20	5.14	169.01	7.72	0.79	5.70	15.75
	Aug 21	5.36	254.36	7.24	0.73	6.05	15.50
	Aug 24	5.14	241.37	8.31	0.74	6.62	15.00
	Aug 25	4.75	242.85	7.04	0.79	5.40	15.50
	Aug 26	4.23	328.19	8.55	0.67	6.76	12.50
	Sept 20	5.69	106.62	7.54	0.84	5.87	21.25
	Sept 26	3.07	55.02	8.11	0.89	5.83	26.00
	Sept 27	2.57	55.63	10.08	0.74	5.35	12.00
Starrs Point 2011	June 4	4.62	281.21	5.36	0.54	6.20	7.00
	Aug 1	5.10	490.66	5.25	0.65	6.37	11.50
	Aug 30	5.75	401.49	3.26	0.65	5.99	11.0
	Aug 30 pm	5.77	446.15	4.06	0.51	6.55	6.50
	Aug 31	5.81	247.74	4.67	0.76	6.95	17.00
	Aug 31 pm	5.88	375.57	4.79	0.73	4.75	10.00
	Sept 1	5.84	328.33	5.02	0.73	6.02	13.00
	Sept 2	5.45	289.69	5.13	0.66	6.05	10.50
Kingsport 2010*	June 25	5.94	13.60		0.67	6.90	12.00
	June 26	5.96	12.05		0.81	8.19	24.00
	June 27	6.53	14.37		0.80	7.63	21.00
	June 28pm	5.83	11.45		0.73	6.32	14.00
	June 29	6.19	10.77		0.40	12.26	9.00
	July 25pm	5.80	16.18	Not available	0.33	7.57	4.00
	July 26	6.29	13.79		0.74	7.37	16.00
	July 28 am	5.83	14.06		0.50	6.23	6.00
	Aug 5 am	5.40	16.43		0.59	12.60	16.00
	Aug 5 pm	4.76	15.69		0.75	8.70	18.00
	Aug 10 am	7.32	12.06		0.72	7.81	16.00
	Aug 10 pm	7.01	21.36		0.56	5.54	6.00

*data are only available for tides with sufficient sediment deposited for analysis and do not reflect the characteristics of tides with limited deposition. In many instances the very low sediment concentrations during Coulter analysis limited DIGS analysis.

Table 3: Comparison of the daily-mean values of tidal elevation, sediment deposition, organic content, and results of deposited DIGS, including floc fraction (f), mean grain size and floc limit (df) at mudflat/creek stations at Starrs Point and Kingsport.   Mean grain size determined using Folk and Ward Method.

The presence of waves or heavy rainfall during the rising tide enhances the availability of sediment as it leads the sediment to be re-suspended, and therefore makes for more sediment to be transported throughout the water column (Allen and Duffy 1998; Friedrichs and Perry 2001; Ganju et al. 2005). Some studies have found waves to be influential to sediment distribution throughout the marsh (Fagherazzi and Priestas 2010; Ganju et al. 2005; van Proosdij et al. 2006a) while Parry (2001) did not find waves to be influencing the distribution of sediment. As Starrs Point is a very sheltered marsh, it could not be expected that waves have the same kind of influence that open marsh systems would have (van Proosdij et al. 2006a). The water was forced to travel through an extensive system of creeks before reaching the study site. Because of this, the waves which may be present in the main channel of the Cornwallis river are mostly dissipated by the time it reaches the site (O'Laughlin and van Proosdij 2012). Therefore, the local waves present are most dominantly present when the wind conditions are high. As the source of the of creek is to the Northeast-East of the creek, that is the direction which produces more waves for Starrs Point marsh and the result of this can be seen with the Aug 1 pm tide which had the wind coming from the East and had a very concentrated tidal bore accompanied with the highest deposition in the creek (Table 3). Although storms and heavy rainfall do increase the amount of sediment in suspension entering the Kingsport site, this increased availability of material does not necessarily bring increased deposition to the system. Other factors influence the ability of this sediment to be deposited.

Opportunity for Sediment Deposition

The opportunity for sediment to be deposited within the marsh system is influenced by water depth (e.g. Temmerman et al. 2003; van Proosdij et al., 2006), notably flooding frequency and inundation time, flow velocity (e.g. Friedrichs and Perry, 2001) and particle characteristics (e.g. grain size, floc content) (Christiansen et al., 2000).
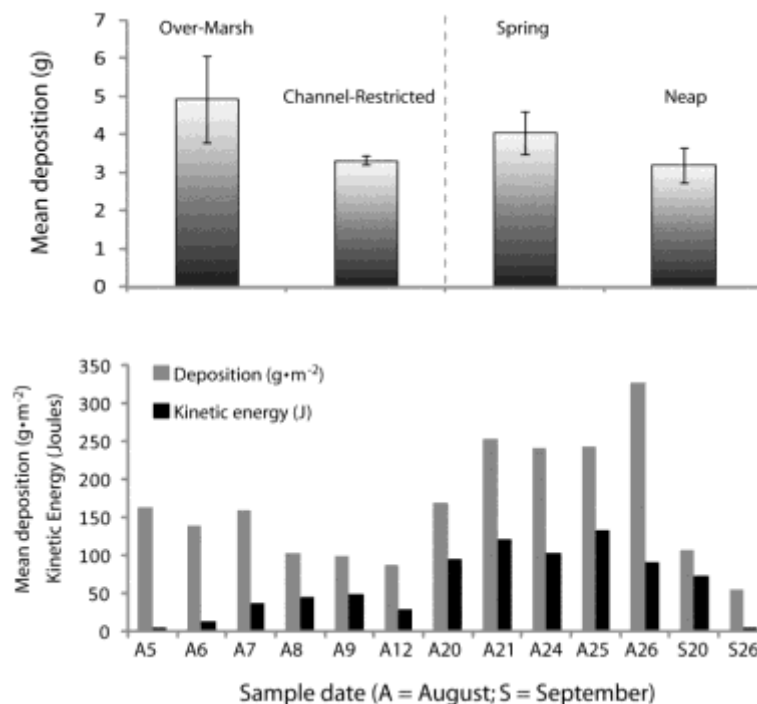
Figure 51: Relationship between tidal kinetic energy and sediment deposition for overmarsh and channel restricted tides at Starrs Point in 2009.

2010					Meteorological conditions			Mean Sediment deposition				
	Time		time		total P	mean WS	mean WD	(g/m^2)				
Date	HT	at ADCP	(min)	Tide	(mm)	(m/s)	(degrees)	per day	plot 1	plot 2	plot 3	plot 4
25-Jun	0:17	5.25	333	SPRING	0	4.6	46.5	-	-	-	-	-
25-Jun	12:46	4.7	317	SPRING	0	1.8	34.4	13.33	12.97	13.69	13.07	13.60
26-Jun	13:36	4.72	318	SPRING	0	4.6	48.0	10.80	10.38	9.94	10.81	12.05
27-Jun	1:51	5.29	333	SPRING	0.7	1.3	58.3	14.55	14.42	16.63	12.78	14.37
28-Jun	2:36	5.17	331	TRANS	25.4	3.7	204.2	4.69	3.74	4.64	4.61	5.77
28-Jun	15:04	4.59	318	TRANS	1.8	1.0	142.9	9.10	8.90	8.09	7.95	11.45
29-Jun	3:20	4.95	330	TRANS	0.6	0.6	159.9	10.91	11.71	9.02	12.15	10.77
25-Jul	0:50	4.97	332	SPRING		no data		13.20	12.41	13.25	13.49	13.66
25-Jul	13:16	4.56	315	SPRING		no data		11.87	7.13	8.25	15.91	16.18
26-Jul	1:38	5.05	329	SPRING		no data		11.78	11.72	9.99	11.62	13.79
28-Jul	2:55	4.98	322	TRANS	0	3.8	98.9	14.34	12.42	16.00	14.86	14.09
28-Jul	15:14	4.59	315	TRANS	0	0.8	141.2	8.39	9.66	7.69	8.60	7.61
29-Jul	3:29	4.82	-	TRANS	3.5	4.4	78.3	25.02	20.58	26.58	29.58	23.34
05-Aug	8:31	4.16	296	TRANS	24.1	3.1	68.8	18.08	18.98	20.83	16.08	16.43
05-Aug	21:00	3.52	-	TRANS	0	2.3	150.1	7.80	3.64	4.70	7.16	15.69
06-Aug	-	-	-	TRANS	24.1	3.6	87.4	13.66	13.97	13.83	13.78	13.07
10-Aug	1:04	6.08	341	SPRING	0.1	1.8	223.3	12.10	11.32	13.85	11.19	12.06
10-Aug	13:33	5.77	330	SPRING	0.9	1.7	166.9	17.00	14.02	15.53	17.10	21.36
11-Aug	1:54	6.33	341	TRANS	0.5	1.4	134.7	15.22	13.14	18.08	13.29	16.35
12-Aug	2:50	6.39	335	TRANS	0	2.1	248.5	14.91	8.54	12.56	13.70	24.83
12-Aug	15:16	6.19	336	TRANS	0.1	1.5	176.9	22.55	22.00	22.88	25.55	19.80
13-Aug	3:41	6.19	329	TRANS	0	1.5	204.9	19.84	18.51	21.51	18.66	20.69
13-Aug	16:10	6.12	336	TRANS	0	1.3	131.7	15.61	11.93	13.51	17.37	19.65
14-Aug	17:01	5.86	330	TRANS	0	1.6	213.4	12.42	11.19	12.26	11.95	14.29
15-Aug	5:26	5.43	325	NEAP	0	1.1	132.2	17.27	16.19	17.09	19.00	16.81
15-Aug	17:52	5.53	329	NEAP	0	1.8	200.2	15.32	12.50	13.53	17.97	17.28
16-Aug	6:14	4.89	317	NEAP	0	1.6	119.9	15.37	14.21	17.98	16.02	13.26
03-Sep	20:26	4.28	-	TRANS	0.2	1.8	269.1					
04-Sep	9:15	4.54	309	TRANS	0.5	7.1	101.9		Hurricane Earl - no traps deployed			
04-Sep	21:32	3.95	336	TRANS	17.6	6.8	271.5					
05-Sep	10:18	4.26	313	TRANS	0	5.5	100.7					
09-Sep	1:36	6.42	336	SPRING	0	2.3	173.8	14.34	18.55	9.70	15.84	13.25
09-Sep	14:02	6.4	337	SPRING	0.1	2.2	106.7	12.91	9.29	9.46	18.74	14.14
10-Sep	2:28	6.45	337	TRANS	0.4	3.0	155.2	10.73	9.65	10.33	11.91	11.02
10-Sep	14:54	6.43	336	TRANS	1.9	2.2	118.8	14.68	14.59	22.40	10.09	11.63
11-Sep	15:40	6.25	332	TRANS	0.1	5.4	209.3	9.82	8.79	11.39	7.14	11.95

Table 4: Summary of meteorological conditions and sediment deposition at Kingsport in 2010. Plot 1 is furthest on the marsh surface while Plot 4 is on the mudflat.

The influence of water depth is most evident within the tidal creek at Starrs Point where there is a clear relationship between tidal prism and kinetic energy (Figure 51).   It was originally hypothesized that by comparing the amount of energy in spring versus neap tides one could see how these differences in energy affected sediment deposition. It was found however to be more useful to distinguish between tides that were either contained within the tidal creek or extended over the marsh surface (Figure 51).   More sediment was

deposited during overmarsh tides than channel restricted tides (Figure 51). These tides also had greater amounts of kinetic energy as well.
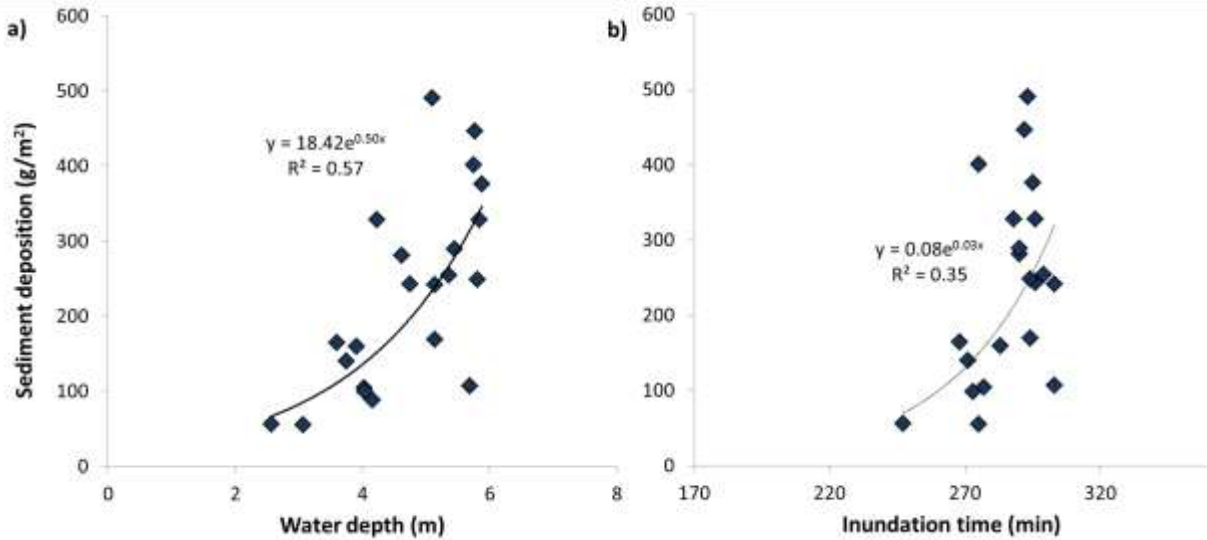
Figure 52: Influence of a) water depth and b) inundation time on sediment deposition within the creek at Starrs Point in 2009 and 2011.
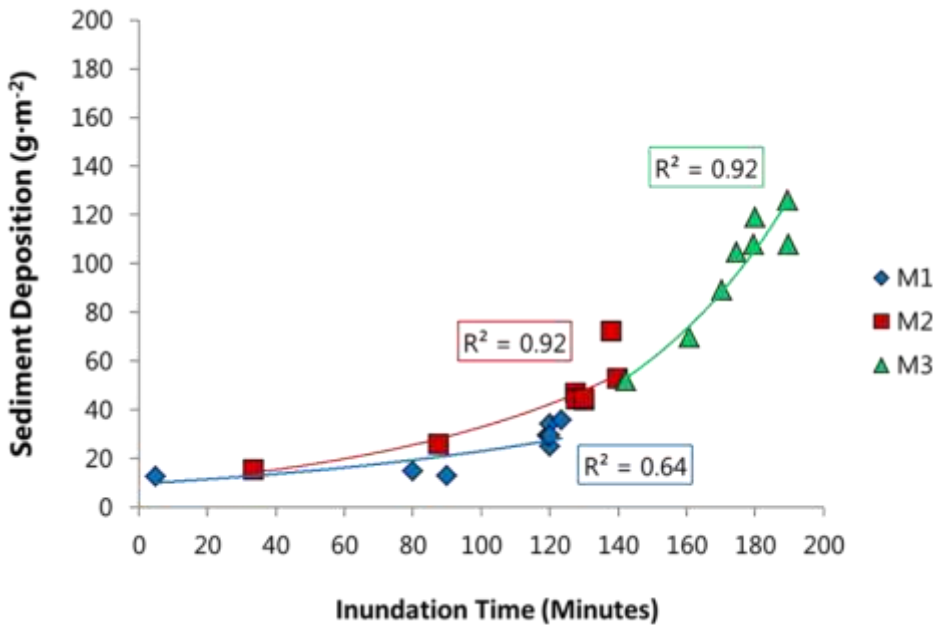
Figure 53: Influence of inundation time on sediment deposition on the marsh surface at Starrs Point in 2011.

In theory, greater depths of water lead to longer inundation times which provide more opportunity for fine particles to settle out of the water column (Voulgaris and Myers, 2004;

Temmerman et al., 2003; van Proosdij et al., 2006).   While there is a positive relationship between water depth or inundation time and deposition within the creek (Figure 52), the relationship is not as strong as on the marsh surface (Figure 53).   The creek did not experience a wide range in inundation times because the topography allows for the water to remain at a stable height locally as the water fills the creek further downstream, therefore although there was a difference in tidal heights, the difference in inundation time where the traps are did not vary considerably. M3 had the highest R^2 value and was also the one which had a relationship closest to a 1:1 relationship. The higher on the marsh the plot was situated, the greater effect inundation time had on deposition, which was at plot M1. With a simple correlation, depth, which is directly proportional to inundation time, had a very strong correlation with deposition, with a Pearson value of 0.946 showing a powerful relationship between depth and deposition.
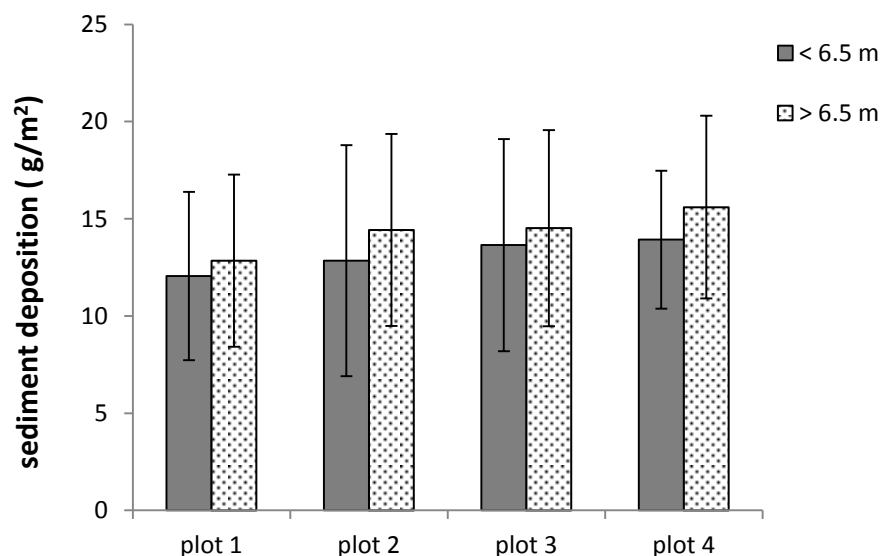
Figure 54: Variation in sediment deposition between marsh and mudflat plots at Kingsport 2010. Plot 1 (furthest up marsh) to Plot 4 (mudflat).   Data are divided according to tides above or below 6.5 m CGVD28 m which corresponds to the top of the main marsh cliff.

At Kingsport, sediment deposition appears to decrease with distance from the mudflat surface, with higher mean deposition for tides greater than 6.5 m CGVD28 (Figure 54).   This corresponds to the water level that would exceed the main marsh cliff near the tower and be part of basin wide circulation patterns rather than local topographic influences. At the plot level however, the relationship between water depth and deposition is weak.   The opportunity for sediment to be deposited is also tied to current velocities. Sufficiently low velocities are required for particle settling however a fine balance exists between velocities that enhance inter-particle collisions resulting in the formation of floc and more rapid deposition and velocities that would serve to break up the flocs.
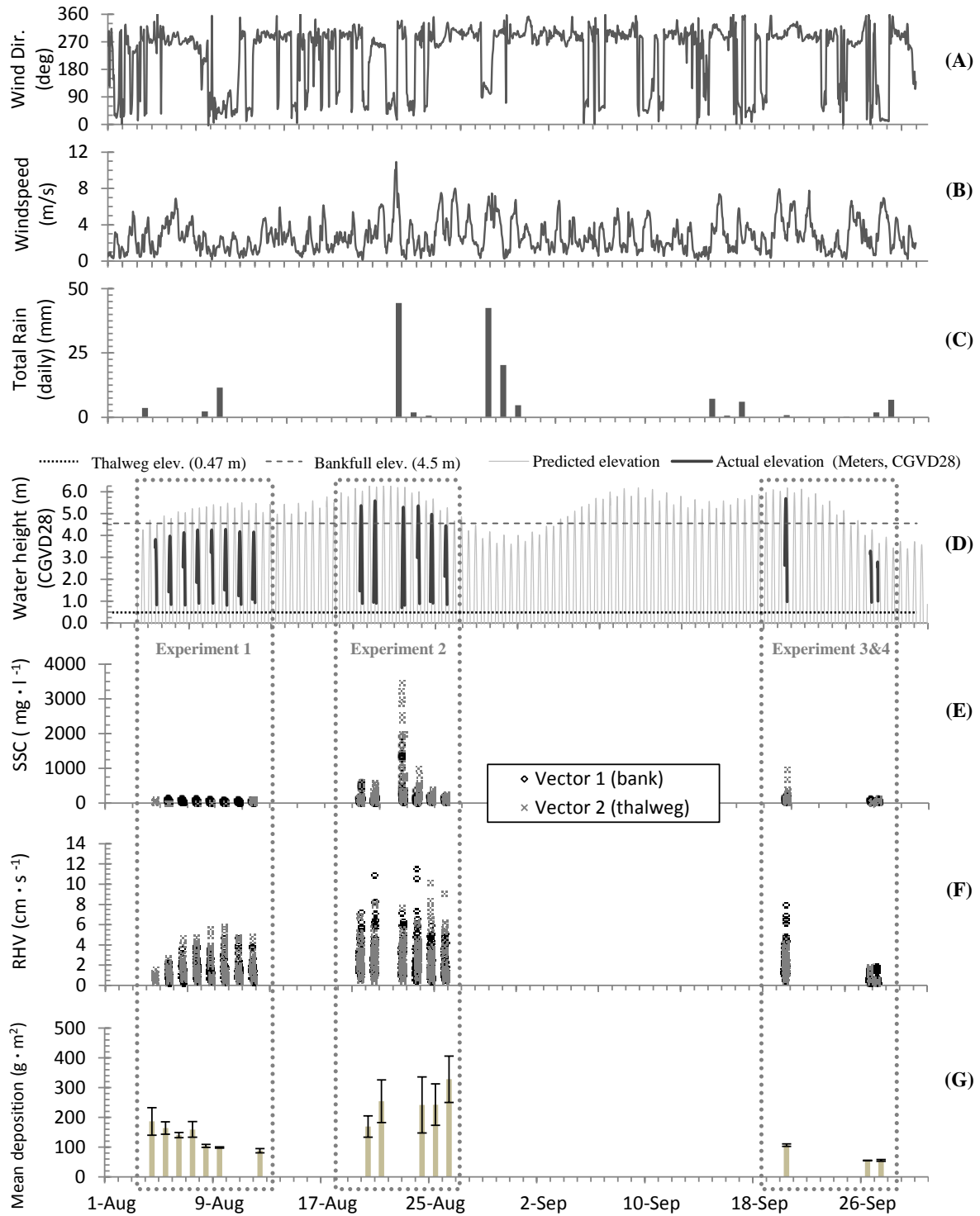
Figure 55: Variation in mean sediment deposition, resolved horizontal velocity (RHV), suspended sediment concentration and meteorological conditions within the tidal creek at Starrs Point in 2009.
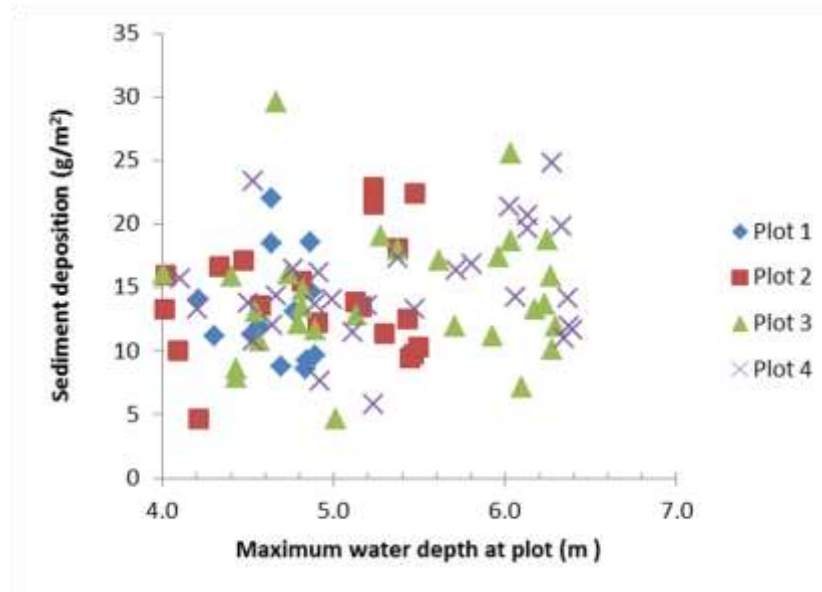
Figure 56: Relationship between depth of water at each plot with corresponding sediment deposition at Kingsport in 2010.
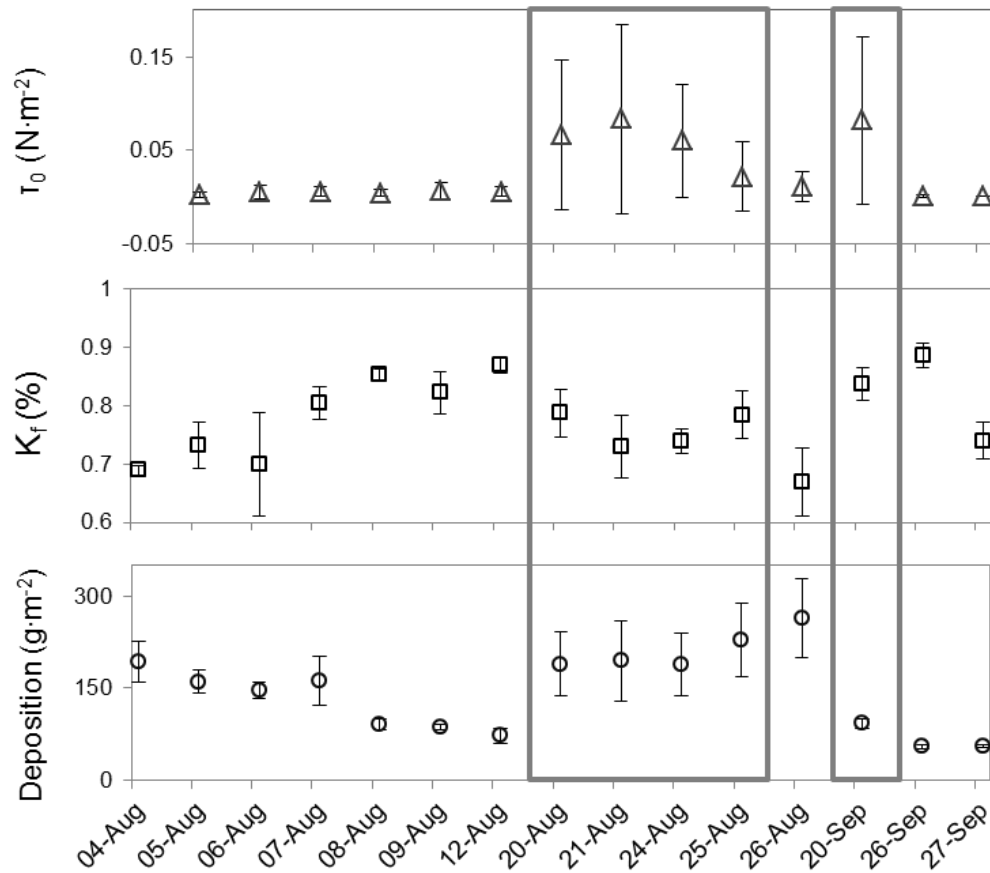
Figure 57: Full-deployment time-series at Starrs Point 2009, showing variation in 5-minute mean values of Kolmogorov microscale (η) and bed shear stress (τ_0), along with daily mean values of floc fraction (f) and deposition. Error bars indicate standard error.

Daily mean values of bed shear stress (τ_0) and the Kolmogorov microscale (η) over the study period are shown in Figure 57. Values of η achieved maximum during channel-restricted tidal cycles and were consistently higher than that of over-marsh tides; in general, peak values for channel-restricted cycles ranged from 4-10 x 103 µm, while that of over-marsh tides ranged from 3-6 x 103 µm. This suggests that turbulence levels associated with typical channel-restricted tidal cycles are sufficient for formation of flocs up to 50% larger than more turbulent over-marsh tides. Turbulent kinetic energy (TKE) was especially low (0.01 – 0.1 J·m3) for the duration of ebb phases of channel-restricted tides, which resulted in peaks to very high η values (20-38 x 103 µm) and suggests that floc formation is most efficient during these phases. Over-marsh tides contrastingly demonstrate maximal values of η around high water, with submergence of the marsh surface; these peak values persist until ebb flow velocity increases (20-40 min following high tide). Combined with reduced bed shear stress (0.001 – 0.05 N·m^{-2}) over the duration of slack tide (30-45 min) during over-marsh cycles, this situation describes an increased potential for floc formation and particle settling. Higher bed shear stress (0.1 – 0.5 N·m^{-2}) values are associated with turbulent flows (TKE < 1.8 J·m3) during initial and final stages of over-marsh tides suggest that existing flocs may be destroyed during these periods. The general pattern of tidal energy over the study period follows this trend, showing increased kinetic energy and TKE with submergence of high- and low-marsh surfaces (e.g. over-marsh tides). This is most notable during early ebb stages in association with gravity-driven drainage.
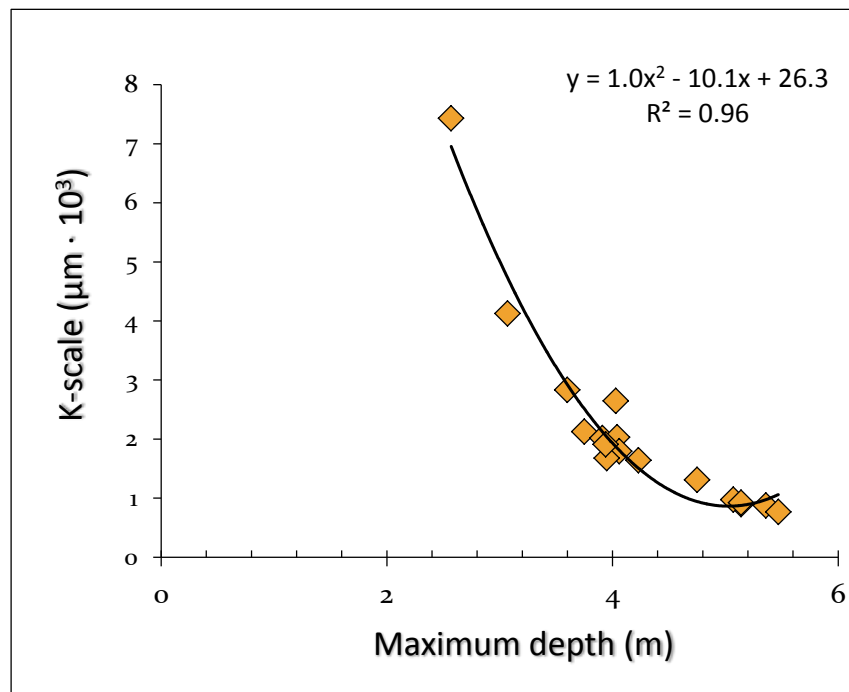
Figure 58: Relationship between Komogrov microscale and water depth within the creek in 2009. The K-scale describes upper size limit of potential floc formation, based solely on flow conditions.

On the marsh surface, when comparing deposition to resolved horizontal velocity (RHV), and including all plots in a simple correlation, RHV had a negative correlative, with a Pearson value of -0.677, with deposition.   There is a very weak correlation (-0.21) at marsh plots in Kingsport (Figure 59).
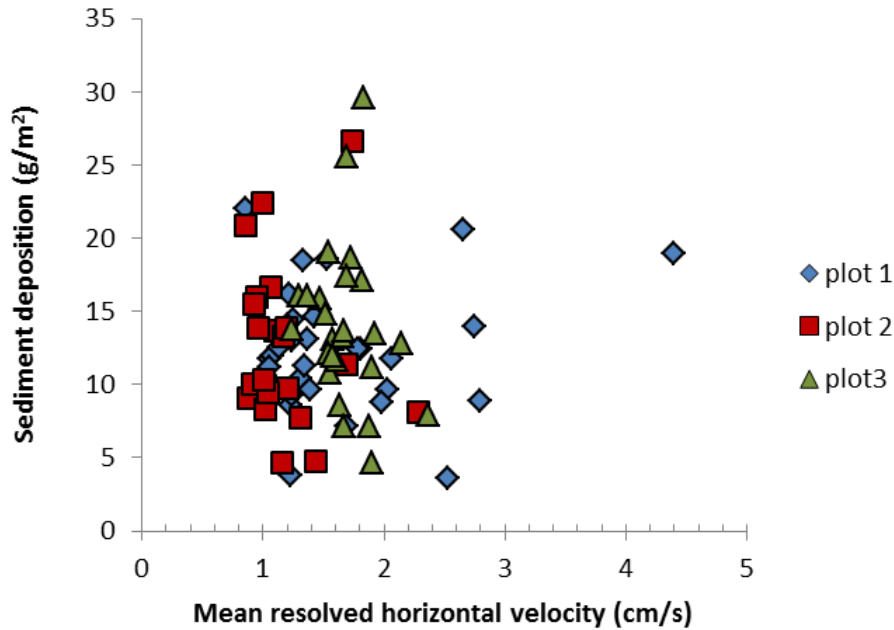
Figure 59: Relationship between mean horizontal velocity and sediment deposition at Kingsport in 2010.

Vegetation also plays a role in influencing how much sediment is deposited on the marsh surface by decreasing flow velocity and physically trapping sediment on its stems and leaves (e.g. Voulgaris and Myes, 2004; Leonard and Croft, 2007).   The marsh surface at both sites was dominated by *Spartina alterniflora* while *Spartina patens* was also observed at station M1 at Starrs Point.
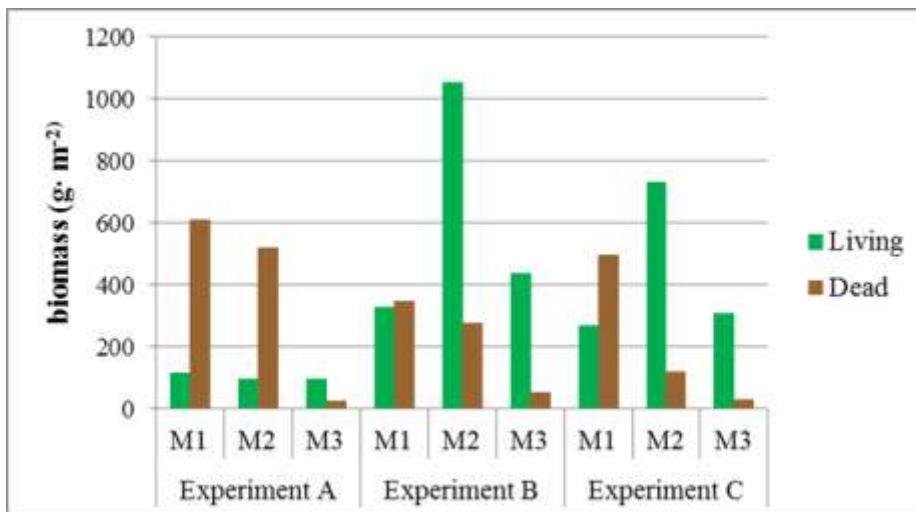
Figure 60: Variation in above ground biomass on the marsh surface at Starrs Point in 2011.

Figure 60 shows that during the two last experiments at Starrs Point, there was much more alive vegetation than dead vegetation. The only tide which occurred in Experiment A with the abundant dead vegetation was Jun 4 am. Plot M1, dominated by *spartina patens*, remained with a dead vegetation dominance throughout the season and plot M3, which was dominated by *spartina alterniflora*, remained with an alive vegetation dominance throughout the season. M2 was the only plot with a transition between a prominent dead dominance during Experiment A to prominent alive dominance during Experiment B and Experiment C. There was generally more deposition when there was a greater amount of live biomass.
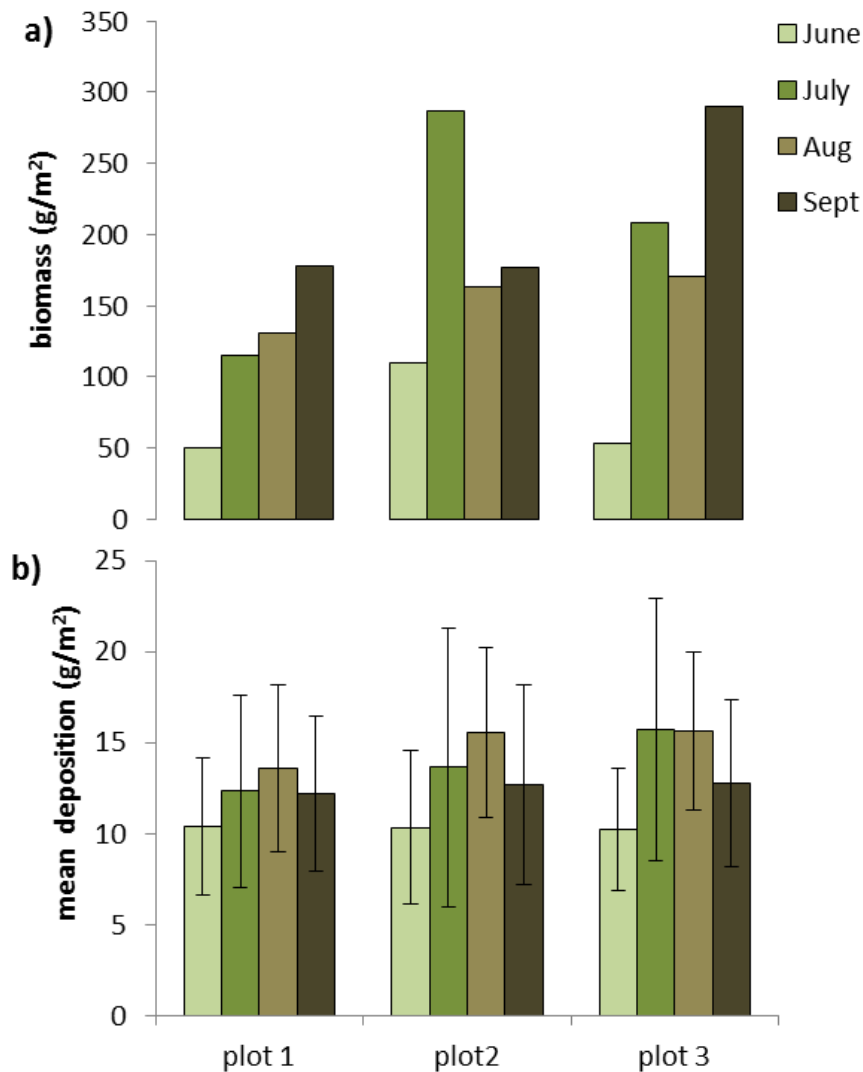
Figure 61: Variation in a) above ground biomass and b) mean sediment deposition at each plot throughout the growing season at Kingsport in 2010. Error bars represent standard deviation.
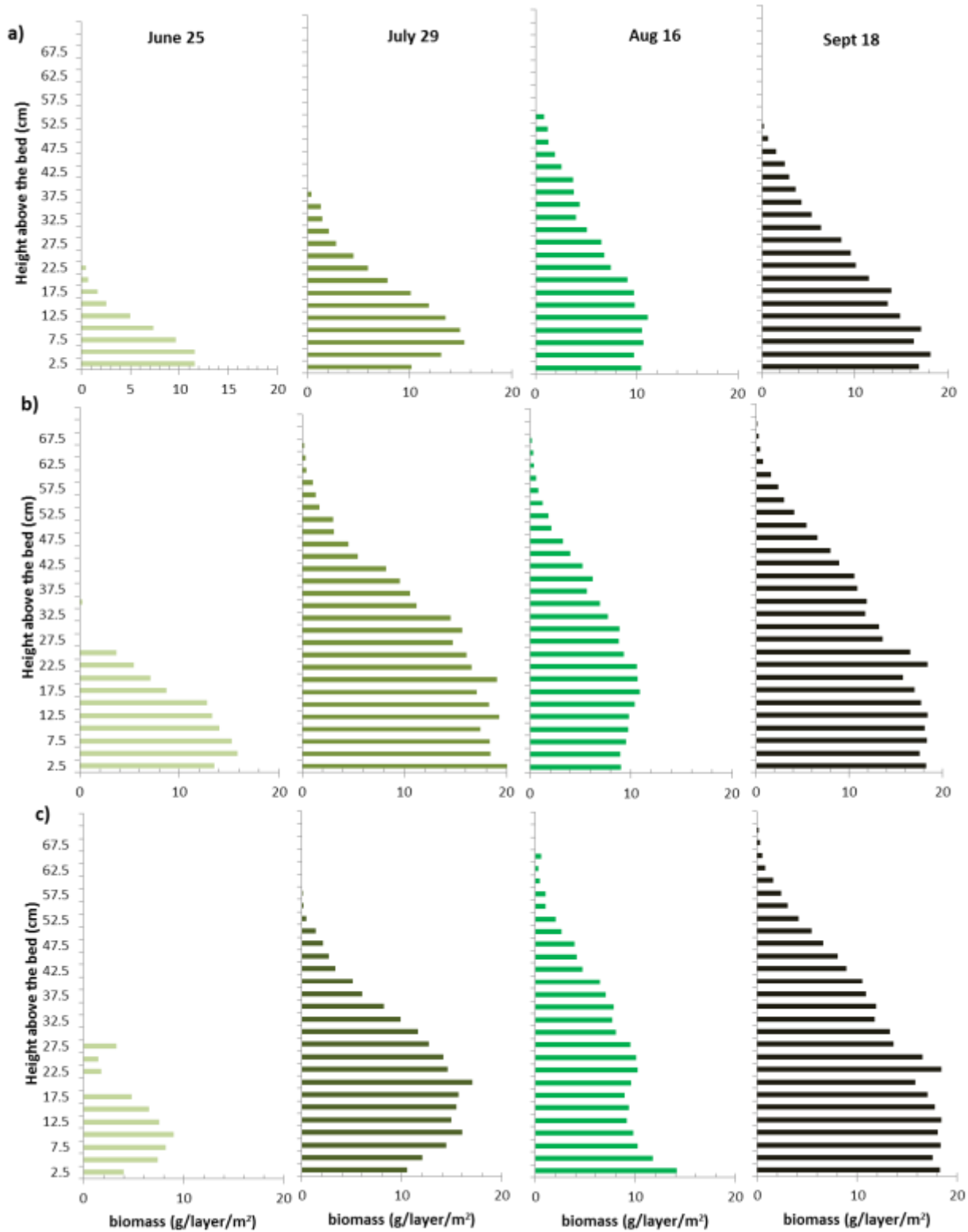
Figure 62: Change in vertical above ground biomass with height over the growing season at Kingsport for a) plot 1, b) plot 2 and c) plot 3.

Although the vegetative biomass at Kingsport was not divided into 'living' or 'dead', it did provide some interesting trends.   The biomass recorded in June was comparable to the amount recorded at Starrs Point early in the growing season. However, by August, *spartina alterniflora* was almost twice as high at Starrs point, particularly adjacent to the creek.   The mean amount of sediment deposited during the June deployment at Kingsport was very similar between plots (Figure 61) and had markedly smaller amounts of biomass.   This pattern is consistent with observations by van Proosdij et al. 2006 in the Cumberland basin who recorded lower amounts of deposition, minimal variation across the marsh surface early in the growing season.   As vegetation increases in height and biomass, it becomes more effective at trapping sediment, particularly through wave attenuation (van Proosdij, et al., 2006).   The dip in biomass in August may be related to snail hervivory.   Examination of the vertical distribution of biomass in Figure 62 potentially supports this observation, particularly at plot 2 when comparing July to August distributions.

The amount of sediment that is eventually deposited on the marsh surface is also related to how these sediments settle through the water column. The settling velocity is affected by both the size of the individual particles and the size of any floc aggregate.   Deposited sediment collected at Starrs Point in both 2009 and 2011 was primarily composed of very fine silt, with a mean grain size of 6.13 (±0.63) µm, and d50 of 6.7 µm. Kingsport deposited sediments (where available) were coarser and more variable, with a mean grain size of 8.26 (± 2.20) µm.   This falls within the fine silt range according to the Wentworth grain size classification. Results of disaggregated inorganic grain size (DIGS) analysis (Table 3, Table 9) show that the mean source slope (m) showed little variation over the course of the study (approximately 0.4 to 0.6), indicating a stable source of sediment supply (Kranck and Milligan, 1996a).   Floc fraction (f), or the proportion of the total suspended mass held in flocs, ranged from 55% to 89%, and was generally maximized on channel-restricted tides (Table 3).

Dissaggregated grain size (DIGS) analyses of suspended materials (Figure 63) shows changes in concentration which agree with that monitored by OBS sensors, where peak concentrations typically occur during initial flood and final ebb stages.   In addition, suspended sediment DIGS show notable fluctuations in concentration near high tide during over-marsh tidal cycles.   Concentration dynamics increase in response to flow accelerations during flooding and drainage of the marsh surface, resulting in alternating periods of re-suspension and potential deposition occurring throughout over-marsh tides (Figure 63, D).   In these instances, potential deposition is characterized by prominent reductions in concentration with declining flow velocity during slack tide phases, truncated by increases in concentration associated with velocity pulses.   In contrast, channel-restricted tides show a near-continuous decrease in suspended concentration throughout

tidal cycles (Figure 63, F), reducing from a maximal maximum associated with the first 1 or 2 samples.
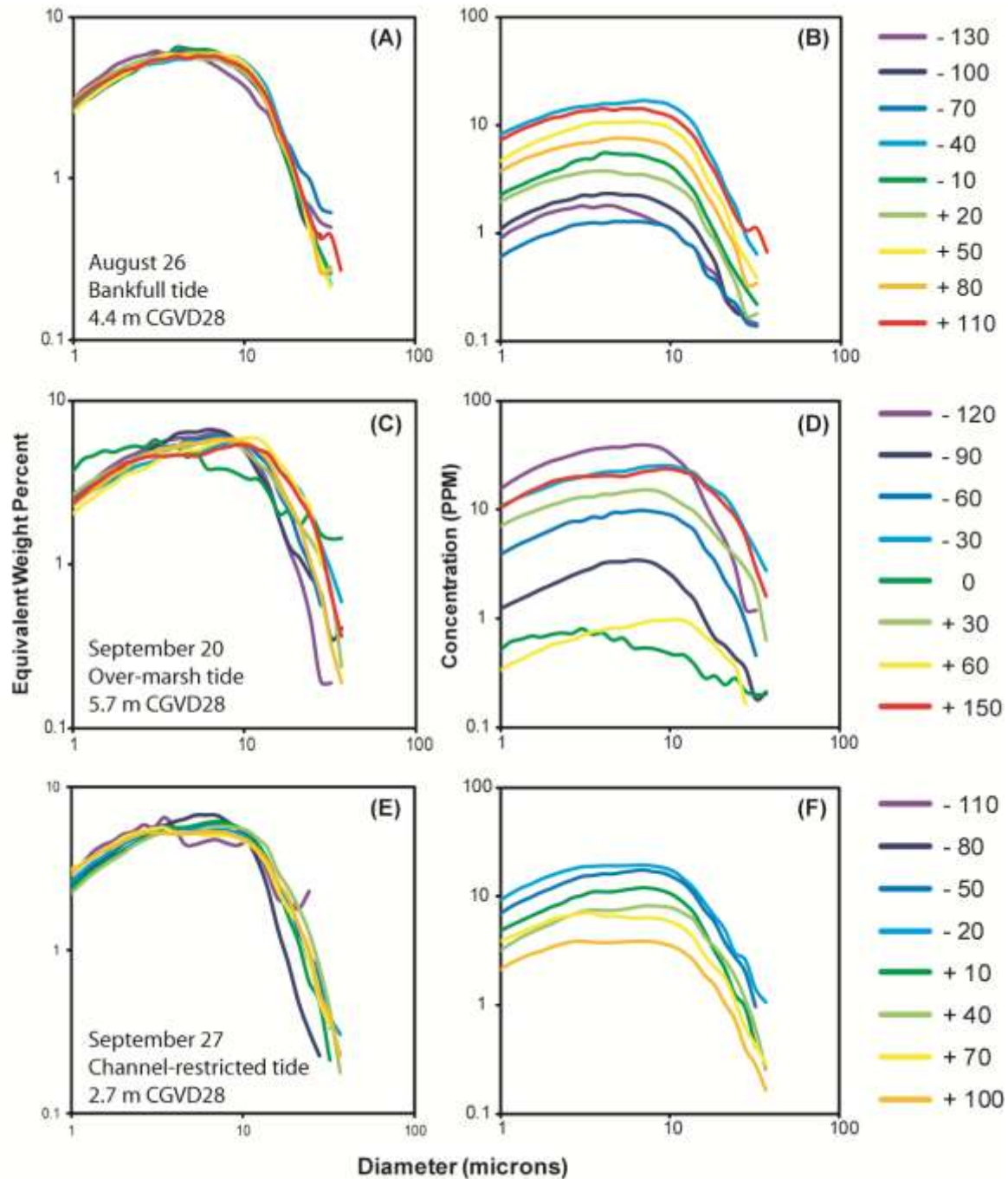
Figure 63: DIGS spectra of suspended sediment samples obtained with the ISCO automated water sampler, and processed using the Coulter Multisizer III. Equivalent weight percent, normalized over the size range, for three tides, is shown in panels A, C and E; corresponding relative changes in concentration (ppm) over the duration of tidal cycles is shown in panels B, D and F. Sample times, in minutes relative to high tide, are shown at right

Suspended sediment DIGS can be linked to DIGS of deposited materials through a residual calculation (C_1-C_2), where the minimum concentration near high tide (C_1) is subtracted from the maximum flood concentration (C_2). This analysis is designed to anticipate the potential contribution to the bed, according to suspended materials, for direct comparison with deposited sediment DIGS. In Figure 64, dashed lines showing 'settled' material illustrate what theoretically was removed from suspension and contributed to the bed, during four tidal cycles. Results suggest variability in the occurrence of particles at both fine and coarse ends of the spectrum, relative to deposited material. Although trapped sediment is slightly coarser, in most cases calculated suspended sediment residuals match well with deposited sediment DIGS. This analysis is not available for Kingsport.
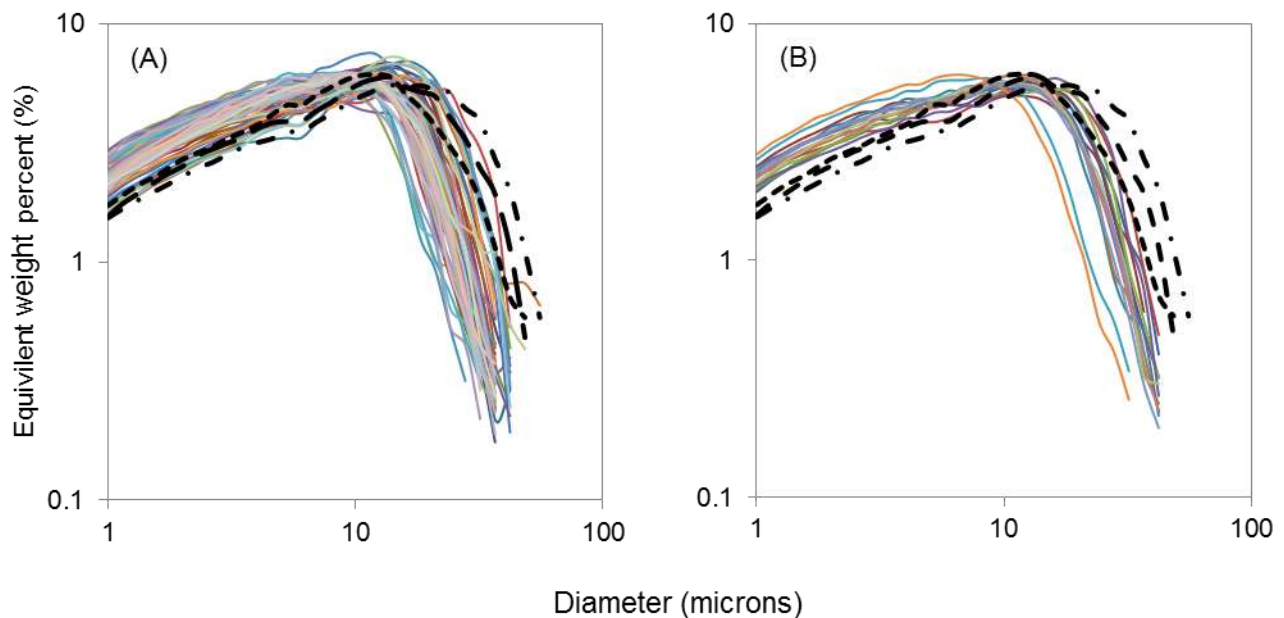
Figure 64: DIGS of surface scrape samples (uppermost 1-3 cm of sediment surface) collected at Starrs Point in 2011 (black dashed lines) are compared with DIGS of deposited sediment collected with surface-mounted sediment traps in 2009 (A) and 2011 (B).

Although flocculation was expected to be strongly correlated with deposition, this was not the case with any of the floc characteristics. Flocculated particles are associated with higher concentrations of suspended sediment making for a muddy environment (Chen et al. 2005; Milligan et al. 2007). In other studies, higher suspended sediment concentrations have been found to lead to higher values of floc limit (Milligan et al. 2007). Here, the suspended sediment concentration correlated with deposition, but the floc fraction, the proportion of grains in flocculated form, and the floc limit, the size at which there is the same flux of flocs as there is of single grains, did not (Table 9). Christiansen et al. (2000) found this pattern of less floc with increasing distance from the creek for all tides with no varying controls between tides.

DISSEMINATION and TECHNOLOGY TRANSFER

Throughout the life of this project there have been numerous opportunities for dissemination of results and technology transfer. The grant provided a major opportunity to standardize sediment processing techniques and approaches (e.g. DIGS) using the Coulter Multisizer 3 between the Particle Dynamics Lab at BIO, Paul Hill's lab at Dalhousie and the In_CoaST research unit at Saint Mary's University. This has significantly increased the capacity of the region to conduct detailed grain size analyses and address fundamental and applied questions of sediment mobility. The project has also played a key role in training 5 HQP ('highly qualified personnel') that will be able to fill a research gap in the region. Casey O'Laughlin completed his graduate thesis within the project and Emma Poirier completed her honours research. She is now continuing her work at the masters level as a Pengrowth scholarship winner and on a new OEER grant. An additional three undergraduate research assistants were also trained.

This research has been presented widely at local (Nova Scotia Energy Research Development Forum, Atlantic Canadian Coastal Estuarine Research Federation, Bay of Fundy Ecosystem Partnership, Atlantic Geological Association) national (Canadian Association of Geographers) and international levels (American Associate of Geographers, Coastal and Estuarine Research Federation). Details are provided in Appendix D.

CONCLUSIONS and RECOMMENDATIONS

The results of this study clearly demonstrate the significant spatial and temporal variability in sediment transport processes and the complexity of interactions between variables. Computer models currently being developed to model sediment transport and deposition should be tested to ensure that they capture at least some of this variability. In addition, models should be run under different conditions (e.g. with storms, varying suspended sediment concentrations, etc…) beyond changes in tidal energy. The amount of sediment deposited, particularly on the marsh surface, appears to be most sensitive to changes in water depth. Therefore even a 5% reduction in tidal amplitude would reduce the number of over-marsh tides by a similar figure, and cause an increase in the occurrence of channel-restricted tides and result in significant changes in inundation time and flooding frequency on the marsh surface. The frequency of marshfull tides can potentially increase as well, in which case amplified erosion of marsh edges may create an additional sediment source. Decreased inundation frequency of high marsh surfaces may impose a sediment deficit in marsh systems, as less material is distributed to the marsh surface from tidal creeks. High marsh areas will likely be the most significantly impacted with a loss of sediment input. This can show impacts in marsh sedimentation and resulting elevation, channel

equilibrium, vegetation community structure, and ecological productivity (Smith and Friedrichs, 2011; Craft *et al.*, 2009; Bertness, 1991).

Potential decreased ebb-flow magnitude is likely to be associated with decreased tidal amplitude, due to less water being put into storage on the marsh surface, as well as less frequent inundation events. Lower magnitude ebb flows may show less capacity for sedimentary work, reducing sediment mobility during ebb phases. The result may be creek infilling and a reduction in bank steepness, which would likely have continued impacts on creek hydrodynamics and sediment transport. Reduced bank steepness may further accelerate creek infilling, through reduction of in-channel currents, such as ebb-phase gravity-driven drainage of marsh surfaces, which mediate bank elevations through ebb-stage re-suspension of newly introduced materials (Reed, 1988). A continuation and exacerbation of this cycle would constitute a non-linear response of fine-grained materials in tidal creeks, and would impact the movement of water in and out of the estuary through changes in deposition and erosion patterns and the resulting basin geometry. Either a circumstance of decreased sediment supply to the marsh surface, or an increase in in-channel sedimentation, will impact the form and function of salt marshes. It has been shown that changes to balanced sediment budgets will show the greatest impact in accretion rates on low marsh surfaces (Chmura *et al.*, 2001).

While this research has led to an increased understanding of the factors controlling sediment transport and deposition, it has also raised our awareness of the spatial and temporal complexity of these processes. Future field data collection efforts should try to get a better picture of the significant fluctuations in suspended sediment concentrations in the exposed marsh and mudflat system, given the challenges during the Kingsport deployment. It would be ideal to couple a LISST device, or autoranging OBS and an in-situ camera to try and describe this fluctuations. In addition, a better method needs to be developed to monitor changes in surface elevation over time since the pins alone were not useful. It is recommended that the research be expanded to include a greater range of seasonal conditions and simultaneous measurements at multiple locations. It will be critical that computer models be tested for a range of environmental conditions and at a sufficiently fine spatial scale to resolve differences in sediment transport processes between un-vegetated creek or mudflat surfaces and the marsh surface. In addition, given the sensitivity of intertidal sediment transport processes and deposition to water depth, it is recommended that a Basin wide GIS assessment be conducted to identify the areas that will be most sensitive (e.g. upper marsh) to changes in tidal amplitude.

- Allen, J.R.L. and Duffy, M.J. 1998. Medium-term sedimentation on high intertidal mudflats and saltmarshes in the Severn Estuary, SW Britain: the role of wind and tide. *Marine Geology*, 150: 1-27.

- Amos CL, Mosher DC. 1985. Erosion and deposition of fine-grained sediments from the Bay of Fundy. *Sedimentology* **32**: 815-832.

- Biron PM, Robson C, Lapointe MF, Gaskin SJ. 2004. Comparing different methods of bed shear stress estimates in simple and complex flow fields. *Earth Surface Processes and Landforms* **29**: 1403-1415. DOI: 10.1002/esp.1111

- Blanton JO, Lin G, Elston SA. 2002. Tidal current asymmetry in shallow estuaries and tidal creeks. *Continental Shelf Research* **22**: 1731-1743.

- Blott, S.J. and Pye, K. (2001) GRADISTAT: a grain size distribution and statistics package for the analysis of unconsolidated sediments. Earth Surface Processes and Landforms 26, 1237-1248.

- Bowron, T.; Neatt, N.; van Proosdij, D.; Lundholm, J. and J. Graham. 2011. Macro-tidal Salt Marsh Ecosystem Response to Culvert Expansion. Restoration Ecology 19(3):307-322. DOI: 10.1111/j.1526-100X.2009.00602.x

- Bryden IG, Grinsted T, Melville GT. 2004. Assessing the potential of a simple channel to deliver useful energy. *Applied Ocean Research* **26**: 198-204. doi:10.1016/j.apor.2005.04.001

- Chmura, G.L., Helmer, L.L., Beecher, C.H. and Sunderland, E.L. 2001. Historical rates of salt marsh accretion on the outer Bay of Fundy. *Canadian Journal of Earth Science*, 38: 1081-1092.

- Christiansen T, Wilberg PL, Milligan TG. 2000. Flow and sediment transport on a tidal salt marsh surface. *Estuarine, Coastal and Shelf Science* **50**: 315-331. DOI: 10.1006/ecss.2000.0548

- Curran KJ, Hill PS, Schnell TM, Milligan TG, Piper DJW. 2004. Inferring the mass fraction of floc-deposited mud: application to fine-grained turbidites. *Sedimentology* **51**: 927-944. DOI: 10.1111/j.1365-3091.2004.00647.x

- Davidson-Arnott RGD, van Proosdij D, Ollerhead J, Schostak L. 2002. Hydrodynamics and sedimentation in salt marshes: examples from a macrotidal marsh, Bay of Fundy. *Geomorphology* **48**: 209-231.

- Dupont F, Hannah C, Greenberg D. 2005. Modelling the Sea Level in the Upper Bay of Fundy. Atmos.-Ocean. **43**(1), 33-47.

- Fagherazzi, S. and Priestas, A. M. 2010. Sediments and water fluxes in a muddy coastline: interplay between waves and tidal channel hydrodynamics. *Earth Surface Processes and Landforms,* 35: 284-293.

- French JR, Stoddart DR. 1992. Hydrodynamics of Salt Marsh Creek Systems: Implications for Marsh Morphological Development and Material Exchange. *Earth Surface Processes and Landforms* **17**: 235-252.

- Friedrichs CT, Perry JE. 2001. Tidal salt marsh morphodynamics: a synthesis. *Journal of Coastal Research* **27**: 7-37.

- Fugate DC, Friedrichs CT. 2002. Determining concentration and fall velocity of estuarine particle populations using ADV, OBS and LISST. *Continental Shelf Research* **22**:1867-1886.

- Ganju, N.K., Schoellhamer, D.H. and Bergamaschi, B.A. 2005. Suspended sediment fluxes in a tidal wetlands: measurement, controlling factors, and error analysis. *Estuaries,* 28(6): 812-822.

- Gordon DC. 1994. Intertidal ecology and potential power impacts, Bay of Fundy, Canada. *Biological Journal of the Linnean Society* **51**: 17-23.

- Graham, G.W., and Manning, A.J. 2007. Floc size and settling velocity within a *Spartina anglica* canopy. *Continental Shelf Research*, 27: 1060-1079.

- Hill PS, Newgard JP, Milligan TG. 2012 Flocculation on a muddy intertidal flat in Willapa Bay, Washington, Part II: Observations of suspended particle size in a secondary channel and adjacent flat. *Continental Shelf Research*: 44 pp.

- Hoitink AJF, Hoekstra P. 2005. Observations of suspended sediment from ADCP and OBS measurements in a mud-dominated environment. *Coastal Engineering* **52**: 103-118. DOI: 10.1016/j.coastaleng.2004.09.005

- Karsten RH, McMillan JM, Lickley MJ, Haynes RD. 2008. Assessment of tidal current energy in the Minas Passage, Bay of Fundy. *Proceedings of the Institution of Mechanical Engineers* **222 (A-J)**: 493-507.

- Kim SC, Friedrichs CT, Maa JP-Y, Wright LD. 2000. Estimating bottom stress in tidal boundary layer from acoustic Doppler velocimeter data. Journal of Hydraulic Engineering, ASCE 126 (6): 399–406.

- Kim SC, Voulgaris G. 2003. Estimation of suspended sediment concentration in estuarine environments using acoustic backscatter from an ADCP. *Proceedings of the Fifth International Conference on Coastal Sediments*, 2003. 10pp.

- Kranck K, Smith P, Milligan TG. 1996a. Grain-size characteristics of fine-grained unflocculated sediments I: 'one-round' distributions. *Sedimentology* **43**: 589-596.

- Kranck K, Smith P, Milligan TG. 1996b. Grain-size characteristics of fine-grained unflocculated sediments II: 'multi-round' distributions. *Sedimentology* **43**: 597-606.

- Kranck K, Milligan TG. 1991. Grain size in oceanography. In: Syvitski, JPM [ed]. *Principles, Methods, and Applications of Particle Size Analysis*. Cambridge University Press: 368 pp.

- Lane et al. 1998 Lane SN, Biron PM, Bradbrook KF, Butler JB, Chandler JH, Crowell MD, McLelland SJ, Richards KS, Roy AG. 1998. Three dimensional measurement of river channel flow processes using acoustic Doppler velocimetry. Earth Surface Processes and Landforms 23: 1247–1267.

- Law BA, Hill PS, Milligan TG, Curran KJ, Wiberg PL, Wheatcroft RA. 2008. Size sorting of fine-grained sediments during erosion: Results from the western Gulf of Lions. *Continental Shelf Research* **28**: 1935-1946.

- Leonard LA, Croft AL. 2006. The effect of standing biomass on flow velocity and turbulence in *Spartina alterniflora* canopies. *Estuarine, Coastal and Shelf Science* **69**: 325-336. DOI: 10.1016/j.ecss.2006.05.004

- MacDonald, G.; Noel, P; van Proosdij, D. and G. Chmura. 2010. The Legacy of Agricultural reclamation on surface hydrology of salt marshes of the Bay of Fundy. Estuaries and Coasts 33:151-160. DOI 10.1007/s12237-009-9222-4

- Milligan TG, Law BA. 2005. The effect of marine agriculture on fine sediment dynamics in coastal inlets. In: Hargrave, B. [ed]. Environmental Effects of Marine Finfish Aquaculture. *The Handbook of Environmental Chemistry* **5**: Water Pollution. Springer, Berlin Heidelbrg New York, 467 pp.

- Neumeier U, Amos CL. 2006. The influence of vegetation on turbulence and flow velocity in European salt-marshes. *Sedimentology* **53**: 259-277. DOI: 10.1111/j.1365-3091.2006.00772x

- O'Laughlin and van Proosdij, 2012

- Polagye BL, Malte PC. 2010. Far-field dynamics of tidal energy extraction in channel networks. *Renewable Energy* **36**: 222-234. DOI:10.1016/j.renene.2010.06.025

- Polagye B, Van Cleve B, Copping A, Kirkendall K (eds). 2011. Environmental effects of tidal energy development. *U.S. Dept. Commerce, NOAA Tech. Memo*. 181 pp.

- Puleo AJ, Johnson RV, Butt T, Kooney TN, Holland KT. 2007. The effect of air bubbles on optical backscatter sensors. Marine Geology 230: 87-97.

- Roy AG, Biron P, De Serres B. 1996. On the necessity of applying a rotation to instantaneous velocity measurements in river flows. Earth Surface Processes and Landforms 21: 817-827.

- Sheldon RW. 1972. Size separation of marine seston by membrane and glass-fiber filters. Limnology and Oceanography 17 (3): 494-498.

- Sheldon RW, Sutcliffe WH. 1969. Retention of marine particles by screens and filters. Limnology and Oceanography 14 (3): 441-444.

- Soulsby RL. 1983. The bottom boundary layer of shelf seas. Elsevier Oceanography Series 35: 189-266.

- Sun X, Chick JP, Bryden IG. 2008. Laboratory-scale simulation of energy extraction from tidal currents. *Renewable Energy* **23**: 1267-1274.

- Temmerman, S., Govers, G., Wartel, S. and Meire, P. 2004. Modelling estuarine variations in tidal marsh sedimentation: response to changing sea level and suspended sediment concentrations. *Marine Geology,* 212: 1-19.

- Thorne PD, Hardcastle PJ, Soulsby RL. 1993. Analysis of acoustic measurements of suspended sediment. Journal of Geophysical Research 98 (C1): 899– 910.

- Thorne PD, Hanes DM. 2002. A review of acoustic measurements of small-scale sediment processes. *Continental Shelf Research* **22**: 603-632

- Turk TR, Risk MJ, Hirtle RWM, Yeo RK. 1980. Sedimentological and biological changes in the Windsor mudflat, and area of induced siltation. *Canadian Journal of Fisheries and Aquatic Sciences* **37**: 1387-1397.

- van Proosdij D, Davidson-Arnott RGD, Ollerhead J. 2006a. Controls on spatial patterns of sediment deposition across a macro-tidal salt marsh surface over single tidal cycles. *Estuarine, Coastal and Shelf Science* **69**: 64-86. DOI: 10.1016/j.ecss.2006.04.022

- van Proosdij D, Milligan T, Bugden G, Butler K. 2009. A tale of two macro-tidal estuaries: differential morphodynamic response of the intertidal zone to causeway construction. *Journal of Coastal Research*, Special Issue **56**: 772-776.

- van Proosdij, D.; Lundholm, J.; Neatt, N.; Bowron, T. and J. Graham. 2010. Ecological Re-engineering of a Freshwater Impoundment for Salt Marsh Restoration in a Hypertidal System. Journal of Ecological Engineering 36(10):1314-1332. DOI:10.1016/j.ecoleng.2010.06.008

- Voulgaris G, Meyers ST. 2004. Temporal variability of hydrodynamics, sediment concentration and sediment settling velocity in a tidal creek. *Continental Shelf Research* **24**: 1659-1683. DOI: 10.1016/j.csr.2004.05.006

- Whitford, 2008 Whitford, J. 2008. Background Report for the Fundy Tidal Energy Strategic Environmental Assessment. OEER Project #1028476, 21pp.

- Yeo RK, Risk MJ. 1979. Fundy tidal power: Environmental sedimentology. *Geoscience Canada* **6 (3)**: 115-121.

APPENDIX A

Sampling locations - Starrs Point (2009 & 2011) and Kingsport (2010 & 2012)						
	Plot ID	**Location**	**Easting**	**Northing**	**Elevation (CGVD28)**	**Instruments deployed**
Starrs Point 2009	V1	bank	392558.63	4995691.969	1.257	ADV, OBS
	V2	thalweg	392558.3	4995694.842	0.469	ADV, OBS
	ADCP	thalweg	392555.73	4995692.86	0.5163	ADCP
	Traps	bank	3925570.4	4995693.415	0.678	Traps
Starrs Point 2011	M1	high marsh	392568.63	4995676.675	4.32	ADV, OBS, traps
	M2	high marsh	392562.06	4995684.149	4.12	ADV, traps
	M3	creek edge	392559.97	4995686.498	3.18	ADV, OBS, traps
	C4	thalweg	392555.14	4995691.959	0.28	ADCP, traps
Kingsport 2010	V1	mid-marsh	392424.18	5001054.38	2.882	ADV, OBS, traps
	V2	low marsh	392425.22	5001047.288	2.104	ADV, traps
	V3	low marsh	392428.88	5001033.888	1.44	ADV, OBS, traps
	M4	mudflat	392430.97	5001025.817	1.344	ADCP, traps

Table 5: Projected geographic coordinates for stations and associated elevations.   Easting and Northing expressed relative to NAD83 CSRS UTM zone 20 datum and elevations are relative to CGD28 vertical datum.

APPENDIX B

Summary of Data Collected

Tidal Conditions – Starr's Point 2009			Data Collected				
Date	Elevation (CGVD28) (m)		ADCP	Bank array ADV/OBS1	Thalweg array ADV/OBS2	Traps	Comments
	Predicted	Observed					
04-Aug-09	3.3	3.6	Channel-Restricted				✓	
05-Aug-09	3.5	3.8	Channel-Restricted	✓		✓	✓	Thalweg array start (V2)
06-Aug-09	3.8	3.9	Channel-Restricted	✓	✓	✓	✓	Bank array start (V1)
07-Aug-09	4.1	4.1	Channel-Restricted	✓	✓	✓	✓	
08-Aug-09	4.3	4.2	Channel-Restricted	✓	✓	✓	✓	
09-Aug-09	4.4	4.2	Channel-Restricted	✓	✓	✓	✓	V2 error (late start)
10-Aug-09	4.5	4.2	Channel-Restricted	✓	✓	✓		Rain: No traps.
11-Aug-09	4.3	4.1	Channel-Restricted	✓	✓	✓		Rain: No traps.
12-Aug-09	4.5	4.1	Channel-Restricted	✓	✓	✓	✓	
20-Aug-09	5.1	5.3	Over-Marsh	✓	✓	✓	✓	
21-Aug-09	5.2	5.5	Over-Marsh	✓	✓	✓	✓	
23-Aug-09	5.2	5.2	Over-Marsh		✓	✓		Hurricane Bill
24-Aug-09	5	5.3	Over-Marsh	✓	✓	✓	✓	
25-Aug-09	4.7	4.9	Over-Marsh	✓	✓	✓	✓	
26-Aug-09	4.3	4.4	Channel-Restricted	✓	✓	✓	✓	
20-Sep-09	5.2	5.7	Over-Marsh	✓	✓	✓	✓	
26-Sep-09	3.3	3.3	Channel-Restricted	✓	✓	✓	✓	
27-Sep-09	2.7	2.7	Channel-Restricted	✓	✓	✓	✓	

Table 6: Summary of data collected at Starrs Point in 2009 associated with Year 1 of Casey O'Laughlin's MSc thesis. Field data collection funded by OEER and PERD.

2010	Conditions						Instruments & Data Sampled						
Date	Tide (time)		Tide height (m)			Spring/Neap	ADCP	OBS & V1	V2	OBS & V3	Sediment Traps	ISCO	rising stage SSC
	CHS	ADCP	CHS	at ADCP	CGVD28								
25-Jun	0:07	0:17	13.7	5.25	6.49	SPRING	✓	✓	✓				
25-Jun	12:37	12:46	13.0	4.7	5.94	SPRING	✓	✓	✓	✓	✓		
26-Jun	13:25	13:36	13.7	4.72	5.96	SPRING	✓	✓	✓	✓	✓		
27-Jun	1:43	1:51	13.7	5.29	6.53	SPRING	✓	✓	✓	✓	✓		
28-Jun	2:27	2:36	13.6	5.17	6.41	TRANS	✓	✓	✓	✓	✓		
28-Jun	14:55	15:04	13.0	4.59	5.83	TRANS	✓	✓	✓	✓			
29-Jun	3:11	3:20	13.5	4.95	6.19	TRANS	✓	✓	✓	✓	✓		
25-Jul	0:36	0:50	13.2	4.97	6.21	SPRING	✓	✓	✓	✓	✓		
25-Jul	13:05	13:16	12.7	4.56	5.80	SPRING	✓	✓	✓	✓	✓		
26-Jul	1:22	1:38	13.4	5.05	6.29	SPRING	✓	✓	✓	✓	✓	✓	
28-Jul	2:47	2:55	13.4	4.98	6.22	TRANS	✓	✓	✓	✓	✓		✓
28-Jul	15:11	15:14	13.1	4.59	5.83	TRANS	✓	✓	✓	✓	✓		✓
29-Jul	3:27	3:29	13.4	4.82	6.06	TRANS	✓	✓	✓	✓	✓		✓
05-Aug	9:11	8:31	11.8	4.16	5.40	TRANS		✓	✓	✓	✓	✓	✓
05-Aug	21:38	21:00	12.6	3.52	4.76	TRANS	✓	✓	✓	✓	✓	✓	✓
06-Aug	10:11	-	12.0	-	-	TRANS		✓	✓	✓	✓	✓	✓
10-Aug	1:15	1:04	14.4	6.08	7.32	SPRING	✓	✓	✓	✓	✓	✓	✓
10-Aug	13:42	13:33	14.1	5.77	7.01	SPRING	✓	✓	✓	✓	✓	✓	✓
11-Aug	2:03	1:54	14.7	6.33	7.57	TRANS	✓	✓	✓	✓	✓		✓
12-Aug	2:49	2:50	14.9	6.39	7.63	TRANS	✓	✓		✓	✓	✓	✓
12-Aug	15:14	15:16	14.7	6.19	7.43	TRANS	✓	✓		✓	✓	✓	✓
13-Aug	3:36	3:41	14.8	6.19	7.43	TRANS	✓	✓		✓	✓	✓	✓
13-Aug	16:00	16:10	14.7	6.12	7.36	TRANS	✓	✓		✓	✓	✓	✓
14-Aug	16:48	17:01	14.5	5.86	7.10	TRANS	✓	✓		✓	✓	✓	✓
15-Aug	5:12	5:26	14.1	5.43	6.67	NEAP	✓	✓		✓	✓	✓	✓
15-Aug	17:37	17:52	14.1	5.53	6.77	NEAP	✓	✓		✓	✓	✓	✓
16-Aug	6:03	6:14	13.5	4.89	6.13	NEAP	✓	✓		✓	✓	✓	✓
03-Sep	21:12	20:26	12.6	4.28	5.52	TRANS	✓	✓		✓			
04-Sep	9:47	9:15	12.2	4.54	5.78	TRANS	✓	✓		✓		✓	
04-Sep	22:14	21:32	12.9	3.95	5.19	TRANS	✓	✓		✓		✓	
05-Sep	10:47	10:18	12.6	4.26	5.50	TRANS	✓	✓		✓			
09-Sep	1:42	1:36	14.8	6.42	7.66	SPRING	✓	✓	✓		✓		✓
09-Sep	14:05	14:02	14.8	6.4	7.64	SPRING	✓	✓	✓		✓		✓
10-Sep	2:28	2:28	14.9	6.45	7.69	TRANS	✓	✓	✓		✓		✓
10-Sep	14:50	14:54	15.0	6.43	7.67	TRANS	✓	✓	✓		✓		✓
11-Sep	15:35	15:40	14.9	6.25	7.49	TRANS	✓	✓	✓	✓	✓		✓

Table 7: Summary of data collected and instruments deployed at Kingsport.

Date	Tide Time (CHS)	Tide Height (m) (CHS)	OBS1 &V1	OBS2 &V2	V3	ADCP	RBR	ISCO	M1	M2	M3	C4
Jun 1	13:17	12.9			✔	✔	✔	✔			✔	✔
Jun 2	1:34	13.7			✔	✔	✔	✔	✔	✔	✔	✔
Jun 2	14:00	13.1			✔	✔	✔	✔			✔	✔
Jun 3	2:18	13.9			✔	✔	✔	✔	✔	✔	✔	✔
Jun 3	14:44	13.3			✔	✔	✔	✔			✔	✔
Jun 4	3:02	14.0		✔	✔	✔	✔	✔	✔	✔	✔	✔
Aug 1	14:49	14.3	✔	✔	✔	✔	✔	✔	✔	✔	✔	✔
Aug 2	3:10	14.7	✔	✔	✔	✔	✔	✔				
Aug 2	15:35	14.5	✔	✔	✔	✔	✔	✔				
Aug 3	3:56	14.7	✔	✔	✔	✔	✔	✔				
Aug 3	16:21	14.5	✔	✔	✔	✔	✔	✔				
Aug 4	4:44	14.4	✔	✔	✔		✔	✔	✔	✔	✔	✔
Aug 30	2:03	14.7	✔	✔	✔	✔	✔	✔	✔	✔	✔	✔
Aug 30	14:26	14.7	✔	✔	✔	✔	✔	✔	✔	✔	✔	✔
Aug 31	2:48	14.9	✔	✔	✔	✔	✔	✔	✔	✔	✔	✔
Aug 31	15:11	14.9	✔	✔	✔	✔	✔	✔	✔	✔	✔	✔
Sep 1	3:34	14.8	✔	✔	✔		✔	✔	✔	✔	✔	✔
Sep 1	15:57	14.9	✔	✔	✔	✔	✔	✔	✔	✔	✔	✔
Sep 2	4:21	14.6	✔	✔	✔	✔	✔	✔	✔	✔	✔	✔

Table 8: Experimental summary at Starrs Point in 2011 that is the basis for Emma Poirier's honours thesis. M1, M2, M3 and C4 represent trap data.

2010 Date	depth (m) at ADCP	Tide	Sediment deposition (g/ m²) plot 1	plot 2	plot 3	plot 4	max water depth at plot (m) 1	2	3	4	V1 (cm/s) flood	ebb	V2 flood	ebb	V3 flood	ebb
25-Jun	5.94	SPRING	12.97	13.69	13.07	13.60	3.14	3.74	4.54	4.64	1.27	1.21	1.20	1.01	1.82	1.34
26-Jun	5.96	SPRING	10.38	9.94	10.81	12.05	3.16	3.76	4.56	4.66	1.43	1.20	1.07	0.97	1.65	1.46
27-Jun	6.53	SPRING	14.42	16.63	12.78	14.37	3.73	4.33	5.13	5.23	1.24	1.27	1.14	0.99	1.76	2.54
28-Jun	6.41	TRANS	3.74	4.64	4.61	5.77	3.61	4.21	5.01	5.11	1.19	1.27	1.21	1.11	1.94	1.87
28-Jun	5.83	TRANS	8.90	8.09	7.95	11.45	3.03	3.63	4.43	4.53	3.37	2.23	2.64	1.92	2.71	2.03
29-Jun	6.19	TRANS	11.71	9.02	12.15	10.77	3.39	3.99	4.79	4.89	1.02	1.10	0.84	0.92	1.85	1.24
25-Jul	6.21	SPRING	12.41	13.25	13.49	13.66	3.41	4.01	4.81	4.91	1.62	2.00	1.27	1.07	1.97	1.89
25-Jul	5.80	SPRING	7.13	8.25	15.91	16.18	3.00	3.60	4.40	4.50	1.57	1.81	1.14	0.89	1.73	1.22
26-Jul	6.29	SPRING	11.72	9.99	11.62	13.79	3.49	4.09	4.89	4.99	1.96	2.16	0.96	0.88	1.7	1.52
28-Jul	6.22	TRANS	12.42	16.00	14.86	14.09	3.42	4.02	4.82	4.92	1.57	2.00	1.02	0.89	1.49	1.55
28-Jul	5.83	TRANS	9.66	7.69	8.60	7.61	3.03	3.63	4.43	4.53	1.71	2.34	1.42	1.21	1.77	1.50
29-Jul	6.06	TRANS	20.58	26.58	29.58	23.34	3.26	3.86	4.66	4.76	2.60	2.70	1.69	1.78	1.89	1.77
05-Aug	5.40	TRANS	18.98	20.83	16.08	16.43	2.60	3.20	4.00	4.10	4.62	4.18	0.99	0.73	1.25	1.35
05-Aug	4.76	TRANS	3.64	4.70	7.16	15.69	1.96	2.56	3.36	3.46	2.52	2.53	1.51	1.37	1.94	1.82
06-Aug		TRANS	13.97	13.83	13.78	13.07					2.61	2.88	1.21	1.17	1.13	1.36
10-Aug	7.32	SPRING	11.32	13.85	11.19	12.06	4.52	5.12	5.92	6.02	1.26	1.43	0.91	1.02	1.82	1.99
10-Aug	7.01	SPRING	14.02	15.53	17.10	21.36	4.21	4.81	5.61	5.71	1.11	1.31	0.96	0.89	2.05	1.59
11-Aug	7.57	TRANS	13.14	18.08	13.29	16.35	4.77	5.37	6.17	6.27	1.18	1.55			1.51	1.81
12-Aug	7.63	TRANS	8.54	12.56	13.70	24.83	4.83	5.43	6.23	6.33	1.12	1.34			1.54	1.79
12-Aug	7.43	TRANS	22.00	22.88	25.55	19.80	4.63	5.23	6.03	6.13	0.91	0.81			1.71	1.67
13-Aug	7.43	TRANS	18.51	21.51	18.66	20.69	4.63	5.23	6.03	6.13	1.40	1.26			1.75	1.70
13-Aug	7.36	TRANS	11.93	13.51	17.37	19.65	4.56	5.16	5.96	6.06	0.92	1.24			1.65	1.74
14-Aug	7.10	TRANS	11.19	12.26	11.95	14.29	4.30	4.90	5.70	5.80	1.08	1.04			1.78	1.38
15-Aug	6.67	NEAP	16.19	17.09	19.00	16.81	3.87	4.47	5.27	5.37	1.21	1.23			1.61	1.48
15-Aug	6.77	NEAP	12.50	13.53	17.97	17.28	3.97	4.57	5.37	5.47	1.21	1.05				
16-Aug	6.13	NEAP	14.21	17.98	16.02	13.26	3.33	3.93	4.73	4.83					1.47	1.27
09-Sep	7.66	SPRING	18.55	9.70	15.84	13.25	4.86	5.46	6.26	6.36	1.57	1.49	1.26	1.15		
09-Sep	7.64	SPRING	9.29	9.46	18.74	14.14	4.84	5.44	6.24	6.34	1.03	1.45	0.88	1.21		
10-Sep	7.69	TRANS	9.65	10.33	11.91	11.02	4.89	5.49	6.29	6.39	1.37	1.41	0.95	1.06		
10-Sep	7.67	TRANS	14.59	22.40	10.09	11.63	4.87	5.47	6.27	6.37	1.28	1.56	0.94	1.05		
11-Sep	7.49	TRANS	8.79	11.39	7.14	11.95	4.69	5.29	6.09	6.19	1.54	2.42	1.22	2.17	1.43	1.92

2010 Date	depth (m) at ADCP	Tide	Sediment deposition (g/ m^2) plot 1	plot 2	plot 3	plot 4	Floc fraction 1	2	3	4	Floc limit 1	2	3	4	source slope 1	2	3	4
25-Jun	6.494	SPRING	-	-	-	-												
25-Jun	5.944	SPRING	12.97	13.69	13.07	13.60		0.27	0.71	0.67		6	21	12		0.75	0.56	0.19
26-Jun	5.964	SPRING	10.38	9.94	10.81	12.05				0.81				24				0.12
27-Jun	6.534	SPRING	14.42	16.63	12.78	14.37	0.82	0.73	0.68	0.80	21	14	18	21	0.44	0.45	0.56	0.44
28-Jun	6.414	TRANS	3.74	4.64	4.61	5.77		0.63	0.61			12	16			18	0.08	
28-Jun	5.834	TRANS	8.90	8.09	7.95	11.45	0.54	0.60	0.71	0.73	12	12	14	14	0.20	0.08	0.19	0.32
29-Jun	6.194	TRANS	11.71	9.02	12.15	10.77	0.59	0.53	0.66	0.40	12	11	12	9	0.23	0.33	0	0.39
25-Jul	6.214	SPRING	12.41	13.25	13.49	13.66												
25-Jul	5.804	SPRING	7.13	8.25	15.91	16.18		0.64	0.61	0.33		12	12	4		0.19	0.43	-0.1
26-Jul	6.294	SPRING	11.72	9.99	11.62	13.79	0.66	0.34	0.72	0.74	16	6	18	16	0.61	0.15	0.43	0.33
28-Jul	6.224	TRANS	12.42	16.00	14.86	14.09	0.81	0.59	0.28	0.50	21	16	3	6	0.40	0.35	-0	-0.1
28-Jul	5.834	TRANS	9.66	7.69	8.60	7.61												
29-Jul	6.064	TRANS	20.58	26.58	29.58	23.34												
05-Aug	5.404	TRANS	18.98	20.83	16.08	16.43	0.76	0.74		0.59	21	18		16	0.46	0.51		0.35
05-Aug	4.764	TRANS	3.64	4.70	7.16	15.69	0.67	0.53	0.77	0.75	14	11	18	18	0.54	0.52	0.38	0.65
06-Aug		TRANS	13.97	13.83	13.78	13.07												
10-Aug	7.324	SPRING	11.32	13.85	11.19	12.06	0.75	0.54	0.75	0.72	14	7	16	16	0.14	0.37	0.39	0.37
10-Aug	7.014	SPRING	14.02	15.53	17.10	21.36	0.63	0.80	0.81	0.56	12	24	21	6	0.72	0.42	0.19	0.45

Table 9: Detailed sediment characteristics, hydrodynamics and deposition at Kingsport in 2010.

APPENDIX D

Detailed list of presentations

- O'Laughlin*, C. and D. van Proosdij. 2010. Spring-neap sediment dynamics within a macro-tidal salt marsh tidal creek: preliminary findings. Oral presentation at the Atlantic Geology Association in Wolfville, NS Feb 6, 2010.

- van Proosdij, D. and C. O'Laughlin. 2010. Effects of tidal energy extraction on sediment dynamics of intertidal ecosystems. Oral presentation at the NS Energy and Research Forum, Halifax, NS. May 26-27, 2010.

- O'Laughlin, C.* and D. van Proosdij. 2010. Effects of Energy Extraction on Intertidal Ecosystems of the Minas Basin. Poster Presentation at the NS Energy and Research Forum, Halifax, NS. May 26-27, 2010.

- van Proosdij, D. and C. O'Laughlin. 2010. Sediment Dynamics of an Intertidal Ecosystem over the Spring/Neap Cycle. Oral presentation at the Canadian Association of Geographers and Canadian Geomorphology Research Group Annual meeting. Regina, Saskatchewan June 1-4, 2010.

- O'Laughlin, C.* and D. van Proosdij. 2010. Spring/Neap Variations in Tidal Creek Hydrodynamics. Oral presentation at the Canadian Association of Geographers and Canadian Geomorphology Research Group Annual meeting. Regina, Saskatchewan June 1-4, 2010.

- O'Laughlin, C and D. van Proosdij. (June 1-5, 2010). *Spring-neap variations in tidal creek hydrodynamics, Bay of Fundy.*   50th Annual Canadian Association of Geographer's Meeting and Canadian Geomorphological Research Group, Regina, Sack.

- D. van Proosdij and C. O'Laughlin. (June 1-5, 2010). *Sediment dynamics within a macro-tidal creek over spring-neap tidal cycles.*   50th Annual Canadian Association of Geographer's Meeting and Canadian Geomorphological Research Group, Regina, Sack.

- van Proosdij, D. & C. O'Laughlin. (Oct 13-14, 2010). *Effects of Energy Extraction on Intertidal Ecosystems of the Minas Basin: Challenges and lessons learnt.* OEER/FORCE Tidal Energy Workshop, Wolfville, NS.

- *van Proosdij, D & C. O'Laughlin (Apr 12-16, 2011). *Sediment Dynamics within a Salt Marsh Tidal Creek.* Coastal and Marine Sciences Specialty Group, American Association of Geographers Annual Meeting, Seattle WA. Invited oral.

- *O'Laughlin, C. and D. van Proosdij (April 12-16, 2011). *Spring-neap Dynamics in Intertidal Hydrodynamics and Sedimentation in the Bay of Fundy.* Coastal and Marine Sciences Specialty Group, American Association of Geographers Annual Meeting, Seattle WA. Poster. Canadian Geomorphological Research Group student poster award.

- van Proosdij, D., C.O'Laughlin*, T. Milligan, R. Mulligan and E. Poirier (Sept 27-30, 2011) *Potential Far Field Effects of Tidal Energy Extraction on Intertidal Ecosystems in the Bay of Fundy.* Bay of Fundy Ecosystem Partnership Bi-annual meeting, St. John New Brunswick. Oral.

- *<u>O'Laughlin, C</u> and D. van Proosdij.(Sept 27-30, 2011). *Intertidal Energy and Sedimentation in the Bay of Fundy.* Bay of Fundy Ecosystem Partnership Bi-annual meeting, St. John New Brunswick. Oral

- *<u>Poirier, E.</u> ; van Proosdij,D and <u>C. O'Laughlin.</u> (Sept 27-30, 2011). *Sedimentary Dynamics within a Hyper-tidal Salt Marsh and Tidal Creek System.* Bay of Fundy Ecosystem Partnership Bi-annual meeting, St. John New Brunswick. Oral

- van Proosdij, D., <u>C. O'Laughlin</u>*, T. Milligan, R. Mulligan and <u>E. Poirier</u> (Sept 27-30, 2011) *Potential Far Field Effects of Tidal Energy Extraction on Intertidal Ecosystems in the Bay of Fundy.* Bay of Fundy Ecosystem Partnership Bi-annual meeting, St. John New Brunswick. Oral.

- *<u>O'Laughlin, C</u> and D. van Proosdij (Sept 27-30, 2011). *Intertidal Energy and Sedimentation in the Bay of Fundy.* Bay of Fundy Ecosystem Partnership Bi-annual meeting, St. John New Brunswick. Oral .

- *<u>Poirier, E.</u> ; van Proosdij,D and <u>C. O'Laughlin.</u> (Sept 27-30, 2011). *Sedimentary Dynamics within a Hyper-tidal Salt Marsh and Tidal Creek System.* Bay of Fundy Ecosystem Partnership Bi-annual meeting, St. John New Brunswick. Oral

- *van Proosdij, D**.,** <u>O'Laughlin, C</u>., Mulligan, R., Milligan, T. and <u>E. Poirier</u>**.** (Nov 5-11, 2011). *Potential far field effects of tidal energy extraction on intertidal ecosystems of the Bay of Fundy.* 21st Coastal Estuarine Research Federation Meeting, Special session on Marine Energy. Daytona Beach, Florida. Oral.

- *<u>O'Laughlin, C</u> and D. van Proosdij.(Nov 5-11, 2011). *Intertidal Energy and Sedimentation in the Bay of Fundy.* 21st Coastal Estuarine Research Federation Meeting, Daytona Beach, Florida. Poster.

- *<u>Poirier, E.</u> ; van Proosdij,D and <u>C. O'Laughlin.</u> (Nov 5-11, 2011). *Sedimentary Dynamics within a Hyper-tidal Salt Marsh and Tidal Creek System. .* 21st Coastal Estuarine Research Federation Meeting, Daytona Beach, Florida. Poster.

- <u>van Proosdij, D.</u>; O'Laughlin, C. and E. Poirier. (Feb 27, 2012). *Sedimentary Processes in a Hyper-intertidal Ecosystem.* Annual Meeting of the American Association of Geographers, New York, USA.

- <u>Poirier, E.</u> and D. van Proosdij. (May 10-11, 2012). *Sediment Dynamics within a Hypertidal Salt Marsh and Tidal Creek System: Results from the Bay of Fundy.* Oral presentation at the Atlantic Canada Coastal and Estuarine Science Association Meeting, Halifax, NS.

- <u>O'Laughlin, C</u> and D. van Proosdij (May 10-11, 2012). *Influence of Flocculation Processes on Sediment Deposition with a Bay of Fundy Tidal Creek.* Oral presentation at the Atlantic Canada Coastal and Estuarine Science Association Meeting, Halifax, NS.

- <u>Poirier, E.</u> and D. van Proosdij. (May 16, 2012). *Sediment Dynamics within a Hypertidal Salt Marsh and Tidal Creek System: Results from the Bay of Fundy.* Poster presentation at the Nova Scotia Energy and Research Development Forum, Halifax, NS.

- <u>O'Laughlin, C</u> and D. van Proosdij (May 16, 2012). *Controls on the Availability and Opportunity for Deposition within a Macrotidal Saltmarsh Creek.* Poster presentation at the Nova Scotia Energy and Research Development Forum, Halifax, NS.

APPENDIX E

Saint Mary's University Financial Grant Statement

Saint Mary's University
Principle Investigator: Dr. Danika van Proosdij, Geogrpaghy Department
OEER and OETR Associations Research Agreement
Research Project: Effects of Energy Extraction on Sediment Dynamics in Intertidal Ecosystems of the Minas Basin
Year 1: December 17, 2009 to May 31, 2010
Year 2: June 01, 2010 to May 31, 2011
Year 3: June 01, 2011 to May 31, 2012

	@ May 31, 2010 Year 1	@May 31, 2011 Year 2	Interim Report @Dec 31, 2011 Year 3	Project Total
Revenue:				
OEER Association	$ 5,000.00	$ 12,500.00	$ 7,500.00	25,000.00
OETR Association	5,000.00	12,500.00	7,500.00	25,000.00
Total Revenue	10,000.00	25,000.00	15,000.00	50,000.00
Expenses:				
Research assistant salaries & benefits	4,235.88	16,709.38	24,162.28	45,107.54
Equipment & Facilities	-			
Materials and Supplies	-	3,232.82	49.36	3,282.18
Travel	-	5,050.93	2,138.24	7,189.17
Dissemination	-			
Overhead	2,098.47	5,259.00	2,670.83	10,028.30
Total Expenses	6,334.35	30,252.13	29,020.71	65,607.19
Excess Revenue over Expenses	3,665.65	(5,252.13)	(14,020.71)	(15,607.19)
Opening Balance	-	3,665.65	(1,586.48)	
Closing Balance May 31	$ 3,665.65	$ (1,586.48)	$ (15,607.19)	$ (15,607.19)

Marcia Kissner
Accountant, Research and Special Projects
Saint Mary's University, Financial Services

Jan 09, 2012
Date